

Applied Methodologies in

# Polymer Research and Technology



Editors

Abbas Hamrang, PhD

Devrim Balköse, PhD



Apple Academic Press



CRC Press  
Taylor & Francis Group

**APPLIED METHODOLOGIES  
IN POLYMER RESEARCH  
AND TECHNOLOGY**

This page intentionally left blank

# APPLIED METHODOLOGIES IN POLYMER RESEARCH AND TECHNOLOGY

*Edited by*

**Abbas Hamrang, PhD, and Devrim Balköse, PhD**

**Gennady E. Zaikov, DSc, and A. K. Haghi, PhD**

*Reviewers and Advisory Board Members*



Apple Academic Press

---

TORONTO NEW JERSEY

CRC Press  
Taylor & Francis Group  
6000 Broken Sound Parkway NW, Suite 300  
Boca Raton, FL 33487-2742

Apple Academic Press, Inc  
3333 Mistwell Crescent  
Oakville, ON L6L 0A2  
Canada

© 2015 by Apple Academic Press, Inc.

Exclusive worldwide distribution by CRC Press an imprint of Taylor & Francis Group, an Informa business

No claim to original U.S. Government works  
Version Date: 20141013

International Standard Book Number-13: 978-1-4822-5434-1 (eBook - PDF)

This book contains information obtained from authentic and highly regarded sources. Reasonable efforts have been made to publish reliable data and information, but the author and publisher cannot assume responsibility for the validity of all materials or the consequences of their use. The authors and publishers have attempted to trace the copyright holders of all material reproduced in this publication and apologize to copyright holders if permission to publish in this form has not been obtained. If any copyright material has not been acknowledged please write and let us know so we may rectify in any future reprint.

Except as permitted under U.S. Copyright Law, no part of this book may be reprinted, reproduced, transmitted, or utilized in any form by any electronic, mechanical, or other means, now known or hereafter invented, including photocopying, microfilming, and recording, or in any information storage or retrieval system, without written permission from the publishers.

For permission to photocopy or use material electronically from this work, please access [www.copyright.com](http://www.copyright.com) (<http://www.copyright.com/>) or contact the Copyright Clearance Center, Inc. (CCC), 222 Rosewood Drive, Danvers, MA 01923, 978-750-8400. CCC is a not-for-profit organization that provides licenses and registration for a variety of users. For organizations that have been granted a photocopy license by the CCC, a separate system of payment has been arranged.

**Trademark Notice:** Product or corporate names may be trademarks or registered trademarks, and are used only for identification and explanation without intent to infringe.

**Visit the Taylor & Francis Web site at**  
**<http://www.taylorandfrancis.com>**

**and the CRC Press Web site at**  
**<http://www.crcpress.com>**

**For information about Apple Academic Press product**  
**<http://www.appleacademicpress.com>**

# ABOUT THE EDITORS

---

## **Abbas Hamrang, PhD**

Abbas Hamrang, PhD, is a professor of polymer science and technology. He is currently a senior polymer consultant and editor and member of the academic boards of various international journals. His research interests include degradation studies of historical objects and archival materials, cellulose-based plastics, thermogravimetric analysis, and accelerated ageing process and stabilization of polymers by chemical and non-chemical methods. His previous involvement in academic and industry sectors at the international level includes deputy vice-chancellor of research and development, senior lecturer, manufacturing consultant, and science and technology advisor.

## **Devrim Balköse, PhD**

Devrim Balköse, PhD, graduated from the Middle East Technical University in Ankara, Turkey, with a degree in chemical engineering. She received her MS and PhD degrees from Ege University, Izmir, Turkey, in 1974 and 1977 respectively. She became associate professor in macromolecular chemistry in 1983 and professor in process and reactor engineering in 1990. She worked as research assistant, assistant professor, associate professor, and professor between 1970–2000 at Ege University. She was the Head of Chemical Engineering Department at Izmir Institute of Technology, Izmir, Turkey, between 2000 and 2009. She is now a faculty member in the same department. Her research interests are in polymer reaction engineering, polymer foams and films, adsorbent development, and moisture sorption. Her research projects are on nanosized zinc borate production, ZnO polymer composites, zinc borate lubricants, antistatic additives, and metal soaps.

This page intentionally left blank

# REVIEWERS AND ADVISORY BOARD MEMBERS

---

## **Gennady E. Zaikov, DSc**

Gennady E. Zaikov, DSc, is Head of the Polymer Division at the N. M. Emanuel Institute of Biochemical Physics, Russian Academy of Sciences, Moscow, Russia, and Professor at Moscow State Academy of Fine Chemical Technology, Russia, as well as Professor at Kazan National Research Technological University, Kazan, Russia. He is also a prolific author, researcher, and lecturer. He has received several awards for his work, including the Russian Federation Scholarship for Outstanding Scientists. He has been a member of many professional organizations and on the editorial boards of many international science journals.

## **A. K. Haghi, PhD**

A. K. Haghi, PhD, holds a BSc in urban and environmental engineering from University of North Carolina (USA); a MSc in mechanical engineering from North Carolina A&T State University (USA); a DEA in applied mechanics, acoustics and materials from Université de Technologie de Compiègne (France); and a PhD in engineering sciences from Université de Franche-Comté (France). He is the author and editor of 65 books as well as 1000 published papers in various journals and conference proceedings. Dr. Haghi has received several grants, consulted for a number of major corporations, and is a frequent speaker to national and international audiences. Since 1983, he served as a professor at several universities. He is currently Editor-in-Chief of the *International Journal of Chemoinformatics and Chemical Engineering* and *Polymers Research Journal* and on the editorial boards of many international journals. He is a member of the Canadian Research and Development Center of Sciences and Cultures (CRDCSC), Montreal, Quebec, Canada.



This page intentionally left blank

# CONTENTS

---

<i>List of Contributors</i> .....	<i>xi</i>
<i>List of Abbreviations</i> .....	<i>xiii</i>
<i>List of Symbols</i> .....	<i>xv</i>
<i>Preface</i> .....	<i>xvii</i>
<b>1. Electrospinning Process: A Comprehensive Review and Update</b> .....	<b>1</b>
S. Rafiei	
<b>2. Aluminium-Coated Polymer Films as Infrared Light Shields for Food Packing</b> .....	<b>109</b>
Esen Arkış and Devrim Balköse	
<b>3. Generalization of Fuels Swelling Data by Means of Linear Free Energy Principle</b> .....	<b>125</b>
Roman Makitra, Halyna Midyana, Liliya Bazylyak, and Olena Palchykova	
<b>4. Trends on New Biodegradable Blends on the Basis of Copolymers 3-Hydroxybutyrate with Hydroxyvalerate and Segmented Polyetherurethane</b> .....	<b>151</b>
Svetlana G. Karpova, Sergei M. Lomakin, Anatolii A. Popov, and Aleksei A. Iordanskii	
<b>5. New Biologically Active Composite Materials on the Basis of Dialdehyde Cellulose</b> .....	<b>159</b>
Azamat A. Khashirov, Azamat A. Zhansitov, Genadiy E. Zaikov, and Svetlana Yu. Khashirova	
<b>6. Microheterogeneous Titanium Ziegler–Natta Catalysts: The Influence of Particle Size on the Isoprene Polymerization</b> .....	<b>167</b>
Elena M. Zakharova, Vadim Z. Mingaleev, and Vadim P. Zakharov	
<b>7. The Role and Mechanism of Bonding Agents in Composite Solid Propellants</b> .....	<b>185</b>
S. A. Vaziri, S. M. Mousavi Motlagh, and M. Hasanzadeh	

<b>8. A Study on Adsorption of Methane on Zeolite 13x at Various Pressures and Temperatures .....</b>	<b>197</b>
Farshid Basiri, Alireza Eslami, Mazyar Sharifzadeh, and Mahdi Hasanzadeh	
<b>9. Importance of the Phase Behavior in Biopolymer Mixtures.....</b>	<b>207</b>
Y. A. Antonov and Paula Moldenaers	
<i>Index</i> .....	237

# LIST OF CONTRIBUTORS

---

## **Esen Arkış**

Izmir Institute of Technology Department of Chemical Engineering, Gülbahçe Urla 35430, Izmir Turkey, Email: esenarkis@iyte.edu.tr

## **Devrim Balköse**

Izmir Institute of Technology Department of Chemical Engineering, Gülbahçe Urla 35430 Izmir Turkey

## **Farshid Basiri**

Department of Chemical Engineering, South Tehran Branch, Islamic Azad University, Tehran, Iran

## **Liliya Bazylyak**

Chemistry of Oxidizing Processes Division; Physical Chemistry of Combustible Minerals Department, Institute of Physical–Organic Chemistry & Coal Chemistry named after L. M. Lytvynenko, National Academy of Science of Ukraine 79053, Ukraine, Email: bazylyak.L.I@nas.gov.ua

## **Alireza Eslami**

Department of Chemical Engineering, South Tehran Branch, Islamic Azad University, Tehran, Iran

## **M. Hasanzadeh**

Department of Textile Engineering, University of Guilan, Rasht, Iran

## **Mahdi Hasanzadeh**

Department of Textile Engineering, University of Guilan, Rasht, Iran, Email: hasanzadeh\_mahdi@yahoo.com

## **Aleksei A. Jordanskii**

Semenov Institute of Chemical Physics, Russian Academy of Sciences, Moscow, Russia

## **Svetlana G. Karpova**

Emmanuel Institute of Biochemical Physics, Russian Academy of Sciences, Moscow, Russia

## **Azamat A. Khashirov**

Kabardino-Balkarian State University, Nalchik 360004, Russia, Russian Federation, Email: new\_kompozit@mail.ru

## **Svetlana Yu. Khashirova**

Kabardino-Balkarian State University, Nalchik 360004, Russia, Russian Federation, Email: new\_kompozit@mail.ru

## **Sergei M. Lomakin**

Emmanuel Institute of Biochemical Physics, Russian Academy of Sciences, Moscow, Russia

## **Roman Makitra**

Chemistry of Oxidizing Processes Division; Physical Chemistry of Combustible Minerals Department; Institute of Physical–Organic Chemistry & Coal Chemistry named after L. M. Lytvynenko, National Academy of Science of Ukraine 79053, Ukraine; Email: bazylyak.L.I@nas.gov.ua

**Halyna Midyana**

Chemistry of Oxidizing Processes Division; Physical Chemistry of Combustible Minerals Department, Institute of Physical–Organic Chemistry & Coal Chemistry named after L. M. Lytvynenko, National Academy of Science of Ukraine 79053, Ukraine, Email: bazylyjak.L.I@nas.gov.ua

**Vadim Z. Mingaleev**

Institute of Organic Chemistry, Ufa Scientific Center of Russian Academy of Sciences, Ufa, Bashkortostan, 450054, Russia

**S. M. Mousavi Motlagh**

Department of Chemical Engineering, Imam Hossien University, Tehran, Iran

**Olena Palchykova**

Institute of Geology and Geochemistry of Combustible Minerals; National Academy of Science of Ukraine 79053, Ukraine

**Anatolii A. Popov**

Emmanuel Institute of Biochemical Physics, Russian Academy of Sciences, Moscow, Russia

**S. Rafiei**

University of Guilan, Rasht, Iran

**Maziyar Sharifzadeh**

Department of Chemical Engineering, Ayatollah Amoli Branch, Islamic Azad University, Amol, Iran

**S. A. Vaziri**

Department of Chemical Engineering, Imam Hossien University, Tehran, Iran

**Genadiy E. Zaikov**

N.M. Emanuel Institute of Biochemical Physics of Russian Academy of Sciences, Moscow 119991, Russia, Russian Federation

**Vadim P. Zakharov**

Bashkir State University, Ufa 450076, Bashkortostan, Russia, Email: zaharovvp@mail.ru

**Elena M. Zakharova**

Institute of Organic Chemistry, Ufa Scientific Center of Russian Academy of Sciences, Ufa, Bashkortostan, 450054, Russia

**Azamat A. Zhansitov**

Kabardino-Balkarian State University, Nalchik 360004, Russia, Russian Federation, Email: new\_kompozit@mail.ru

# LIST OF ABBREVIATIONS

---

ACs	active sites
CS	cuckoo search
DAC	dialdehyde cellulose
DAGA	diallylguanidine acetate
DAGTFA	diallylguanidine trifluoroacetate
DE	differential evolution
DLS	dynamic light scattering
DSS	dextran sulfate sodium salt
ESEM	environment scanning electron microscope
FPLC	fast protein liquid chromatography
MCC	microcrystalline cellulose
MWD	molecular weight distribution
NPBA	neutral polymeric bonding agent
OM	optical microscopy
PHB	poly(3-hydroxybutyrate)
PMMA	poly (methylmethacrylate)
PSO	particle swarm optimization
SA	sodium alginate
SALS	small angle light scattering
SC	sodium caseinate
SPEUs	segmented polyetherurethanes

This page intentionally left blank

# LIST OF SYMBOLS

---

$\delta_1$ and $\delta_2$	Hildebrand's parameters
$\rho_2$	density of a polymer into solution
$V_1$	molar volume of the solvent
$T_m$	melting temperature
$P_{\max}$	maximum pressure of each isotherm
$S$	number of point per isotherm per gas
$C^{\text{exp}}$	methane concentrations (experimental)
$C^{\text{cal}}$	methane concentrations (calculated)
$U_e$	electrophoretic mobility
$\epsilon$	dielectric constant
$\eta$	viscosity
$z\rho$	zeta potential
$k$	Boltzmann's constant
$T$	temperature
$n$	dumbbells density
$p$	unit vector in nanoelement axis direction
$\omega_{ij}$	rotation rate tensor
$\gamma_{ij}$	deformation tensor
$D_r$	rotary diffusivity
$\theta$	shape factor
$l$	mean segment length
$V$	velocity
$h$	fabric thickness
$m$	equivalent mass
$\alpha$	surface charge parameter



This page intentionally left blank

# PREFACE

---

Polymers are substances that contain a large number of structural units joined by the same type of linkage. These substances often form into a chain-like structure. Starch, cellulose, and rubber all possess polymeric properties. Today, the polymer industry has grown to be larger than the aluminum, copper, and steel industries combined. Polymers already have a range of applications that far exceeds that of any other class of material available to man. Current applications extend from adhesives, coatings, foams, and packaging materials to textile and industrial fibers, elastomers, and structural plastics. Polymers are also used for most nanocomposites, electronic devices, biomedical devices, and optical devices, and are precursors for many newly developed high-tech ceramics.

This book presents leading-edge research in this rapidly changing and evolving field. Successful characterization of polymer systems is one of the most important objectives of today's experimental research of polymers. Considering the tremendous scientific, technological, and economic importance of polymeric materials, not only for today's applications but for the industry of the twenty-first century, it is impossible to overestimate the usefulness of experimental techniques in this field. Since the chemical, pharmaceutical, medical, and agricultural industries, as well as many others, depend on this progress to an enormous degree, it is critical to be as efficient, precise, and cost-effective in our empirical understanding of the performance of polymer systems as possible. This presupposes our proficiency with, and understanding of, the most widely used experimental methods and techniques. This book is designed to fulfill the requirements of scientists and engineers who wish to be able to carry out experimental research in polymers using modern methods.

Polymer nanocomposites are materials that possess unique properties. These properties are enhanced properties of the polymer matrix. Some of the improved properties are thermal stability, permeability to gases, flammability, mechanical strength and photodegradability. At complete dispersion of the new layers in the polymer matrix, these enhanced properties

are obtained. The unique properties of the material makes it suitable in applications as, food and beverage packaging, automobile parts, furniture, carrier bags, electrical gadgets, and so on.

# CHAPTER 1

---

## ELECTROSPINNING PROCESS: A COMPREHENSIVE REVIEW AND UPDATE

S. RAFIEI

---

### CONTENTS

1.1	Introduction.....	2
1.2	Nanostructured Materials.....	4
1.3	Nanofiber Technology .....	13
1.4	Design Multifunctional Product by Nanostructures .....	23
1.5	Multifunctional Nanofiber-Based Structure .....	33
1.6	Concluding Remarks of Multifunctional Nanostructure Design ...	49
1.7	Introduction to Theoretical Study of Electrospinning Process .....	49
1.8	Study of Electrospinning Jet Path.....	51
1.9	Electrospinning Drawbacks .....	54
1.10	Modeling the Electrospinning Process .....	56
1.11	Electrospinning Simulation.....	95
	Keywords .....	95
	References.....	96

## 1.1 INTRODUCTION

Understanding the nanoworld makes up one of the frontiers of modern science. One reason for this is that technology based on nanostructures promises to be hugely important economically [1–3]. Nanotechnology literally means any technology on a nanoscale that has applications in the real world. It includes the production and application of physical, chemical, and biological systems at scales ranging from individual atoms or molecules to submicron dimensions, as well as the integration of the resulting nanostructures into larger systems. Nanotechnology is likely to have a profound impact on our economy and society in the early twenty-first century, comparable with that of semiconductor technology, information technology, or cellular and molecular biology. Science and technology research in nanotechnology promises breakthroughs in areas such as materials and manufacturing [4], nanoelectronics [5], medicine and healthcare [6], energy [7], biotechnology [8], information technology [9], and national security [10]. It is widely felt that nanotechnology will be the next Industrial Revolution [9].

As far as “nanostructures” are concerned, one can view this as objects or structures whereby at least one of its dimensions is within nanoscale. A “nanoparticle” can be considered as a zero dimensional nanoelement, which is the simplest form of nanostructure. It follows that a “nanotube” or a “nanorod” is a one-dimensional nanoelement from which slightly more complex nanostructure can be constructed of Refs. [11–12].

Following this fact, a “nanoplatelet” or a “nanodisk” is a two-dimensional element which, along with its one-dimensional counterpart, is useful in the construction of nanodevices. The difference between a nanostructure and a nanodevice can be viewed upon as the analogy between a building and a machine (whether mechanical, electrical, or both) [1]. It is important to know that as far as nanoscale is concerned, these nanoelements should not be considered only as an element that forms a structure while they can be used as a significant part of a device. For example, the use of carbon nanotube as the tip of an atomic force microscope (AFM) would have it classified as a nanostructure. The same nanotube, however, can be used as a single-molecule circuit, or as part of a miniaturized electronic component, thereby appearing as a nanodevice. Hence, the function, along with the structure, is essential in classifying which nanotech-

nology subarea it belongs to. This classification will be discussed in detail in further sections [11, 13].

As long as nanostructures clearly define the solids' overall dimensions, the same cannot be said so for nanomaterials. In some instances, a nanomaterial refers to a nanosized material; whereas in other instances, a nanomaterial is a bulk material with nanoscaled structures. Nanocrystals are other groups of nanostructured materials. It is understood that a crystal is highly structured and that the repetitive unit is indeed small enough. Hence, a nanocrystal refers to the size of the entire crystal itself being nanosized, but not of the repetitive unit [14].

Nanomagnetics are the other types of nanostructured materials that are known as highly miniaturized magnetic data storage materials with very high memory. This can be attained by taking advantage of the electron spin for memory storage; hence, the term "spin-electronics," which has since been more popularly and more conveniently known as "spintronics" [1, 9, 15]. In nanobioengineering, the novel properties of nanoscale are taken advantage of for bioengineering applications. The many naturally occurring nanofibrous and nanoporous structure in the human body further adds to the impetus for research and development in this subarea. Closely related to this is molecular functionalization whereby the surface of an object is modified by attaching certain molecules to enable desired functions to be carried out such as for sensing or filtering chemicals based on molecular affinity [16–17].

With the rapid growth of nanotechnology, nanomechanics are no longer the narrow field that it used to be [13]. This field can be broadly categorized into the molecular mechanics and the continuum mechanics approaches that view objects as consisting of discrete many-body system and continuous media, respectively. As long as the former inherently includes the size effect, it is a requirement for the latter to factor in the influence of increasing surface-to-volume ratio, molecular reorientation, and other novelties as the size shrinks. As with many other fields, nanotechnology includes nanoprocessing novel materials processing techniques by which nanoscale structures and devices are designed and constructed [18–19].

Depending on the final size and shape, a nanostructure or nanodevice can be created from the top-down or the bottom-up approach. The former refers to the act of removing or cutting down a bulk to the desired size; whereas, the latter takes on the philosophy of using the fundamental building blocks—such as atoms and molecules, to build up nanostructures

in the same manner. It is obvious that the top-down and the bottom-up nanoprocessing methodologies are suitable for the larger and two smaller ends, respectively, in the spectrum of nanoscale construction. The effort of nanopatterning—or patterning at the nanoscale— would hence fall into nanoprocessing [1, 12, 18].

## 1.2 NANOSTRUCTURED MATERIALS

Strictly speaking, a nanostructure is any structure with one or more dimensions measuring in the nanometer ( $10^{-9}\text{m}$ ) range. Various definitions refine this further, stating that a nanostructure should have a characteristic dimension lying between 1nm and 100 nm, putting nanostructures as intermediate in size between a molecule and a bacterium. Nanostructures are typically probed either optically (spectroscopy, photoluminescence ...), or in transport experiments. This field of investigation is often given the name mesoscopic transport, and the following considerations give an idea of the significance of this term[1–2, 12, 20–21].

What makes nanostructured materials very interesting and award them with their unique properties is that their size is smaller than critical lengths that characterize many physical phenomena. In general, physical properties of materials can be characterized by some critical length, a thermal diffusion length, or a scattering length, for example. The electrical conductivity of a metal is strongly determined by the distance that the electrons travel between collisions with the vibrating atoms or impurities of the solid. This distance is called the mean free path or the scattering length. If the sizes of the particles are less than these characteristic lengths, it is possible that new physics or chemistry may occur [1, 9, 17].

Several computational techniques have been used to simulate and model nanomaterials. Since the relaxation times can vary anywhere from picoseconds to hours, it becomes necessary to employ Langevin dynamics besides molecular dynamics in the calculations. Simulation of nanodevices through the optimization of various components and functions provides challenging and useful task[20, 22]. There are many examples where simulation and modeling have yielded impressive results, such as nanoscale lubrication [23]. Simulation of the molecular dynamics of DNA has been successful to some extent [24]. Quantum dots and nanotubes have been modeled satisfactorily [25–26]. First principles calculations of

nanomaterials can be problematic if the clusters are too large to be treated by Hartree–Fock methods and too small for density functional theory [1]. In the next section various classifications of these kinds of materials are considered in detail.

### **1.2.1 NANOSTRUCTURED MATERIALS AND THEIR CLASSIFICATIONS**

Nanostructure materials as a subject of nanotechnology are low-dimensional materials comprising building units of a submicron or nanoscale size at least in one direction and exhibiting size effects. The first classification idea of NSMs was given by Gleiter in 1995 [3]. A modified classification scheme for these materials, in which 0D, 1D, 2D, and 3D are included suggested in later researches [21]. These classifications are given below.

#### **1.2.1.1 0D NANOPARTICLES**

A major feature that distinguishes various types of nanostructures is their dimensionality. In the past 10 years, significant progress has been made in the field of 0D nanostructure materials. A rich variety of physical and chemical methods have been developed for fabricating these materials with well-controlled dimensions[3, 18]. Recently, 0D nanostructured materials such as uniform particles arrays (quantum dots), heterogeneous particles arrays, core-shell quantum dots, onions, hollow spheres, and nanolenses have been synthesized by several research groups[21]. They have been extensively studied in light-emitting diodes (LEDs), solar cells, single-electron transistors, and lasers.

#### **1.2.1.2 1D NANOPARTICLES**

In the past decade, 1D nanostructured materials have focused an increasing interest due to their importance in research and developments and have a wide range of potential applications [27]. It is generally accepted that these materials are ideal systems for exploring a large number of novel phenomena at the nanoscale and investigating the size and dimensionality dependence of functional properties. They are also expected to play a



significant role as both interconnects and the key units in fabricating electronic, optoelectronic, and EEDs with nanoscale dimensions. The most important types of this group are nanowires, nanorods, nanotubes, nanobelts, nanoribbons, hierarchical nanostructures, and nanofibers [1, 18, 28].

### **1.2.1.3 2D NANOPARTICLES**

2D nanostructures have two dimensions outside of the nanometric size range. In recent years, synthesis of 2D nanomaterial has become a focal area in materials research, owing to their many low-dimensional characteristics different from the bulk properties. Considerable research attention has been focused over the past few years on the development of them. Two-dimensional nanostructured materials with certain geometries exhibit unique shape-dependent characteristics and subsequent utilization as building blocks for the key components of nanodevices[21]. In addition, these materials are particularly interesting not only for basic understanding of the mechanism of nanostructure growth but also for investigation and developing novel applications in sensors, photocatalysts, nanocontainers, nanoreactors, and templates for 2D structures of other materials. Some of the 3D nanoparticles are junctions (continuous islands), branched structures, nanoprisms, nanoplates, nanosheets, nanowalls, and nanodisks [1].

### **1.2.1.4 3D NANOPARTICLES**

Owing to the large specific surface area and other superior properties over their bulk counterparts arising from quantum size effect, they have attracted considerable research interest and many of them have been synthesized in the past 10 years [1, 12]. It is well known that the behaviors of NSMs strongly depend on the sizes, shapes, dimensionality and morphologies, which are thus the key factors to their ultimate performance and applications. Therefore, it is of great interest to synthesize 3D NSMs with a controlled structure and morphology. In addition, 3D nanostructures are an important material due to its wide range of applications in the area of catalysis, magnetic material and electrode material for batteries [2]. Moreover, the 3D NSMs have recently attracted intensive research interests because the nanostructures have higher surface area and supply enough absorption sites for all involved molecules in a small space [58]. On the contrary, such



gas-phase, liquid-phase, and solid-phase methods based on the state of the reaction system. The gas-phase method includes gas-phase evaporation method (resistance heating, high-frequency induction heating, plasma heating, electron beam heating, laser heating, electric heating evaporation method, vacuum deposition on the surface of flowing oil, and exploding wire method), chemical vapor reaction (heating heat pipe gas reaction, laser-induced chemical vapor reaction, plasma-enhanced chemical vapor reaction), chemical vapor condensation, and sputtering method. Liquid-phase method for synthesizing nanoparticles mainly includes precipitation, hydrolysis, spray, solvent thermal method (high temperature and high pressure), solvent evaporation pyrolysis, oxidation reduction (room pressure), emulsion, radiation chemical synthesis, and sol-gel processing. The solid-phase method includes thermal decomposition, solid-state reaction, spark discharge, stripping, and milling method [30, 33].

In other classification, there are two general approaches to the synthesis of nanomaterials and the fabrication of nanostructures, bottom-up and top-down approach. The first one includes the miniaturization of material components (up to atomic level) with further self-assembly process leading to the formation assembly of nanostructures. During self-assembly, the physical forces operating at nanoscale are used to combine basic units into larger stable structures. Typical examples are quantum dot formation during epitaxial growth and formation of nanoparticles from colloidal dispersion. The latter uses larger (macroscopic) initial structures, which can be externally controlled in the processing of nanostructures. Typical examples include etching through the mask, ball milling, and application of severe plastic deformation [3, 13]. Some of the most common methods are described in the sections that follow.

### **1.2.3 PLASMA-BASED METHODS**

Metallic, semiconductive, and ceramic nanomaterials are widely synthesised by hot and cold plasma methods. A plasma is sometimes referred to as being “hot” if it is nearly fully ionized, or “cold” if only a small fraction, (e.g., 1%), of the gas molecules are ionized, but other definitions of the terms “hot plasma” and “cold plasma” are common. Even in cold plasma, the electron temperature is still typically several thousand degrees Celsius. In general, the related equipment consists of an arc-melting chamber and a

collecting system. The thin films of alloys were prepared from highly pure metals by arc melting in an inert gas atmosphere. Each arc-melted ingot was flipped over and remelted three times. Then, the thin films of alloy were produced by arc melting a piece of bulk materials in a mixing gas atmosphere at a low pressure. Before the ultrafine particles were taken out from the arc-melting chamber, they were passivated with a mixture of inert gas and air to prevent the particles from burning up [34–35].

Cold plasma method is used for producing nanowires in large scale and bulk quantity. The general equipment of this method consists of a conventional horizontal quartz tube furnace and an inductively coupled coil driven by a 13.56 MHz radiofrequency (RF) power supply. This method often is called as an RF plasma method. During RF plasma method, the starting metal is contained in a pestle in an evacuated chamber. The metal is heated above its evaporation point using high-voltage RF coils wrapped around the evacuated system in the vicinity of the pestle. Helium gas is then allowed to enter the system, forming a high-temperature plasma in the region of the coils. The metal vapor nucleates on the He gas atoms and diffuses up to a colder collector rod where nanoparticles are formed. The particles are generally passivated by the introduction of some gas such as oxygen. In the case of aluminum nanoparticles, the oxygen forms a layer of aluminum oxide about the particle [1, 36].

#### **1.2.4 CHEMICAL METHODS**

Chemical methods have played a significant role in developing materials imparting technologically important properties through structuring the materials on the nanoscale. However, the primary advantage of chemical processing is its versatility in designing and synthesizing new materials that can be refined into the final end products. The secondary most advantage that the chemical processes offer over physical methods is a good chemical homogeneity, as a chemical method offers mixing at the molecular level. On the contrary, chemical methods frequently involve toxic reagents and solvents for the synthesis of nanostructured materials. Another disadvantage of the chemical methods is the unavoidable introduction of byproducts that require subsequent purification steps after the synthesis in other words, this process is time-consuming. Despite these facts, probably the most useful methods of synthesis in terms of their potential to be

scaled up are chemical methods [33, 37]. There are a number of different chemical methods that can be used to make nanoparticles of metals, and we will give some examples. Several types of reducing agents can be used to produce nanoparticles such as  $\text{NaBEt}_3\text{H}$ ,  $\text{LiBEt}_3\text{H}$ , and  $\text{NaBH}_4$  where Et denotes the ethyl ( $-\text{C}_2\text{H}_5$ ) radical. For example, nanoparticles of molybdenum (Mo) can be reduced in toluene solution with  $\text{NaBEt}_3\text{H}$  at room temperature, providing a high yield of Mo nanoparticles having dimensions of 1–5 nm [30].

#### 1.2.4.1 THERMOLYSIS AND PYROLYSIS

Nanoparticles can be made by decomposing solids at high temperature having metal cations, and molecular anions or metal organic compounds. The process is called thermolysis. For example, small lithium particles can be made by decomposing lithium oxide,  $\text{LiN}_3$ . The material is placed in an evacuated quartz tube and heated to  $400^\circ\text{C}$  in the apparatus. At about  $370^\circ\text{C}$ , the  $\text{LiN}_3$  decomposes, releasing  $\text{N}_2$  gas, which is observed by an increase in the pressure on the vacuum gauge. In a few minutes, the pressure drops back to its original low value, indicating that all the  $\text{N}_2$  has been removed. The remaining lithium atoms coalesce to form small colloidal metal particles. Particles less than 5 nm can be made by this method. Passivation can be achieved by introducing an appropriate gas [1].

Pyrolysis is commonly a solution process in which nanoparticles are directly deposited by spraying a solution on a heated substrate surface, where the constituent react to form a chemical compound. The chemical reactants are selected such that the products other than the desired compound are volatile at the temperature of deposition. This method represents a very simple and relatively cost-effective processing method (particularly, in regard to equipment costs) as compared to many other film deposition techniques [30].

The other pyrolysis-based method that can be applied in nanostructures production is a laser pyrolysis technique that requires the presence in the reaction medium of a molecule absorbing the  $\text{CO}_2$  laser radiation [38–39]. In most cases, the atoms of a molecule are rapidly heated via vibrational excitation and are dissociated. But in some cases, a sensitizer gas such as  $\text{SF}_6$  can be directly used. The heated gas molecules transfer their energy to the reaction medium by collisions leading to dissociation

of the reactive medium without, in the ideal case, dissociation of this molecule. Rapid thermalization occurs after dissociation of the reactants due to transfer collision. Nucleation and growth of NSMs can take place in the as-formed supersaturated vapor. The nucleation and growth period is very short time (0.1–10 ms). Therefore, the growth is rapidly stopped as soon as the particles leave the reaction zone. The flame-excited luminescence is observed in the reaction region where the laser beam intersects the reactant gas stream. Since there is no interaction with any walls, the purity of the desired products is limited by the purity of the reactants. However, because of the very limited size of the reaction zone with a faster cooling rate, the powders obtained in this wellness reactor present a low degree of agglomeration. The particle size is small ( $\sim 5\text{--}50$  nm range) with a narrow size distribution. Moreover, the average size can be manipulated by optimizing the flow rate, and, therefore, the residence time in the reaction zone [39–40].

#### 1.2.4.2 LASER-BASED METHODS

The most important laser-based techniques in the synthesis of nanoparticles are pulsed laser ablation. As a physical gas-phase method for preparing nanosized particles, pulsed laser ablation has become a popular method to prepare high-purity and ultrafine nanomaterials of any composition [41–42]. In this method, the material is evaporated using pulsed laser in a chamber filled with a known amount of a reagent gas and by controlling condensation of nanoparticles onto the support. It is possible to prepare nanoparticles of mixed molecular composition such as mixed oxides/nitrides and carbides/nitrides or mixtures of oxides of various metals by this method. This method is capable of a high rate of production of 2–3 g/min [40].

Laser chemical vapor deposition method is the next laser-based technique in which photoinduced processes are used to initiate the chemical reaction. During this method, three kinds of activation should be considered. First, if the thermalization of the laser energy is faster than the chemical reaction, pyrolytic, and/or photothermal activation is responsible for the activation. Second, if the first chemical reaction step is faster than the thermalization, photolytical (nonthermal) processes are responsible for the excitation energy. Third, combinations of the different types of activation

are often encountered. During this technique, a high intensity laser beam is incident on a metal rod, causing evaporation of atoms from the surface of the metal. The atoms are then swept away by a burst of helium and passed through an orifice into a vacuum where the expansion of the gas causes cooling and formation of clusters of the metal atoms. These clusters are then ionized by UV radiation and passed into a mass spectrometer that measures their mass: charge ratio [1, 41–43].

Laser-produced nanoparticles have found many applications in medicine, biophotonics, in the development of sensors, new materials, and solar cells. Laser interactions provide a possibility of chemical clean synthesis, which is difficult to achieve under more conventional NP production conditions [42]. Moreover, a careful optimization of the experimental conditions can allow a control over size distributions of the produced nanoclusters. Therefore, many studies were focused on the investigation the laser nanofabrication. In particular, many experiments were performed to demonstrate nanoparticles formation in vacuum, in the presence of a gas or a liquid. Nevertheless, it is still difficult to control the properties of the produced particles. It is believed that numerical calculations can help explain experimental results and to better understand the mechanisms involved [43].

Despite rapid development in laser physics, one of the fundamental questions still concerns the definition of proper ablation mechanisms and the processes leading to the nanoparticles formation. Apparently, the progress in laser systems implies several important changes in these mechanisms, which depend on both laser parameters and material properties. Among the more studied ablation mechanisms there are thermal, photochemical and photomechanical ablation processes. Frequently, however, the mechanisms are mixed, so that the existing analytical equations are hardly applicable. Therefore, numerical simulation is needed to better understand and to optimize the ablation process [44].

Thus far, thermal models are commonly used to describe nanosecond (and longer) laser ablation. In these models, the laser-irradiated material experiences heating, melting, boiling, and evaporation. In this way, three numerical approaches were used [29, 45]:

*Atomistic approach* based on such methods as molecular dynamics (MD) and direct Monte Carlo (DSMC) simulation. Typical calculation results provide detailed information about atomic positions, velocities, kinetic, and potential energy.

*Macroscopic approach* based hydrodynamic models. These models allow the investigations of the role of the laser-induced pressure gradient, which is particularly important for ultra-short laser pulses. The models are based on a one fluid two-temperature approximation and a set of additional models (equation of state) that determines thermal properties of the target.

*Multiscale approach* based on the combination of two approaches cited above was developed by several groups and was shown to be particularly suitable for laser applications.

### 1.3 NANOFIBER TECHNOLOGY

Nanofiber consists of two terms “nano” and “fiber,” as the latter term looks more familiar. Anatomists observed fibers as any of the filament constituting the extracellular matrix of connective tissue, or any elongated cells or thread-like structures, muscle fiber, or nerve fiber. According to textile industry, fiber is a natural or synthetic filament, such as cotton or nylon, capable of being spun into simply as materials made of such filaments. Physiologists and biochemists use the term “fiber” for indigestible plant matter consisting of polysaccharides such as cellulose, that when eaten stimulates intestinal peristalsis. Historically, the term “fiber” or “fibre” in British English comes from Latin “fibra.” Fiber is a slender, elongated thread-like structure. Nano is originated from Greek word “nanos” or “nannos” refer to “little old man” or “dwarf.” The prefixes “nanos” or “nano” as nannoplanktons or nanoplanktons used for very small planktons measuring 2–20  $\mu\text{m}$ . In modern “nano” is used for describing various physical quantities within the scale of a billionth as nanometer (length), nanosecond (time), nanogram (weight), and nanofarad (charge) [1, 4, 9, 46]. As mentioned earlier, nanotechnology refers to the science and engineering concerning materials, structures, and devices, which has at least one dimension is 100nm or less. This term also refers for a fabrication technology, where molecules, specification, and individual atoms that have at least one dimension in nanometers or less is used to design or built objects. Nanofiber, as the name suggests, is the fiber having a diameter range in nanometer. Fibrous structure having at least 1D in nanometer or less is defined as nanofiber according to National Science Foundation (NSC). The term “nano” describes the diameter of the fibrous shape at anything below one micron or 1,000 nm [4, 18].



Nanofiber technology is a branch of nanotechnology whose primary objective is to create materials in the form of nanoscale fibers in order to achieve superior functions [1–2, 4]. The unique combination of high specific surface area, flexibility, and superior directional strength makes such fibers a preferred material form for many applications ranging from clothing to reinforcements for aerospace structures. Indeed, while the primary classification of nanofibers is that of nanostructure or nanomaterial, other aspects of nanofibers such as its characteristics, modeling, application, and processing would enable nanofibers to penetrate into many subfields of nanotechnology [4, 46–47].

It is obvious that nanofibers would geometrically fall into the category of 1D nanoscale elements that include nanotubes and nanorods. However, the flexible nature of nanofibers would align it along with other highly flexible nanoelements such as globular molecules (assumed as 0D soft matter), as well as solid and liquid films of nanothickness (2D). A nanofiber is a nanomaterial in view of its diameter, and can be considered a nanostructured material material if filled with nanoparticles to form composite nanofibers [1, 48].

The study of the nanofiber mechanical properties as a result of manufacturing techniques, constituent materials, processing parameters, and other factors would fall into the category of nanomechanics. Indeed, while the primary classification of nanofibers is that of nanostructure or nanomaterial, other aspects of nanofibers such as its characteristics, modeling, application, and processing would enable nanofibers to penetrate into many subfields of nanotechnology [1, 18].

Although the effect of fiber diameter on the performance and processibility of fibrous structures has long been recognized, the practical generation of fibers at the nanometer scale was not realized until the rediscovery and popularization of the electrospinning technology by Professor Darrell Reneker almost a decade ago [49–50]. The ability to create nanoscale fibers from a broad range of polymeric materials in a relatively simple manner using the electrospinning process, coupled with the rapid growth of nanotechnology in recent years have greatly accelerated the growth of nanofiber technology. Although there are several alternative methods available for generating fibers in a nanometer scale, none of the methods matches the popularity of the electrospinning technology due largely to the simplicity of the electrospinning process[18]. These methods will be discussed in the sections that follow.

### **1.3.1 VARIOUS NANOFIBER PRODUCTION METHODS**

As was discussed in detail, nanofiber is defined as the fiber having at least 1D in nanometer range that can be used for a wide range of medical applications for drug delivery systems, scaffold formation, wound healing and widely used in tissue engineering, skeletal tissue, bone tissue, cartilage tissue, ligament tissue, blood vessel tissue, neural tissue, and so on. It is also used in dental and orthopedic implants [4, 51–52]. Nanofiber can be formed using different techniques including drawing, template synthesis, phases separation, self-assembly, and electrospinning.

#### **1.3.1.1 DRAWING**

In 1998, nanofibers were fabricated with citrate molecules through the process of drawing for the first time [53]. During drawing process, the fibers are fabricated by contacting a previously deposited polymer solution droplet with a sharp tip and drawing it as a liquid fiber that is then solidified by rapid evaporation of the solvent owing to the high surface area. The drawn fiber can be connected to another previously deposited polymer solution droplet, thereby forming a suspended fiber. Here, the predeposition of droplets significantly limits the ability to extend this technique, especially in 3D configurations and hard-to-access spatial geometries. Further, there is a specific time in which the fibers can be pulled. The viscosity of the droplet continuously increases with time due to solvent evaporation from the deposited droplet. The continual shrinkage in the volume of the polymer solution droplet affects the diameter of the fiber drawn and limits the continuous drawing of fibers [54].

To overcome the above-mentioned limitation, it is appropriate to use hollow glass micropipettes with a continuous polymer dosage. It provides greater flexibility in drawing continuous fibers in any configuration. Moreover, this method offers increased flexibility in the control of key parameters of drawing such as waiting time before drawing (because the required viscosity of the polymer edge drops), the drawing speed or viscosity, thus enabling repeatability and control on the dimensions of the fabricated fibers. Thus, drawing process requires a viscoelastic material that can undergo strong deformations while being cohesive enough to support the stresses developed during pulling [54–55].

### 1.3.1.2 *TEMPLATE SYNTHESIS*

Template synthesis implies the use of a template or mold to obtain a desired material or structure. Hence, the casting method and DNA replication can be considered as template-based synthesis. In the case of nanofiber creation by Feng et al. [56], the template refers to a metal oxide membrane with through-thickness pores of nanoscale diameter. Under the application of water pressure on the one side and restraint from the porous membrane causes extrusion of the polymer which, upon coming into contact with a solidifying solution, gives rise to nanofibers whose diameters are determined by the pores [1, 57].

This method is an effective route to synthesize nanofibrils and nanotubes of various polymers. The advantage of the template synthesis method is that the length and diameter of the polymer fibers and tubes can be controlled by the selected porous membrane, which results in more regular nanostructures. General feature of the conventional template method is that the membrane should be soluble so that it can be removed after synthesis so as to obtain single fibers or tubes. This restricts practical application of this method and gives rise to a need for other techniques [1, 56–57].

### 1.3.1.3 *PHASE SEPARATION METHOD*

This method consists of five basic steps: polymer dissolution, gelation, solvent extraction, freezing, and freeze-drying. In this process, it is observed that gelation is the most difficult step to control the porous morphology of nanofiber. Duration of gelation varied with polymer concentration and gelation temperature. At low gelation temperature, nanoscale fiber network is formed; whereas, high gelation temperature led to the formation of platelet-like structure. Uniform nanofiber can be produced as the cooling rate is increased, polymer concentration affects the properties of nanofiber, as polymer concentration is increased porosity of fiber decreased and mechanical properties of fiber are increased [1, 58].

### 1.3.1.4 *SELF-ASSEMBLY*

Self-assembly refers to the build-up of nanoscale fibers using smaller molecules. In this technique, a small molecule is arranged in a concentric man-

ner so that they can form bonds among the concentrically arranged small molecules that, upon extension in the plane-s normal, give the longitudinal axis of a nanofiber. The main mechanism for a generic self-assembly is the intramolecular forces that bring the smaller unit together. A hydrophobic core of alkyl residues and a hydrophilic exterior lined by peptide residues was found in obtained fiber. It is observed that the nanofibers produced with this technique have a diameter range of 5–8 nm approximately and are several microns in length [1, 59].

Although there are a number of techniques used for the synthesis of nanofiber, electrospinning represents an attractive technique to fabricate polymeric biomaterial into nanofibers. Electrospinning is one of the most commonly utilized methods for the production of nanofiber. It has a wide advantage over the previously available fiber formation techniques because here electrostatic force is used instead of conventionally used mechanical force for the formation of fibers. This method will be debated comprehensively in the sections that follow.

#### 1.3.1.5 ELECTROSPINNING OF NANOFIBERS

Electrospinning is a straightforward and cost-effective method to produce novel fibers with diameters in the range of from less than 3 nm to over 1 mm, which overlaps contemporary textile fiber technology. During this process, an electrostatic force is applied to a polymeric solution to produce nanofiber [60–61] with diameter ranging from 50 to 1,000 nm or greater [49, 62–63]; Due to surface tension, the solution is held at the tip of syringe. Polymer solution is charged due to applied electric force. In the polymer solution, a force is induced due to mutual charge repulsion that is directly opposite to the surface tension of the polymer solution. Further increases in the electrical potential led to the elongation of the hemispherical surface of the solution at the tip of the syringe to form a conical shape known as “Taylor cone.” [50, 64]. The electric potential is increased to overcome the surface tension forces to cause the formation of a jet, ejects from the tip of the Taylor cone. Due to elongation and solvent evaporation, charged jet instable and gradually thins in air primarily [62, 65–67]. The charged jet forms randomly oriented nanofibers that can be collected on a stationary or rotating grounded metallic collector [50]. Electrospinning

provides a good method and a practical way of producing polymer fibers with diameters ranging from 40 to 2,000 nm [49–50].

### 1.3.1.5 1 THE HISTORY OF ELECTROSPINNING METHODOLOGY

William Gilbert discovered the first record of the electrostatic attraction of a liquid in 1,600 [68]. The first electrospinning patent was submitted by John Francis Cooley in 1900 [69]. After that in 1914, John Zeleny studied on the behavior of fluid droplets at the end of metal capillaries that caused the beginning of the mathematical model the behavior of fluids under electrostatic forces [65]. Between 1931 and 1944, Anton Formhals took out at least 22 patents on electrospinning [69]. In 1938, N.D. Rozenblum and I.V. Petryanov-Sokolov generated electrospun fibers, which they developed into filter materials [70]. Between 1964 and 1969, Sir Geoffrey Ingram Taylor produced the beginnings of a theoretical foundation of electrospinning by mathematically modeling the shape of the (Taylor) cone formed by the fluid droplet under the effect of an electric field [71–72]. In the early 1990s, several research groups (such as Reneker) demonstrated electrospun nanofibers. Since 1995, the number of publications about electrospinning has been increasing exponentially every year [69].

### 1.3.1.5 2 ELECTROSPINNING PROCESS

Electrospinning process can be explained in five significant steps including the following [48, 73–75]:

1. *Charging of the polymer fluid*: The syringe is filled with a polymer solution, the polymer solution is charged with a very high potential around 10–30 kV. The nature of the fluid and polarity of the applied potential free electrons, ions, or ion pairs are generated as the charge carriers form an electrical double layer. This charging induction is suitable for conducting fluid, but for nonconducting fluid charge directly injected into the fluid by the application of electrostatic field.
2. *Formation of the cone jet (Taylor cone)*: The polarity of the fluid depends on the voltage generator. The repulsion between the sim-

ilar charges at the free electrical double-layer works against the surface tension and fluid elasticity in the polymer solution to deform the droplet into a conical-shaped structure, that is known as a Taylor cone. Beyond a critical charge density Taylor cone becomes unstable and a jet of fluid is ejected from the tip of the cone.

3. *Thinning of the jet in the presence of an electric field:* The jet travels a path to the ground; this fluid jet forms a slender continuous liquid filament. The charged fluid is accelerated in the presence of an electrical field. This region of fluid is generally linear and thin.
4. *Instability of the jet:* Fluid elements accelerated under electric field and thus stretched and succumbed to one or more fluid instabilities that distort as they grow following many spiral and distort the path before collected on the collector electrode. This region of instability is also known as whipping region.
5. *Collection of the jet:* Charged electrospun fibers travel downfield until its impact with a lower potential collector plate. The orientation of the collector affects the alignment of the fibers. Different types of collector also affect the morphology and the properties of producing nanofiber. Different types of collectors are used—rotating drum collector, moving belt collector, rotating wheel with bevelled edge, multifilament thread, parallel bars, simple mesh collector, and so on.

### 1.3.1.5 3 ELECTROSPINNING SETUPS

Electrospinning is conducted at room temperature with atmospheric conditions. The typical setup of electrospinning apparatus is shown in Figure 1.1. Basically, an electrospinning system consists of three major components: a high-voltage power supply, a spinneret (such as a pipette tip), and a grounded collecting plate (usually a metal screen, plate, or rotating mandrel) and utilizes a high-voltage source to inject charge of a certain polarity into a polymer solution or melt, which is then accelerated toward a collector of opposite polarity [73, 76–77]. Most of the polymers are dissolved in some solvents before electrospinning, and when it completely dissolves, forms polymer solution. The polymer fluid is then introduced into the capillary tube

for electrospinning. However, some polymers may emit unpleasant or even harmful smells; therefore, the processes should be conducted within chambers having a ventilation system. In the electrospinning process, a polymer solution held by its surface tension at the end of a capillary tube is subjected to an electric field and an electric charge is induced on the liquid surface due to this electric field. When the electric field applied reaches a critical value, the repulsive electrical forces overcome the surface tension forces. Eventually, a charged jet of the solution is ejected from the tip of the Taylor cone and an unstable and a rapid whipping of the jet occurs in the space between the capillary tip and collector, which leads to evaporation of the solvent, leaving a polymer behind. The jet is only stable at the tip of the spinneret and after that instability starts. Thus, the electrospinning process offers a simplified technique for fiber formation [50, 73, 78–79].

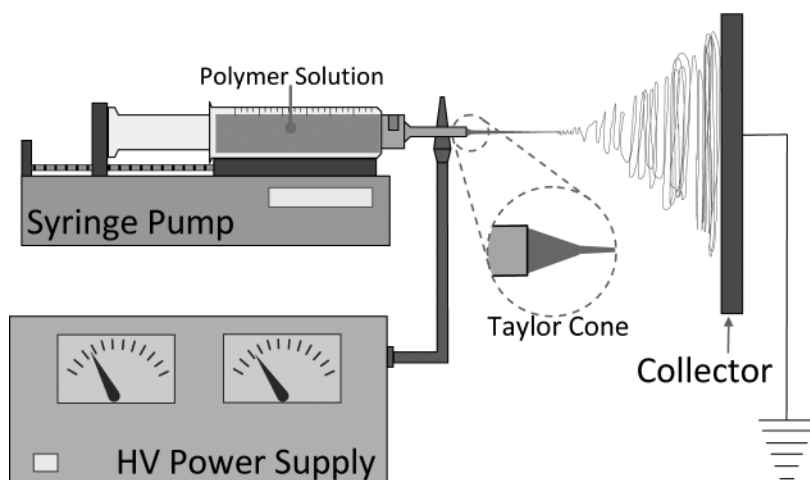


**FIGURE 1.1** Scheme of a conventional electrospinning set-up.

#### 1.3.1.5.4 THE EFFECTIVE PARAMETERS ON ELECTROSPINNING

The electrospinning process is generally governed by many parameters that can be classified broadly into solution parameters, process parameters,

and ambient parameters. Each of these parameters significantly affects the fiber morphology obtained as a result of electrospinning; and by proper manipulation of these parameters, we can get nanofibers of desired morphology and diameters. These effective parameters are sorted as below [63, 67, 73, 76]: (a) Polymer solution parameters that includes molecular weight and solution viscosity, surface tension, solution conductivity, and dielectric effect of solvent and (b) processing parameters that include voltage, feed rate, temperature, effect of collector, and the diameter of the orifice of the needle.

### **(a) Polymer solution parameters**

#### **(1) Molecular weight and solution viscosity**

The higher the molecular weight of the polymer increases molecular entanglement in the solution, the higher the increase in viscosity. The electrospun jet eject with high viscosity during it is stretched to a collector electrode leading to formation of continuous fiber with higher diameter, but very high viscosity makes difficult to pump the solution and also lead to the drying of the solution at the needle tip. As a very low viscosity lead in bead formation in the resultant electrospun fiber; therefore, the molecular weight and viscosity should be acceptable to form nanofiber [48, 80].

#### **(2) Surface tension**

Lower viscosity leads to decrease in surface tension resulting bead formation along the fiber length because the surface area is decreased, but at the higher viscosity effect of surface tension is nullified because of the uniform distribution of the polymer solution over the entangled polymer molecules. Therefore, lower surface tension is required to obtain smooth fiber and lower surface tension can be achieved by adding of surfactants in polymer solution [80–81].

#### **(3) Solution conductivity**

Higher conductivity of the solution followed a higher charge distribution on the electrospinning jet which leads to increase in stretching of the solution during fiber formation. Increased conductivity of the polymer solution lowers the critical voltage for the electrospinning. Increased charge leads to the higher bending instability leading to the higher deposition area of the fiber being formed, as a result jet path is increased and finer fiber



is formed. Solution conductivity can be increased by the addition of salt or polyelectrolyte or increased by the addition of drugs and proteins that dissociate into ions when dissolved in the solvent formation of smaller diameter fiber [67, 80].

#### **4) Dielectric effect of solvent**

Higher the dielectric property of the solution lesser is the chance of bead formation and smaller is the diameter of electrospun fiber. As the dielectric property is increased, there is increase in the bending instability of the jet and the deposition area of the fiber is increased. As jet path length is increased fine fiber deposit on the collector [67, 80].

### **(b) Processing condition parameters**

#### **(1) Voltage**

Taylor cone stability depends on the applied voltage; at higher voltage, greater amount of charge causes the jet to accelerate faster leading to smaller and unstable Taylor cone. Higher voltage leads to greater stretching of the solution due to fiber with small diameter formed. At lower voltage, the flight time of the fiber to a collector plate increases that led to the formation of fine fibers. There is greater tendency to bead formation at high voltage because of increased instability of the Taylor cone, and these beads join to form thick diameter fibers. It is observed that the better crystallinity in the fiber obtained at higher voltage. Instead of DC if AC voltage is provided for electrospinning, it forms thicker fibers [48, 80].

#### **(2) Feed rate**

As the feed rate is increased, there is an increase in the fiber diameter because greater volume of solution is drawn from the needle tip [80].

#### **3) Temperature**

At high temperature, the viscosity of the solution is decreased, and there is increase in higher evaporation rate that allows greater stretching of the solution and a uniform fiber is formed [82].

#### 4) Effect of collector

In electrospinning, collector material should be conductive. The collector is grounded to create stable potential difference between needle and collector. A nonconducting material collector reduces the amount of fiber being deposited with lower packing density. But in case of conducting collector, there is accumulation of closely packed fibers with higher packing density. Porous collector yields fibers with lower packing density as compared with nonporous collector plate. In porous collector plate, the surface area is increased so residual solvent molecules gets evaporated fast as compared with nonporous. Rotating collector is useful in getting dry fibers as it provides more time to the solvents to evaporate. It also increases fibermorphology [83]. The specific hat target with proper parameters has a uniform surface electric field distribution, the target can collect the fiber mats of uniform thickness and thinner diameters with even-size distribution[80].

#### 5) Diameter of pipette orifice

Orifice with small diameter reduces the clogging effect due to less exposure of the solution to the atmosphere and leads to the formation of fibers with smaller diameter. However, very small orifice has the disadvantage that it creates problems in extruding droplets of solution from the tip of the orifice [80].

### 1.4 DESIGN MULTIFUNCTIONAL PRODUCT BY NANOSTRUCTURES

The largest variety of efficient and elegant multifunctional materials is seen in natural biological systems, which occur sometimes in the simple geometrical forms in human-made materials. The multifunctionality of a material could be achieved by designing the material from the micro- to macroscales (bottom up design approach), mimicking the structural formations created by nature [84]. Biological materials present around us have a large number of ingenious solutions and serve as a source of inspiration. There are different ways of producing multifunctional materials that depend largely on whether these materials are structural composites, smart materials, or nanostructured materials. The nanostructure materials are most challenging and innovative processes, introducing, in the manu-

facturing, a new approaches such as self-assembly and self-replication. For biomaterials involved in surface-interface-related processes, common geometries involve capillaries, dendrites, hair, or fin-like attachments supported on larger substrates. It may be useful to incorporate similar hierarchical structures in the design and fabrication of multifunctional synthetic products that include surface sensitive functions such as sensing, reactivity, charge storage, transport property, or stress transfer. Significant effort is being directed to fabricate and understand materials that involve multiple-length scales and functionalities. Porous fibrous structures can behave like lightweight solids providing significantly higher surface area compared to compact ones. Depending on what is attached on their surfaces, or what matrix is infiltrated in them, these core structures can be envisioned in a wide variety of surface active components or net-shape composites. If nanoelements can be attached in the pores, the surface area within the given space can be increased by several orders of magnitude, thereby increasing the potency of any desired surface functionality. Recent developments in electrospinning have made these possible, thanks to a coelectrospinning polymer suspension [85]. This opens up the possibility of taking a functional material of any shape and size, and attaching nanoelements on them for added surface functionality. The fast-growing nanotechnology with modern computational/experimental methods gives the possibility to design multifunctional materials and products in human surroundings. Smart clothing, portable fuel cells, and medical devices are some of them. Research in nanotechnology began with applications outside of everyday life and is based on discoveries in physics and chemistry. The reason for that is need to understand the physical and chemical properties of molecules and nanostructures in order to control them. For example, nanoscale manipulation results in new functionalities for textile structures, including self-cleaning, sensing, actuating, and communicating. Development of precisely controlled or programmable medical nanomachines and nanorobots is great promise for nanomedicine. Once nanomachines are available, the ultimate dream of every medical man becomes reality. The miniaturization of instruments on micro- and nanodimensions promises to make our future lives safer with more humanity. A new approach in material synthesis is a computational-based material development. It is based on multiscale material and process modeling spanning, on a large spectrum of time as well as on length scales. Multiscale materials design means to design materials from a molecular scale up to a macroscale. The ability to manipulate at

atomic and molecular level is also creating materials and structures that have unique functionalities and characteristics. Therefore it will be and revolutionizing next-generation technology ranging from structural materials to nanoelectro-mechanical systems (NEMs), for medicine and bioengineering applications. Recent research development in nanomaterials has been progressing at a tremendous speed for it can totally change the ways in which materials can be made with unusual properties. Such research includes the synthetic of nanomaterials, manufacturing processes, in terms of the controls of their nanostructural and geometrical properties, mouldability, and mixability with other matrix for nanocomposites. The cost of designing and producing a novel multifunctional material can be high and the risk of investment to be significant [12, 22].

Computational materials research that relies on multiscale modeling has the potential to significantly reduce development costs of new nanostructured materials for demanding applications by bringing physical and microstructural information into the realm of the design engineer. As there are various potential applications of nanotechnology in design multifunctional product, only some of the well-known properties come from by nanotreatment are critically highlighted [12, 22, 30]. This section reviews current research in nanotechnology application of the electrospinning nanofiber, from fiber production, and development to end uses as multifunctional nanostructure device and product. The electrospinning phenomena are described from experimental viewpoint to its simulation as multiscale problem.

## **1.4.1 THE MULTIFUNCTIONAL MATERIALS AND PRODUCTS**

### **1.4.1.1 RESPONSIVE NANOPARTICLES**

There are several directions in the research and development of the responsive nanoparticle (RNP) applications (Figure 1.2). Development of particles that respond by changing stability of colloidal dispersions is the first direction. Stimuli-responsive emulsions and foams could be very attractive for various technologies in coating industries, cosmetic, and personal care. The RNPs compete with surfactants; and hence, the costs for the particle production will play a key role. The main challenge is the development of robust and simple methods for the synthesis of RNPs

from inexpensive colloidal particles and suspensions. That is indeed not a simple job since most of commercially available NPs are more expensive than surfactants. Another important application of RNPs for tunable colloidal stability of the particle suspensions is a very broad area of biosensors [86–87].

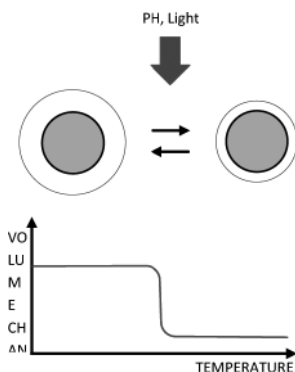


**FIGURE 1.2** Stimuli-responsive nanoparticles.

The second direction is stimuli-responsive capsules that can release the cargo upon external stimuli. The capsules are interesting for biomedical applications (drugs delivery agents) and for composite materials (release of chemicals for self-healing). The most challenging task in many cases is to engineering systems capable to work with demanded stimuli. It is not a simple job for many biomedical applications where signalling biomolecules are present in very small concentrations and a range of changes of many properties is limited by physiological conditions. A well-known challenge is related to the acceptable size production of capsules. Many medical applications need capsules less than 50 nm in diameter. Fabrication of capsules with a narrow pore-size distribution and tunable sizes could dramatically improve the mass transport control [86, 88].

A hierarchically organized multicompart RNP are in the focus. These particles could respond to weak signals, multiple signals, and could demonstrate a multiple response. They can perform logical operations with multiple signals, store energy, absorb and consume chemicals, and synthesize and release chemicals. In other words, they could operate as an autonomous intelligent minidevice. The development of such RNPs can be considered as a part of biomimetics inspired by living cells or logic

extension of the bottom up approach in nanotechnology. The development of the intelligent RNPs faces numerous challenges related to the coupling of many functional building blocks in a single hierarchically structured RNP. These particles could find applications for intelligent drug delivery, removal of toxic substances, diagnostics in medicine, intelligent catalysis, microreactors for chemical synthesis and biotechnology, new generation of smart products for personal use, and others [88–89].

#### 1.4.1.2 NANOCOATINGS

In general, the coating's thickness is at least an order of magnitude lower than the size of the geometry to be coated. The coating's thickness less than 10 nm is called nanocoating. Nanocoatings are materials that are produced by shrinking the material at the molecular level to form a denser product. Nanostructure coatings have an excellent toughness, good corrosion resistance, wear, and adhesion properties. These coatings can be used to repair component parts instead of replacing them, resulting in significant reductions in maintenance costs. In addition, the nanostructure coatings will extend the service life of the component due to the improved properties over conventional coatings [90–91].

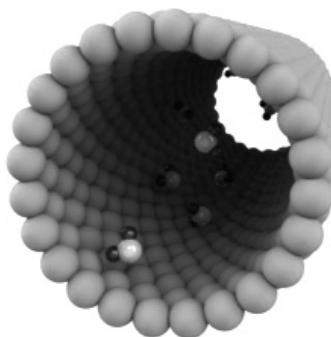


**FIGURE 1.3** Nanocoatings.

#### 1.4.1.3 FIBROUS NANOSTRUCTURE

The nanofibers are basic building block for plants and animals. From the structural viewpoint, a uniaxial structure is able to transmit forces along

its length and reducing required mass of materials. Nanofibers serve as another platform for multifunctional hierarchical example. The successful design concepts of nature, the nanofiber, become an attractive basic building component in the construction of hierarchically organized nanostructures. To follow nature's design, a process that is able to fabricate nanofiber from a variety of materials and mixtures becomes a prerequisite [92–93].

Control of the nanofibers arrangement is also necessary to optimize structural requirements. Finally, incorporation of other components into the nanofibers is required to form a complex, hierarchically organized composite. A nanofiber fabrication technique known as electrospinning process has the potential to play a vital role in the construction of a multilevel nanostructure [94]. In this chapter, we will introduce electrospinning as a potential technology for use as a platform for multifunctional, hierarchically organized nanostructures. Electrospinning is a method of producing superfine fibers with diameters ranging from 10 nm to 100 nm. Electrospinning occurs when the electrical forces at the surface of a polymer solution overcome the surface tension and cause an electrically charged jet of polymer solution to be ejected. A schematic drawing of the electrospinning process is shown in Figure 1.3. The electrically charged jet undergoes a series of electrically induced instabilities during its passage to the collection surface, which results in complicated stretching and looping of the jet [50, 60]. This stretching process is accompanied by the rapid evaporation of the solvent molecules, further reducing the jet diameter. Dry fibers are accumulated on the surface of the collector, resulting in a nonwoven mesh of nanofibers.

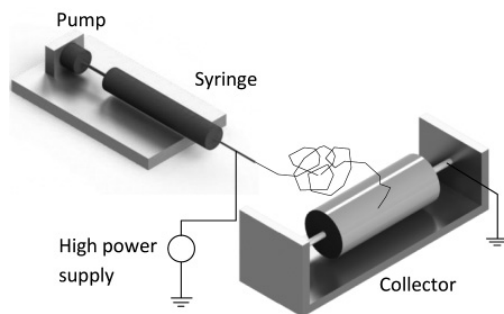


**FIGURE 1.4** The electrospinning process.

Basically, an electrospinning system consists of three major components: a high-voltage power supply, an emitter (e.g., a syringe), and a grounded collecting plate (usually a metal screen, plate, or rotating mandrel). There are a wide range of polymers that used in electrospinning and are able to form fine nanofibers within the submicron range and used for varied applications. Electrospun nanofibers have been reported as being from various synthetic polymers, natural polymers or a blend of both including proteins, nucleic acids [74]. The electrospinning process is solely governed by many parameters, classified broadly into rheological, processing, and ambient parameters. Rheological parameters include viscosity, conductivity, molecular weight, and surface tension; whereas process parameters include applied electric field, tip to collector distance, and flow rate. Each of these parameters significantly affects the fibers morphology obtained as a result of electrospinning, and by proper manipulation of these parameters we can get nanofibers fabrics of desired structure and properties on multiple material scale (Figure 1.5).

Among these variables, ambient parameters encompass the humidity and temperature of the surroundings that play a significant role in determining the morphology and topology of electrospun fabrics. Nanofibrous assemblies such as nonwoven fibrous sheet, aligned fibrous fabric, continuous yarn, and 3D structure have been fabricated using electrospinning [51]. Physical characteristics of the electrospun nanofibers can also be manipulated by selecting the electrospinning conditions and solution. Structure organization on a few hierarchical levels (see Figure 1.4) has been developed using electrospinning. Such hierarchy and multifunctionality potential will be described in the sections that follow. Finally, we will describe how electrospun multifunctional, hierarchically organized nanostructure can be used in applications such as healthcare, defence and security, and environmental.

The slender-body approximation is widely used in electrospinning analysis of common fluids [51]. The presence of nanoelements (nanoparticles, carbon nanotube, clay) in suspension jet complicate replacement 3D axisymmetric with 1D equivalent jet problem under solid–fluid interaction force on nanolevel domain. The applied electric field induced dipole moment, while torque on the dipole rotate and align the nanoelement with electric field. The theories developed to describe the behavior of the suspension jet fall (Figure 1.6) into two levels: macroscopic and microscopic. The macroscopic-governing equations of the electrospinning are equation



of continuity, conservation of the charge, balance of momentum, and electric field equation. Conservation of mass for the jet requires that [61, 95].

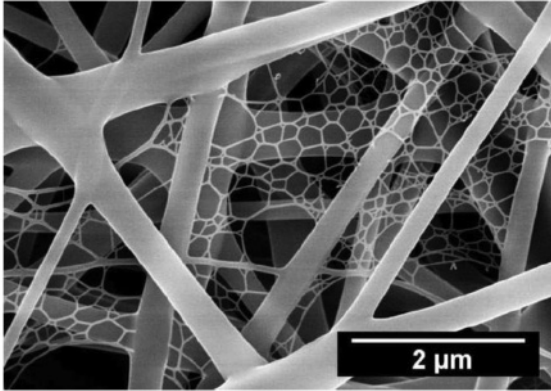


FIGURE 1.5 Multiscale electrospun fabric.

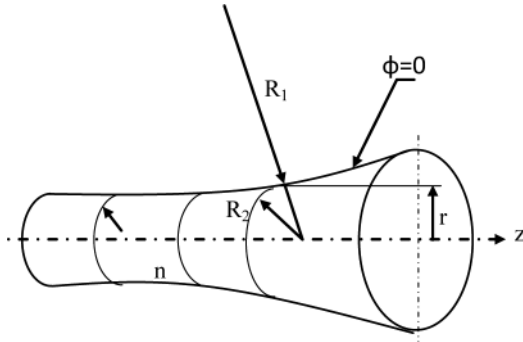


FIGURE 1.6 Geometry of the jet flow.

For polymer suspension stress tensor  $\tau_{ij}$  come from polymeric  $\hat{\tau}_{ij}$  and solvent contribution tensor via constitutive equation:

$$\tau_v = \hat{\tau}_v + n_s \cdot \dot{\gamma}_v \tag{1.4.1}$$

where  $\eta_s$  is solvent viscosity and  $\gamma_{ij}$  strain rate tensor. The polymer contribution tensor  $\hat{\tau}_{ij}$  depends on microscopic models of the suspension. Microscopic approach represents the microstructural features of material by means of a large number of micromechanical elements (beads, platelet,

rods), obeying stochastic differential equations. The evolution equations of the microelements arise from a balance of momentum on the elementary level. For example, rheological behavior of the dilute suspension of the carbon nanotubes (CNTs) in polymer matrix can be described as FENE dumbbell model [96].

$$\lambda \langle Q \cdot Q \rangle^\nabla = \delta_v - \frac{c \langle Q \cdot Q \rangle}{1 - \text{tr} \langle Q \cdot Q \rangle / b_{\text{max}}} \quad (1.4.2)$$

where  $\langle Q \cdot Q \rangle$  is the suspension configuration tensor (see Figure 1.7),  $c$  is a spring constant, and  $b_{\text{max}}$  is maximum CNT extensibility. Subscript  $\nabla$  represent the upper convected derivative, and  $\lambda$  denote a relaxation time. The polymeric stress can be obtained from the following relation:

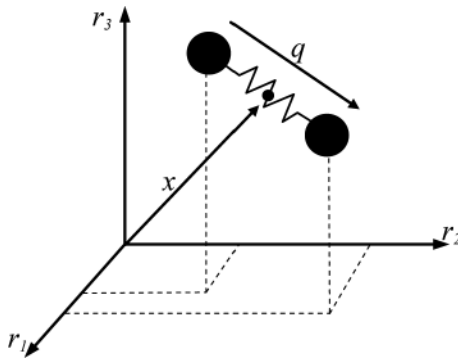


FIGURE 1.7 FENE dumbbell model.

$$\frac{\hat{\tau}_v}{nkT} = \delta_v - \frac{c \langle Q \cdot Q \rangle}{1 - \text{tr} \langle Q \cdot Q \rangle / b_{\text{max}}} \quad (1.4.3)$$

where  $k$  is Boltzmann's constant,  $T$  is temperature, and  $n$  is dumbbells density. Orientation probability distribution function  $\psi$  of the dumbbell vector  $Q$  can be described by the Fokker–Planck equation, neglecting rotary diffusivity.

$$\frac{\partial \psi}{\partial t} + \frac{\partial}{\partial Q} (\psi \cdot Q) = 0 \quad (1.4.4)$$

Solution equations (1.4.3) and (1.4.4), with supposition that flow in orifice is Hamel flow [97], give value orientation probability distribution function  $\psi$  along streamline of the jet. Rotation motion of a nanoelement (e.g., CNTs) in a Newtonian flow can be described as short fiber suspension model as another rheological model [8].

$$\frac{dp}{dt} = \frac{1}{2} \omega_v P_i + \frac{1}{2} \Theta \left[ \frac{d\gamma_v}{dt} P_j - \frac{d\gamma_{kl}}{dt} P_k P_t P_l \right] - D_r \frac{1}{\psi} \frac{\partial \psi}{\partial t} \quad (1.4.5)$$

where  $p$  is a unit vector in nanoelement axis direction,  $\omega_{ij}$  is the rotation rate tensor,  $\gamma_{ij}$  is the deformation tensor,  $D_r$  is the rotary diffusivity, and  $\theta$  is shape factor. Microscopic models for evolution of suspension microstructure can be coupled to macroscopic transport equations of mass and momentum to yield micro–macro multiscale flow models. The presence of the CNTs in the solution contributes to new form of instability with influences on the formation of the electrospun mat. The high strain rate on the nanoscale with complicated microstructure requires innovative research approach from the computational modeling viewpoint [98].

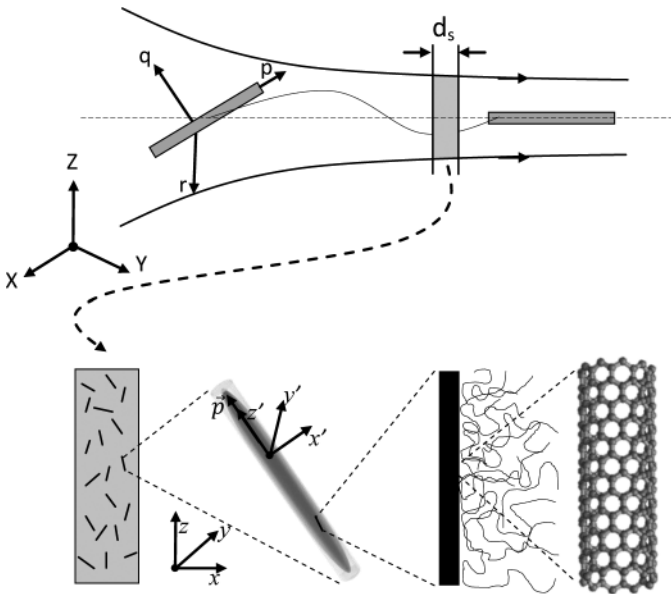


**FIGURE 1.8** The CNTs alignment in jet flow.

By the illustrated multiscale treatment (Figure 1.8), the CNT suspension in the jet, one time as short flexible cylinder in solution (microscale), and second time as coarse grain system with polymer chain particles and CNT(nanoscale level).

## 1.5 MULTIFUNCTIONAL NANOFIBER-BASED STRUCTURE

The variety of materials and fibrous structures that can be electrospun allow for the incorporation and optimization of various functions to the nanofiber, either during spinning or through postspinning modifications. A schematic of the multilevel organization of an electrospun fiber based composite is shown in Figure 1.9.

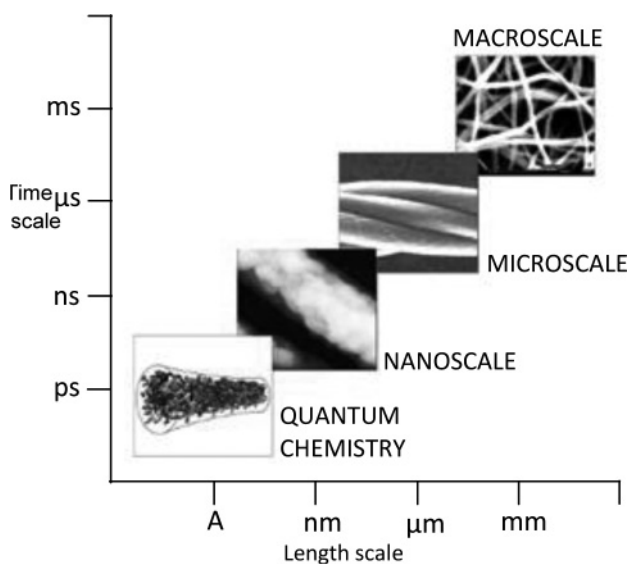


**FIGURE 1.9** Multiscale electrospun fabrics.

Based on current technology, at least four different levels of organization can be put together to form a nanofiber-based hierarchically organized structure. At the first level, nanoparticles or a second polymer can be mixed into the primary polymer solution and electrospun to form composite nanofiber. Using a dual-orifice spinneret design, a second layer of material can be coated over an inner core material during electrospinning

to give rise to the second-level organization. Two solution reservoirs, one leading to the inner orifice and the other to the outer orifice will extrude the solutions simultaneously. Otherwise, other conditions for electrospinning remain the same. Rapid evaporation of the solvents during the spinning process reduces mixing of the two solutions, thereby forming core-shell nanofiber. At the same level, various surface coating or functionalization techniques may be used to introduce additional property to the fabricated nanofiber surface. Chemical functionality is a vital component in advance multifunctional composite material to detect and respond to changes in its environment. Thus, various surface modifications techniques have been used to construct the preferred arrangement of chemically active molecules on the surface with the nanofiber as a supporting base. The third-level organization will see the fibers oriented and organized to optimize its performance. A multilayered nanofiber membrane or mixed materials nanofibers membrane can be fabricated *in situ* through selective spinning or using a multiple orifice spinneret design, respectively. Finally, the nanofibrous assembly may be embedded within a matrix to give the fourth-level organization. The resultant structure will have various properties and functionality due its hierarchical organization. Nanofiber structure at various levels have been constructed and tested for various applications and will be covered in the following sections. To follow surface functionality and modification, jet flow must be solved on multiple scale level. All above scale (nanoscale) can be solved by using particle method together with coarse-grain method on supramolecular level [50–51].

### **1.5.1 NANOFIBER EFFECTIVE PROPERTIES**

The effective properties of the nanofiber can be determined by homogenization procedure using representative volume element (RVE). There is need for incorporating more physical information on microscale to precisely determine material behavior model. For electrospun suspension with nanoelements (CNTs), a concentric composite cylinder embedded with a capped carbon nanotube represents RVE as shown in Figure 1.10. A carbon nanotube with a length  $2l$ , radii  $2a$  is embedded at the center of matrix materials with a radii  $R$  and length  $2L$ .

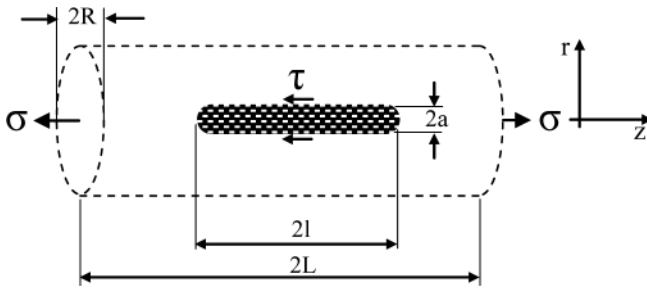


**FIGURE 1.10** The nanofiber representative volume element.

The discrete atomic nanotube structure replaced the effective (solid) fiber having the same length and outer diameter as a discrete nanotube with effective Young's nanotube modulus determined from atomic structure. The stress and strain distribution in RVE was determined using modified shear-lag model [99]. For the known stress and strain distribution under RVE, elastic effective properties quantificators can be calculated. The effective axial module  $E_{33}$ , and the transverse module  $E_{11} = E_{22}$ , can be calculated as follow:

$$\begin{aligned} E_{33} &= \frac{\langle \sigma_{zz} \rangle}{\langle \varepsilon_{zz} \rangle} \\ E_{11} &= \frac{\langle \sigma_{xx} \rangle}{\langle \varepsilon_{xx} \rangle} \end{aligned} \quad (1.4.6)$$

where denotes a volume average under volume  $V$  as defined by

$$\langle \Xi \rangle = \frac{1}{V} \int_V \Xi(x, y, z) \cdot dV. \quad (1.4.7)$$

The three-phase concentric cylindrical shell model has been proposed to predict effective modulus of nanotube reinforced nanofibers. The modulus of nanofiber depends strongly on the thickness of the interphase and CNTs diameter [12].

### 1.5.2 NETWORK MACROSCOPIC PROPERTIES

Macroscopic properties of the multifunctional structure determine final value of the any engineering product. The major objective in the determi-

nation of macroscopic properties is the link between atomic and continuum types of modeling and simulation approaches. The multiscale method such as quasicontinuum, bridge method, coarse-grain method, and dissipative particle dynamics are some popular methods of solution [98, 100]. The main advantage of the mesoscopic model is its higher computational efficiency than the molecular modeling without a loss of detailed properties at molecular level. Peridynamic modeling of fibrous network is another promising method, which allows damage, fracture, and long-range forces to be treated as natural components of the deformation of materials [101]. In the first stage, effective fiber properties are determined by homogenization procedure; whereas in the second stage, the point-bonded stochastic fibrous network at mesoscale is replaced by continuum plane stress model. Effective mechanical properties of nanofiber sheets at the macroscale level can be determined using the 2D Timoshenko beam network (figure 1.11). The critical parameters are the mean number of crossings per nanofiber, total nanofiber crossing in sheet and mean segment length [102]. Let us first consider a general planar fiber network characterized by fibre concentration  $n$  and fibre angular and length distribution  $\psi(\phi, l)$ , where  $\phi$  and  $l$  are fiber orientation angle and fiber length, respectively. The fibre radius  $r$  is considered uniform and the fibre concentration  $n$  is defined as the number of fiber per unite area.

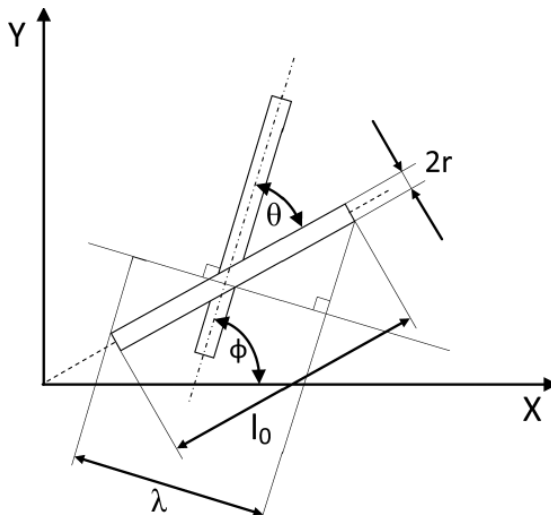


**FIGURE 1.11** The fiber contact analysis.

The Poisson probability distribution can be applied to define the fiber segment length distribution for electrospun fabrics, a portion of the fiber between two neighboring contacts:

$$f(\ell) = \frac{1}{\bar{\ell}} \exp(-\ell/\bar{\ell}) \quad (1.4.8)$$

where  $\bar{\ell}$  is the mean segment length. The total number fiber segments  $N$  in the rectangular region  $b \times h$ :

$$\bar{N} = \{n \cdot \ell_0 (\langle \lambda \rangle + 2r) - 1\} \cdot n \cdot b \cdot h \quad (1.4.9)$$

With

$$\langle \lambda \rangle = \int_0^\phi \int_0^\infty \psi(\theta, \ell) \cdot \lambda(\theta) \cdot d\ell \cdot d\theta \quad (1.4.10)$$

where the dangled segments at fiber ends have been excluded. The fiber network will be deformed in several ways. The strain energy in fiber segments comes from bending, stretching, and shearing modes of deformation can be calculated as follows (see Figure 1.12)

$$\begin{aligned} U = & N \cdot \ell_0 \cdot b \cdot h \frac{1}{2} \iint \frac{E \cdot A}{\ell} \varepsilon_{xx}^2 \cdot \psi(\varphi, \ell) \cdot \ell \cdot d\ell \cdot d\varphi \\ & + n \cdot \ell_0 \cdot \{ (\langle \lambda \rangle + 2r) - 1 \} \cdot b \cdot h \cdot \frac{1}{2} \left\{ \iint \frac{G \cdot A}{\ell} \cdot \gamma_{xy}^2 \cdot \psi(\varphi, \ell) \cdot \ell \cdot d\ell \cdot d\varphi \right. \\ & \left. + \iint \frac{3 \cdot E \cdot I}{\ell^3} \gamma_{xy}^2 \cdot \psi(\varphi, \ell) \cdot \ell \cdot d\ell \cdot d\varphi \right\} \end{aligned} \quad (1.4.11)$$

where  $A$  and  $I$  are beam cross-section area and moment of inertia, respectively. The first term on right-hand side is stretching mode, whereas the second and last terms are shear-bending modes, respectively.



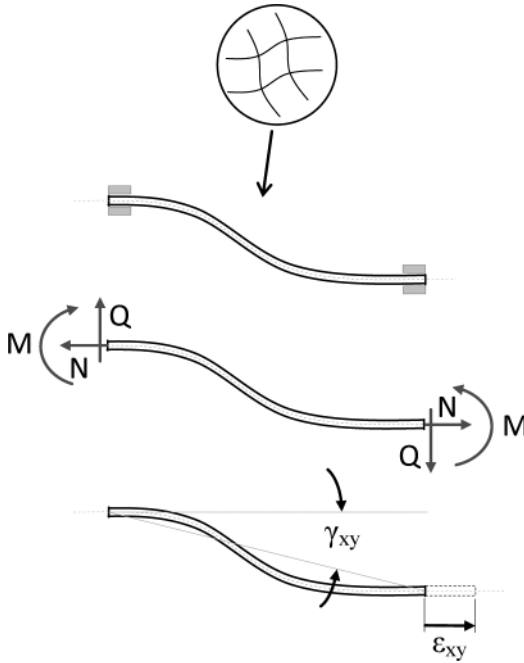


**FIGURE 1.12** Fiber network 2D model.

The effective material constants for fiber network can be determined using homogenization procedure concept for fiber network. The strain energy fiber network for representative volume element is equal to strain energy continuum element with effective material constant. The strain energy of the representative volume element under plane stress conditions are as follows:

$$U = \frac{1}{2} \cdot \langle \epsilon_v \rangle \cdot C_{vkl} \langle \epsilon_{kl} \rangle \cdot V \tag{1.4.12}$$

where is  $V$ .  $b$ .  $h$ .  $2$ .  $r$  representative volume element,  $C_{ijkl}$  are effective elasticity tensor. The square bracket  $\langle \rangle$  means macroscopic strain value. Microscopic deformation tensor was assume of a fiber segments  $\epsilon_{ij}$  is compatible with effective macroscopic strain  $\langle \epsilon_{ij} \rangle$  of effective continuum

(affine transformation). This is bridge relations between fiber segment microstrain  $\varepsilon_{ij}$  and macroscopic strain  $\langle \varepsilon_{ij} \rangle$  in the effective medium. Properties of this nanofibrous structure on the macro scale depend on the 3D joint morphology. The joints can be modeled as contact torsional elements with spring and dashpot [102]. The elastic energy of the whole random fiber network can be calculated numerically, from the local deformation state of the each segment by finite element method [103]. The elastic energy of the network is then the sum of the elastic energies of all segments. We consider here tensile stress, and the fibers are rigidly bonded to each other at every fiber–fiber crossing points. To mimic the microstructure of electrospun mats, we generated fibrous structures with fibers positioned in horizontal planes, and stacked the planes on top of one another to form a 2D or 3D structure. The representative volume element dimensions are considered to be an input parameter that can be used among other parameters to control the solid volume fraction of the structure, density number of fiber in the simulations. The number of intersections/unit area and mean lengths are obtained from image analysis of electrospun sheets. For the random point field, the stochastic fiber network was generated. Using polar coordinates and having the centerline equation of each fiber, the relevant parameters confined in the simulation box is obtained. The procedure is repeated until reaching the desired parameters is achieved [22, 95, 104]. The nonload-bearing fiber segments were removed and trimmed to keep dimensions  $b \times h$  of the representative window (see Figure 1.13).

A line representative network model is replaced by finite element beam mesh. The finite element analyses were performed in a network of 100 fibers, for some CNTs volume fractions values. Nanofibers were modeled as equivalent cylindrical beam as mentioned above. Effective mechanical properties of nanofiber sheets at the macroscale level can be determined using the 2D Timoshenko beam network.

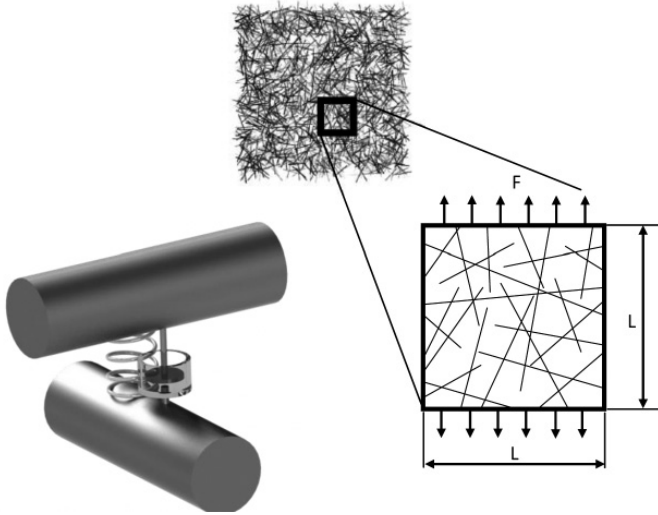


**FIGURE 1.13** Representative volume element of the network.

For a displacement-based form of beam element, the principle of virtual work is assumed valid. For a beam system, a necessary and sufficient condition for equilibrium is that the virtual work done by sum of the external forces and internal forces vanish for any virtual displacement  $\delta W = 0$ . The  $W$  is the virtual work that the work is done by imaginary or virtual displacements.

$$\delta W = \iiint_v v \delta \varepsilon_v + \iiint_v F_j \delta u_s dV + \iint_A T \delta u_l dA \quad (1.4.13)$$

where  $\varepsilon$  is the strain,  $\sigma$  is the stress,  $F$  is the body force,  $\delta u$  is the virtual displacement, and  $T$  is the traction on surface  $A$ . The symbol  $\delta$  is the variational operator designating the virtual quantity. Finite element interpolation for displacement field [15]:

$$\{u\} = [N]\{\hat{u}\} \quad (1.4.14)>$$

where is  $\{u\}$   $u$  displacement vector of arbitrary point and  $\{\hat{u}\}$  is nodal displacement point's vector.  $[N]$  is shape function matrix. After FEM procedure, the problem is reduced to the solution of the linear system of equations

$$[K_e] \cdot \{u\} = \{f\} \quad (1.4.15)$$

where  $\{u\}$  is global displacement vector,  $\{f\}$  is the global nodal force vector, and  $[K_e]$  is the global stiffness matrix. Finite element analyses were performed for computer generated network of 100 fibers. The comparison of calculated data with experimental data [99] for nanotube sheet shows some discrepancies (Figure 1.14). A rough morphological network model for the sheets can explain this on the one hand and simple joint morphology on the other hand [103].

$$\{u\} = [N]\{\hat{u}\}$$

**FIGURE 1.14** The stress–strain curve.

### 1.5.3 FLOW IN FIBER NETWORK

Electrospun nanofiber materials are becoming an integral part of many recent applications and products. Such materials are currently being used in tissue engineering, air and liquid filtration, protective clothing's, drug delivery, and many others. Permeability of fibrous media is important in many applications, therefore during the past few decades, there have been many original studies dedicated to this subject. Depending on the fiber diameter and the air thermal conditions, there are four different regimes of flow around a fiber:

- a) Continuum regime ( $K_N \leq 10^{-3}$ ),
- b) Slip-flow regime ( $10^{-3} \leq K_N \leq 0.25$ ),
- c) Transient regime ( $0.25 \leq K_N \leq 10$ ),
- d) Free molecule regime ( $N_K \geq 10$ ),

Here,  $K_N = 2\lambda / d$  is the fiber Knudson number, where  $\lambda = RT / \sqrt{2N} \pi \cdot d^2 p$  is the mean free path of gas molecules,  $d$  is fiber diameter, and  $N$  is Avogadro number. Air flow around most electrospun nanofibers is typically in the slip or transition flow regimes. In the context of air filtration, the 2D analytical work of Kuwabara [105] has long been used for predicting the permeability across fibrous filters. The analytical expression has been modified by Brown [106] to develop an expression for predicting the permeability across filter media operating in the slip flow regime. The ratio of the slip to no-slip pressure drops obtained from the simplified 2D

models may be used to modify the more realistic, and so more accurate, existing 3D permeability models in such a way that they could be used to predict the permeability of nanofiber structure. To test this supposition, for above developed 3D virtual nanofibrous structure, the Stokes flow equations solved numerically inside these virtual structures with an appropriate slip boundary condition that is developed for accounting the gas slip at fiber surface.

### 1.5.3.1 FLOW FIELD CALCULATION

A steady-state, laminar, incompressible model has been adopted for the flow regime inside our virtual media. Implemented in the Fluent code is used to solve continuity and conservation of linear momentum in the absence of inertial effects [107]:

$$\nabla \cdot v = 0 \quad (1.4.16)$$

$$\nabla P = \mu \cdot \Delta^2 v \quad (1.4.17)$$

The grid size required to mesh the gap between two fibers around their crossover point is often too small. The computational grid used for computational fluid dynamics (CFD) simulations needs to be fine enough to resolve the flow field in the narrow gaps, and at the same time coarse enough to cover the whole domain without requiring infinite computational power. Permeability of a fibrous material is often presented as a function of fiber radius,  $r$ , and solid volume fraction  $\alpha$ , of the medium. Here, we use the continuum regime analytical expressions of Jackson and James [108], developed for 3D isotropic fibrous structures given as follows:

$$\frac{k}{r^2} = \frac{3r^2}{20a} [-\ell n(\alpha) - 0.931] \quad (1.4.18)$$

Brown [106] has proposed an expression for the pressure drop across a fibrous medium based on the 2D cell model of Kuwabara[105] with the slip boundary condition:

$$\Delta P_{SLIP} = \frac{4\mu\alpha \cdot hV \cdot (1 + 1.996K_N)}{r^2[\hat{K} + 1.996K_N(-0.5 \cdot \ln\alpha - 0.25 + 0.25\alpha^2)]} \quad (1.4.19)$$

$$\hat{K} = -0.5 \cdot \ln\alpha - 0.25 + 0.25\alpha^2$$

where  $K^* = -0.5 \cdot \ln\alpha - 0.75 + \alpha - 0.25\alpha^2$ , Kuwabara hydrodynamic factor,  $h$  is fabric thickness, and  $V$  is velocity. As discussed in the some reference [101-108], permeability (or pressure drop) models obtained using ordered 2D fiber arrangements are known for underpredicting the permeability of a fibrous medium. To overcome this problem, if a correction factor can be derived based on the above 2D expression, and used with the realistic expressions developed for realistic 3D fibrous structures. From Eq. (1.4.19), we have for the case of no-slip boundary condition ( $K_N = 0$ ):

$$\Delta P_{NONSLIP} = \frac{4\mu\alpha \cdot hV}{r^2\hat{K}} \quad (1.4.20)$$

The correction factor is defined as follows:

$$\Xi = \frac{\Delta P_{NONSLIP}}{\Delta P_{SLIP}} \quad (1.4.21)$$

to be used in modifying the original permeability expressions of Jackson and James [109], and/or any other expression based on the no-slip boundary condition, in order to incorporate the slip effect. For instance, the modified expression of Jackson and James can be presented as follows:

$$k_z = \frac{3r^2}{20\alpha} [-\ln(\alpha) - 0.931] \cdot \Xi \quad (1.4.22)$$

Operating pressure has no influence on the pressure drop in the continuum region, whereas pressure drop in the free molecular region is linearly proportional to the operating pressure. Although there are many equations available for predicting the permeability of fibrous materials made up of coarse fibers, there are no accurate “easy-to-use” permeability expressions that can be used for nanofiber media. On Figure 1.15 are shown corrected Jackson and James data (blue line). Points on figure are CFD numerical data.

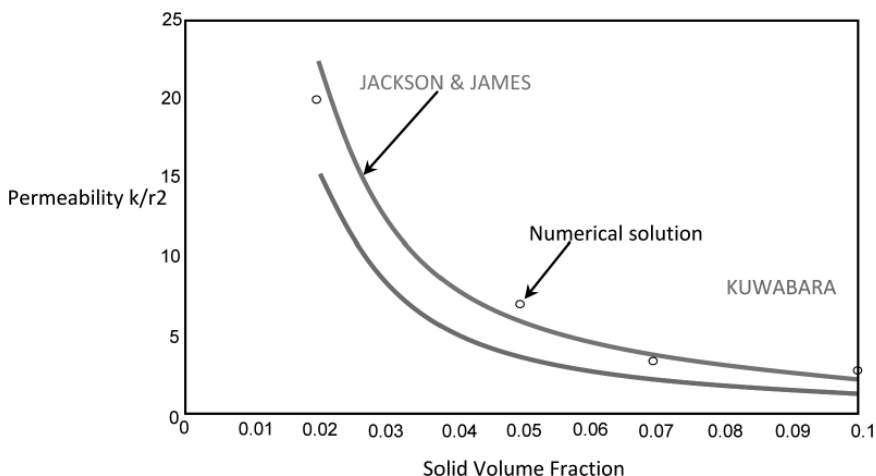


FIGURE 1.15 Permeability  $k/r^2$  dependence on solid volume fraction.

## 1.5.4 SOME ILLUSTRATIVE EXAMPLES

### 1.5.4.1 FUEL CELL EXAMPLE

Fuel cells are electrochemical devices capable of converting hydrogen or hydrogen-rich fuels into electrical current by a metal catalyst. There are many kinds of fuel cells, such as proton exchange mat (PEM) fuel cells, direct methanol fuel cells, alkaline fuel cells, and solid oxide fuel cells [110]. PEM fuel cells are the most important ones among them because of high power density and low operating temperature. Pt nanoparticle catalyst is a main component in fuel cells. The price of Pt has driven up the cell cost and limited the commercialization. Electrospun materials have been prepared as alternative catalyst with high catalytic efficiency, good durability, and affordable cost. Binary PtRh and PtRu nanowires were synthesized by electrospinning, and they had better catalytic performance than commercial nanoparticle catalyst because of the one-dimensional features [111]. Pt nanowires also showed higher catalytic activities in a polymer electrolyte membrane fuel cell [112]. Instead of direct use as catalyst, catalyst supporting material is another important application area for electrospun nanofibers. Pt clusters were electrodeposited on a carbon nanofiber mat for methanol oxidation, and the catalytic peak current of the composite catalyst reached 420 mA/mg compared with 185 mA/mg of a commercial

Pt catalyst [113]. Pt nanoparticles were immobilized on polyimide-based nanofibers using a hydrolysis process and Pt nanoparticles were also loaded on the carbon nanotube containing polyamic acid nanofibers to achieve high catalytic current with long-term stability [114]. Proton exchange mat is the essential element of PEM fuel cells and normally made of a Nafion film for proton conduction. Because pure Nafion is not suitable for electrospinning due to its low viscosity in solution, it is normally mixed with other polymers to make blend nanofibers. Blend Nafion/PEO nanofibers were embedded in an inert polymer matrix to make a proton conducting mat [115], and a high proton conductivity of 0.06–0.08 S/cm at 15 °C in water and low water swelling of 12–23 wt% at 25 °C were achieved [116].

#### 1.5.4.2 PROTECTIVE CLOTHING EXAMPLE

The development of smart nanotextiles has the potential to revolutionize the functionality of our clothing and the fabrics in our surroundings (Figure 1.16). This is made possible by such developments as new materials, fibers, and finishing; inherently conducting polymers; carbon nanotubes; an antimicrobial nanocoatings. These additional functionalities have numerous applications in healthcare, sports, military applications, fashion, and so on. Smart textiles become a critical part of the emerging area of body sensor networks incorporating sensing, actuation, control and wireless data transmission [51–52, 117].

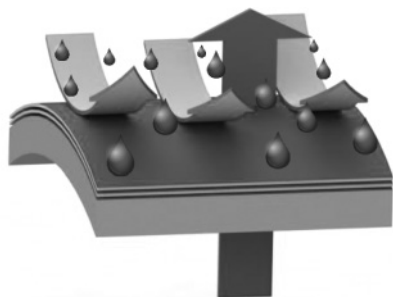


**FIGURE 1.16** Ultrathin layer for selective transport.



### 1.5.4.3 MEDICAL DEVICE

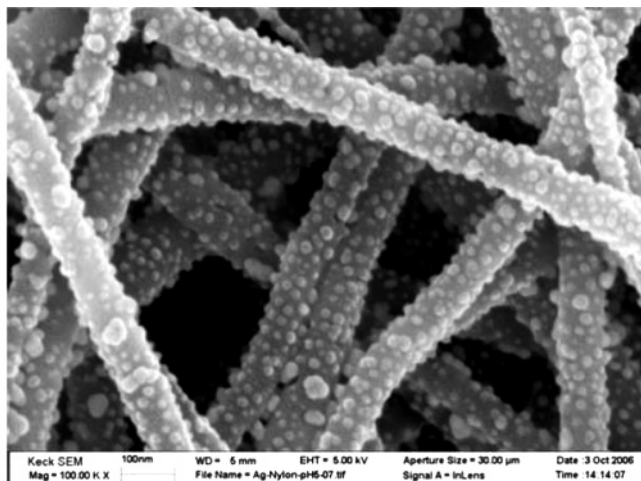


FIGURE 1.17 Cotton coated with silver.

Basic engineered nanomaterial and biotechnology products will enormously be useful in future medical applications. We know nanomedicine as the monitoring, repair, construction, and control of biological systems at the nanoscale level, using engineered nanodevices and nanostructures. The upper portion of the dress contains cotton coated with silver nanoparticles. Silver possesses (Figure 1.17) natural antibacterial qualities that are strengthened at the nanoscale, thus giving the ability to deactivate many harmful bacteria and viruses. The silver infusion also reduces the need to wash the garment, since it destroys bacteria, and the small size of the particles prevents soiling and stains [16, 118].

#### 1.5.4.3.1 DRUG DELIVERY AND RELEASE CONTROL

Controlled release is an efficient process of delivering drugs in medical therapy. It can balance the delivery kinetics, immunize the toxicity and side effects, and improve patient convenience [119]. In a controlled-release system, the active substance is loaded into a carrier or device first, and then released at a predictable rate *in vivo* when administered by an

injected or noninjected route. As a potential drug delivery carrier, electrospun nanofibers have exhibited many advantages. The drug loading is very easy to implement via electrospinning process, and the high applied voltage used in electrospinning process had little influence on the drug activity. The high specific surface area and short diffusion passage length give the nanofiber drug system higher overall release rate than the bulk material (e.g., film). The release profile can be finely controlled by modulation of nanofiber morphology, porosity, and composition.

Nanofibers for drug release systems mainly come from biodegradable polymers and hydrophilic polymers. Model drugs that have been studied include water soluble [120], poor water-soluble [121], and water insoluble drugs [122]. The release of macromolecules, such as DNA [123] and bioactive proteins from nanofibers was also investigated. In most cases, water-soluble drugs, including DNA and proteins, exhibited an early-stage burst [124]. For some applications, preventing postsurgery induced adhesion for instance, and such an early burst release will be an ideal profile because most infections occur within the first few hours after surgery. A recent study also found that when a poorly water soluble drug was loaded into PVP nanofibers [125], 84.9% of the drug can be released in the first 20 seconds when the drug-to-PVP ratio was kept as 1:4, which can be used for fast drug delivery systems. However, for a long-lasting release process, it would be essential to maintain the release at an even and stable pace, and any early burst release should be avoided. For a water insoluble drug, the drug release from hydrophobic nanofibers into buffer solution is difficult. However, when an enzyme capable of degrading nanofibers exists in the buffer solution, the drug can be released at a constant rate because of the degradation of nanofibers [122]. For example, when rifampin was encapsulated in PLA nanofibers, no drug release was detected from the nanofibers. However, when the buffer solution contained proteinase K, the drug release took place nearly in zero-order kinetics, and no early burst release happened. Similarly, initial burst release did not occur for poor water-soluble drugs, but the release from a nonbiodegradable nanofiber could follow different kinetics [126]. In another example, blending a hydrophilic but water-insoluble polymer (PEG-g-CHN) with PLGA could assist in the release of a poor water-soluble drug Ibuprofen [127]. However, when a water soluble polymer was used, the poorly soluble drug was released accompanied with dissolving of the nanofibers, leading to a low burst release [128]. The early burst release can be reduced when the drug

is encapsulated within the nanofiber matrix. When an amphiphilic block copolymer, PEG-b-PLA was added into Mefoxin/PLGA nanofibers, the cumulative amount of the released drug at earlier time points was reduced and the drug release was prolonged [129]. The reason for the reduced burst release was attributed to the encapsulation of some drug molecules within the hydrophilic block of the PEG-b-PLA. Amphiphilic block copolymer also assisted the dispersion and encapsulation of water-soluble drug into nanofibers when the polymer solution used an oleophilic solvent, such as chloroform, during electrospinning [130]. In this case, a water-in-oil emulsion can be electrospun into uniform nanofibers, and drug molecules are trapped by hydrophilic chains. The swelling of the hydrophilic chains during releasing assists the diffusion of drug from nanofibers to the buffer. Coating nanofibers with a shell could be an effective way to control the release profile.

When a thin layer of hydrophobic polymer, such as poly (p-xylylene) (PPX), was coated on PVA nanofibers loaded with bovine serum albumin (BSA)/luciferase, the early burst release of the enzyme was prevented [131]. Fluorination treatment [132] on PVA nanofibers introduced functional C-F groups and made the fiber surface hydrophobic, which dramatically decreased the initial drug burst and prolonged the total release time. The polymer shell can also be directly applied via a coaxial coelectrospinning process, and the nanofibers produced are normally named “core-sheath” bicomponent nanofibers. In this case, even a pure drug can be entrapped into nanofiber as the core, and the release profile was less dependent on the solubility of drug released [133]. A research has compared the release behavior of two drug-loaded PLLA nanofibers prepared using blend and coaxial electrospinning [134]. It was found that the blend fibers still showed an early burst release, while the threads made of core-sheath fibers provided a stable release of growth factor and other therapeutic drugs. In addition, the early burst release can also be lowered via encapsulating drugs into nanomaterial, followed by incorporating the drug-loaded nanomaterials into nanofibers. For example, halloysite nanotubes loaded with tetracycline hydrochloride were incorporated into PLGA nanofibers and showed greatly reduced initial burst release [135].

## 1.6 CONCLUDING REMARKS OF MULTIFUNCTIONAL NANOSTRUCTURE DESIGN

Electrospinning is a simple, versatile, and cost-effective technology that generates nonwoven fibers with high surface area to volume ratio, porosity, and tunable porosity. Because of these properties, this process seems to be a promising candidate for various applications especially nanostructure applications. Electrospun fibers are increasingly being used in a variety of applications, such as tissue engineering scaffolds, wound healing, drug delivery, immobilization of enzymes, as membrane in biosensors, protective clothing, cosmetics, affinity membranes, filtration applications, and so on. In summary, mother nature has always used hierarchical structures such as capillaries and dendrites to increase multifunctional of living organs. Material scientists are at beginning to use this concept and create multiscale structures where nanotubes, nanofillers can be attached to larger surfaces and subsequently functionalized. In principle, many more applications can be envisioned and created. Despite several advantages and success of electrospinning there are some critical limitations in this process such as small pore size inside the fibers. Several attempts in these directions are being made to improve the design through multilayering, inclusion of nanoelements and blending with polymers with different degradation behavior. As new architectures develop, a new wave of surface-sensitive devices related to sensing, catalysis, photovoltaic, cell scaffolding, and gas storage applications is bound to follow.

## 1.7 INTRODUCTION TO THEORETICAL STUDY OF ELECTROSPINNING PROCESS

Electrospinning is a procedure in which an electrical charge to draw very fine (typically on the micro- or nanoscale) fibers from polymer solution or molten. Electrospinning shares characteristics of both and conventional solution dry spinning of fibers. The process does not require the use of coagulation chemistry or high temperatures to produce solid threads from solution. This makes the process more efficient to produce the fibers using large and complex molecules. Recently, various polymers have been successfully electrospun into ultrafine fibers mostly in solvent solution and some in melt form [79, 136]. Optimization of the alignment and

morphology of the fibers is produced by fitting the composition of the solution and the configuration of the electrospinning apparatus such as voltage, flow rate, and and so on. As a result, the efficiency of this method can be improved [137]. Mathematical and theoretical modeling and simulating procedure will assist to offer an in-depth insight into the physical understanding of complex phenomena during electrospinning and might be very useful to manage contributing factors toward increasing production rate [75, 138].

Despite the simplicity of the electrospinning technology, industrial applications of it are still relatively rare, mainly due to the notable problems with very low fiber production rate and difficulties in controlling the process [67].

Modeling and simulation (M&S) give information about how something will act without actually testing it in real. The model is a representation of a real object or system of objects for purposes of visualizing its appearance or analyzing its behavior. Simulation is a transition from a mathematical or computational model for description of the system behavior based on sets of input parameters [104, 139]. Simulation is often the only means for accurately predicting the performance of the modeled system [140]. Using simulation is generally cheaper and safer than conducting experiments with a prototype of the final product. In addition, simulation can often be even more realistic than traditional experiments, as they allow the free configuration of environmental and operational parameters and can often be run faster than in real time. In a situation with different alternatives analysis, simulation can improve the efficiency, in particular when the necessary data to initialize can easily be obtained from operational data. Applying simulation adds decision support systems to the tool box of traditional decision support systems [141].

Simulation permits set up a coherent synthetic environment that allows for integration of systems in the early analysis phase for a virtual test environment in the final system. If managed correctly, the environment can be migrated from the development and test domain to the training and education domain in real systems under realistic constraints [142].

A collection of experimental data and their confrontation with simple physical models appears as an effective approach toward the development of practical tools for controlling and optimizing the electrospinning process. On the contrary, it is necessary to develop theoretical and numerical models of electrospinning because of demanding a different optimization

procedure for each material[143]. Utilizing a model to express the effect of electrospinning parameters will assist researchers to make an easy and systematic way of presenting the influence of variables and by means of that, the process can be controlled. In addition, it causes to predict the results under a new combination of parameters. Therefore, without conducting any experiments, one can easily estimate features of the product under unknown conditions [95].

## 1.8 STUDY OF ELECTROSPINNING JET PATH

To yield individual fibers, most, if not all of the solvents must be evaporated by the time the electrospinning jet reaches the collection plate. As a result, volatile solvents are often used to dissolve the polymer. However, clogging of the polymer may occur when the solvent evaporates before the formation of the Taylor cone during the extrusion of the solution from several needles. To maintain a stable jet while still using a volatile solvent, an effective method is to use a gas jacket around the Taylor cone through two coaxial capillary tubes. The outer tube that surrounds the inner tube will provide a controlled flow of inert gas which is saturated with the solvent used to dissolve the polymer. The inner tube is then used to deliver the polymer solution. For 10 wt% poly (L-lactic acid) (PLLA) solution in dichloromethane, electrospinning was not possible due to clogging of the needle. However, when N<sub>2</sub> gas was used to create a flowing gas jacket, a stable Taylor cone was formed and electrospinning was carried out smoothly.

### 1.8.1 THE THINNING JET (JET STABILITY)

The conical meniscus eventually gives rise to a slender jet that emerges from the apex of the meniscus and propagates downstream. Hohman et al. [60] first reported this approach for the relatively simple case of Newtonian fluids. This suggests that the shape of the thinning jet depends significantly on the evolution of the surface charge density and the local electric field. As the jet thins down and the charges relax to the surface of the jet, the charge density and local field quickly pass through a maximum, and the current due to advection of surface charge begins to dominate over that due to bulk conduction.

The crossover occurs on the length scale given by [6]:

$$L_N = \left( K^4 Q^7 \rho^3 (\ln X)^2 / 8\pi^2 E_\infty I^5 \varepsilon^{-2} \right)^{1/5} \quad (1.6.1)$$

This length scale defines the “nozzle regime” over which the transition from the meniscus to the steady jet occurs. Sufficiently far from the nozzle regime, the jet thins less rapidly and finally enters the asymptotic regime, where all forces except inertial and electrostatic forces cease to influence the jet. In this regime, the radius of the jet decreases as follows:

$$h = \left( \frac{Q^3 \rho}{2\pi^2 E_\infty I} \right)^{1/4} z^{-1/4} \quad (1.6.2)$$

Here,  $z$  is the distance along the centerline of the jet. Between the “nozzle regime” and the “asymptotic regime,” the evolution of the diameter of the thinning jet can be affected by the viscous response of the fluid. Indeed by balancing the viscous and the electrostatic terms in the force balance equation, it can be shown that the diameter of the jet decreases:

$$h = \left( \frac{6\mu Q^2}{\pi E_\infty I} \right)^{1/2} z^{-1} \quad (1.6.3)$$

In fact, the straight jet section has been studied extensively to understand the influence of viscoelastic behavior on the axisymmetric instabilities [93] and crystallization [60] and has even been used to extract extensional viscosity of polymeric fluids at very high strain rates.

For highly strain-hardening fluids, Yu et al. [144] demonstrated that the diameter of the jet decreased with a power-law exponent of  $-1/2$ , rather than  $-1/4$  or  $-1$ , as discussed earlier for Newtonian fluids. This  $-1/2$  power-law scaling for jet thinning in viscoelastic fluids has been explained in terms of a balance between electromechanical stresses acting on the surface of the jet and the viscoelastic stress associated with extensional strain hardening of the fluid. In addition, theoretical studies of viscoelastic fluids predict a change in the shape of the jet due to non-Newtonian fluid behavior. Both Yu et al. [144] and Han et al. [145] have demonstrated that substantial elastic stresses can be accumulated in the fluid as a result of the highstrain rate in the transition from the meniscus into the jetting region.

This elastic stress stabilizes the jet against external perturbations. Further downstream the rate of stretching slows down, and the longitudinal stresses relax through viscoelastic processes. The relaxation of stresses following an extensional deformation, such as those encountered in electrospinning, has been studied in isolation for viscoelastic fluids [146]. Interestingly, Yu et al. [144] also observed that, elastic behavior notwithstanding, the straight jet transitions into the whipping region when the jet diameter becomes of the order of 10 mm.

### **1.8.2 THE WHIPPING JET (JET INSTABILITY)**

While it is in principle possible to draw out the fibers of small diameter by electrospinning in the cone-jet mode alone, the jet does not typically solidify enough en route to the collector and succumbs to the effect of force imbalances that lead to one or more types of instability. These instabilities distort the jet as they grow. A family of these instabilities exists, and can be analyzed in the context of various symmetries (axisymmetric or nonaxisymmetric) of the growing perturbation to the jet.

Some of the lower modes of this instability observed in electrospinning have been discussed in a separate review [81]. The “whipping instability” occurs when the jet becomes convectively unstable and its centerline bends. In this region, small perturbations grow exponentially, and the jet is stretched out laterally. Shin et al. [62] and Fridrikh et al. [63] have demonstrated how the whipping instability can be largely responsible for the formation of solid fiber in electrospinning. This is significant, since as recently as the late 1990s, the bifurcation of the jet into two more or less equal parts (also called “splitting” or “splaying”) were thought to be the mechanism through which the diameter of the jet is reduced, leading to the fine fibers formed in electrospinning. In contrast to “splitting” or “splaying,” the appearance of secondary, smaller jets from the primary jet have been observed more frequently and *in situ* [64, 147]. These secondary jets occur when the conditions on the surface of the jet are such that perturbations in the local field, for example, due to the onset of the slight bending of the jet, is enough to overcome the surface tension forces and invoke a local jetting phenomenon.



The conditions necessary for the transition of the straight jet to the whipping jet has been discussed in the works of Ganan-Calvo [148], Yarin et al. [64], Reneker et al. [66], and Hohman et al. [60].

During this whipping instability, the surface charge repulsion, surface tension, and inertia were considered to have more influence on the jet path than Maxwell's stress, which arises due to the electric field and finite conductivity of the fluid. Using the equations reported by Hohman et al. [60] and Fridrikh et al. [63] obtained an equation for the lateral growth of the jet excursions arising from the whipping instability far from the onset and deep into the nonlinear regime. These developments have been summarized in the review article by Rutledge and Fridrikh.

The whipping instability is postulated to impose the stretch necessary to draw out the jet into fine fibers. As discussed earlier, the stretch imposed can make an elastic response in the fluid, especially if the fluid is polymeric in nature. An empirical rheological model was used to explore the consequences of nonlinear behavior of the fluid on the growth of the amplitude of the whipping instability in numerical calculations [63, 79]. There, it was observed that the elasticity of the fluid significantly reduces the amplitude of oscillation of the whipping jet. The elastic response also stabilizes the jet against the effect of surface tension. In the absence of any elasticity, the jet eventually breaks up and forms an aerosol. However, the presence of a polymer in the fluid can stop this breakup if

$$\tau / \left( \frac{\rho h^3}{\gamma} \right)^{1/2} \geq 1 \quad (1.6.4)$$

where  $\tau$  is the relaxation time of the polymer,  $\rho$  is the density of the fluid,  $h$  is a characteristic radius, and  $\gamma$  is the surface tension of the fluid.

## 1.9 ELECTROSPINNING DRAWBACKS

Electrospinning has attracted much attention both to academic research and industry application because electrospinning (1) can fabricate continuous fibers with diameters down to a few nanometers, (2) is applicable to a wide range of materials such as synthetic and natural polymers, metals as well as ceramics and composite systems, (3) and can prepare nanofibers with low cost and high yielding [47].

Despite the simplicity of the electrospinning technology, industrial applications of it are still relatively rare, mainly due to the notable problems of very low fiber production rate and difficulties in controlling the process [50, 67]. The usual feedrate for electrospinning is about 1.5ml/hr. Given a solution concentration of 0.2g/ml, the mass of nanofiber collected from a single needle after an hour is only 0.3g. In order for electrospinning to be commercially viable, it is necessary to increase the production rate of the nanofibers. To do so, multiple-spinning setup is necessary to increase the yield while at the same time maintaining the uniformity of the nanofiber mesh [48].

Optimization of the alignment and morphology of the fibers which is produced by fitting the composition of the solution and the configuration of the electrospinning apparatus such as voltage, flow rate, and so on, can be useful to improve the efficiency of this method [137]. Mathematical and theoretical modeling and simulating procedure will assist to offer an in-depth insight into the physical understanding of complex phenomena using electrospinning and might be very useful to manage contributing factors toward increasing production rate [75, 138].

At present, nanofibers have attracted the attention of researchers due to their remarkable micro and nanostructural characteristics, high surface area, small pore size, and the possibility of their producing 3D structure that enables the development of advanced materials with sophisticated applications [73].

Controlling the property, geometry, and mass production of the nanofibers is essential to comprehend quantitatively how the electrospinning process transforms the fluid solution through a millimeter diameter capillary tube into solid fibers that are four to five orders smaller in diameter [74].

As mentioned earlier, the electrospinning gives us the impression of being a very simple and easily controlled technique for the production of nanofibers. But, in reality, the process is very intricate. Thus, electrospinning is usually described as the interaction of several physical instability processes. The bending and stretching of the jet are mainly caused by the rapidly whipping which is an essential element of the process induced by these instabilities. Until now, little is known about the detailed mechanisms of the instabilities and the splaying process of the primary jet into multiple filaments. It is thought to be responsible that the electrostatic forces over-

come surface tensions of the droplet during undergoing the electrostatic field and the deposition of jets formed nanofibers [47].

Although electrospinning has been become an indispensable technique for generating functional nanostructures, many technical issues still need to be resolved. For example, it is not easy to prepare nanofibers with a same scale in diameters by electrospinning; it is still necessary to investigate systematically the correlation between the secondary structure of nanofiber and the processing parameters; the mechanical properties, photoelectric properties, and other property of single fiber should be systematically studied and optimized; the production of nanofiber is still in laboratory level, and it is extremely important to make efforts for scaled-up commercialization; nanofiber from electrospinning has a the low production rate and low mechanical strength which hindered its commercialization; in addition, another more important issue should be resolved is how to treat the solvents volatilized in the process.

Until now, lots of efforts have been put on the improvement of electrospinning installation, such as the shape of collectors, modified spinnerets, and so on. The application of multijets electrospinning provides a possibility to produce nanofibers in industrial scale. The development of equipments which can collect the poisonous solvents and the application of melt electrospinning, which would largely reduce the environment problem, create a possibility of the industrialization of electrospinning. The application of water as the solvent for electrospinning provide another approach to reduce environmental pollution, which is the main fact hindered the commercialization of electrospinning. In summary, electrospinning is an attractive and promising approach for the preparation of functional nanofibers due to its wide applicability to materials, low cost and high production rate [47].

## 1.10 MODELING THE ELECTROSPINNING PROCESS

The electrospinning process is a fluid dynamics-related problem. Controlling the property, geometry, and mass production of the nanofibers is essential to comprehend quantitatively how the electrospinning process transforms the fluid solution through a millimeter diameter capillary tube into solid fibers that are four to five orders smaller in diameter [74]. Although information on the effect of various processing parameters and

constituent material properties can be obtained experimentally, theoretical models offer in-depth scientific understanding which can be useful to clarify the affecting factors that cannot be exactly measured experimentally. Results from modeling also explained how processing parameters and fluid behavior lead to the nanofiber of appropriate properties. The term “properties” refers to basic properties (i.e., fiber diameter, surface roughness, and fiber connectivity), physical properties (i.e., stiffness, toughness, thermal conductivity, electrical resistivity, thermal expansion coefficient, and density) and specialized properties (i.e., biocompatibility, degradation curve, and for biomedical applications) [48, 73].

For example, the developed models can be used for the analysis of mechanisms of jet deposition and alignment on various collecting devices in arbitrary electric fields [149].

Various methods formulated by researchers are prompted by several applications of nanofibers. It would be sufficient to briefly describe some of these methods to observed similarities and disadvantages of these approaches. An abbreviated literature review of these models will be discussed in the sections that follow.

### **1.10.1 MODELING ASSUMPTIONS**

Just as in any other process modeling, a set of assumptions are required for the following reasons:

- a. To furnish industry-based applications whereby speed of calculation, but not accuracy, is critical
- b. To simplify, hence enabling checkpoints to be made before more detailed models can proceed
- c. For enabling the formulations to be practically traceable

The first assumption to be considered as far as electrospinning is concerned is conceptualizing the jet itself. Even though the most appropriate view of a jet flow is that of a liquid continuum, the use of nodes connected in series by certain elements that constitute rheological properties has proven successful [64, 66]. The second assumption is the fluid constitutive properties. In the discrete node model [66], the nodes are connected in series by a Maxwell unit, that is, a spring and dashpot in series, for quantifying the viscoelastic properties.

In analyzing viscoelastic models, we apply two types of elements: the dashpot element that describes the force as being in proportion to the velocity (recall friction), and the spring element which describes the force as being in proportion to elongation. One can then develop viscoelastic models using combinations of these elements. Among all possible viscoelastic models, the Maxwell model was selected by Reneker et al. [66] due to its suitability for liquid jet as well as its simplicity. Other models are either unsuitable for liquid jet or too detailed.

In the continuum models a power law can be used for describing the liquid behavior under shear flow for describing the jet flow [150]. At this juncture, it can be noted that the power law is characterized from a shear flow, whereas the jet flow in electrospinning undergoes elongational flow. This assumption will be discussed in detail in the subsequent sections.

The other assumption that should be applied in electrospinning modeling is about the coordinate system. The method for coordinate system selection in electrospinning process is similar to other process modeling, the system that best bring out the results by (i) allowing the computation to be performed in the most convenient manner and, more importantly, (ii) enabling the computation results to be accurate. In view of the linear jet portion during the initial first stage of the jet, the spherical coordinate system is eliminated. Assuming the second stage of the jet to be perfectly spiraling, due to bending of the jet, the cylindrical coordinate system would be ideal. However, experimental results have shown that the bending instability portion of the jet is not perfectly expanding spiral. Hence, the Cartesian coordinate system, which is the most common of all coordinate system, is adopted.

Depending on the processing parameters (i.e., applied voltage and volume flow rate) and the fluid properties (i.e., surface tension and viscosity) as many as 10 modes of electrohydrodynamically driven liquid jet have been identified [151]. The scope of jet modes is highly abbreviated in this chapter because most electrospinning processes that lead to nanofibers consist of only two modes, the straight jet portion, and the spiraling (or whipping) jet portion. Insofar as electrospinning process modeling is involved, the following classification indicates the considered modes or portion of the electrospinning jet.

1. Modeling the criteria for jet initiation from the droplet [Senador et al. [152]; Yarin et al.[64]

2. Modeling the straight jet portion [153–154] Spivak et al. [150, 155]
3. Modeling the entire jet [Reneker et al. [66]; Yarin et al.[156]; Hohman et al. [60–61]

### 1.10.2 CONSERVATION RELATIONS

Balance of the producing accumulation is, particularly, a basic source of quantitative models of phenomena or processes. Differential balance equations are formulated for momentum, mass, and energy through the contribution of local rates of transport expressed by the principle of Newton's, Fick's, and Fourier laws. For a description of more complex systems such as electrospinning that involved strong turbulence of the fluid flow, characterization of the product property is necessary and various balances are required [157].

The basic principle used in modeling of chemical engineering process is a concept of balance of momentum, mass and energy, which can be expressed in a general form as follows:

$$A = I + G - O - C \quad (1.8.1)$$

where

A is the accumulation built up within the system.

I is the input entering through the system surface.

G is the generation produced in system volume.

O is the output leaving through system boundary.

C is consumption used in system volume.

The form of expression depends on the level of the process phenomenon description. [157–158]

According to the electrospinning models, the jet dynamics are governed by a set of three equations representing mass, energy, and momentum conservation for the electrically charge jet [159].

**1.1.1. IN ELECTROSPINNING MODELING FOR SIMPLIFICATION OF DESCRIBING THE PROCESS, RESEARCHERS CONSIDER AN ELEMENT OF THE JET AND THE JET VARIATION VERSUS TIME IS NEGLECTED.**

**1.1.2. MASS CONSERVATION**

The concept of mass conservation is widely used in many fields such as chemistry, mechanics, and fluid dynamics. Historically, mass conservation was discovered in chemical reactions by Antoine Lavoisier in the late eighteenth century, and was of decisive importance in the progress from alchemy to the modern natural science of chemistry. The concept of matter conservation is useful and sufficiently accurate for most chemical calculations, even in modern practice [160].

The equations for the jet follow from Newton's Law and the conservation laws obey, namely, conservation of mass and conservation of charge [60].

According to the conservation of mass equation

$$\pi R^2 v = Q \quad (1.8.2)$$

$$\frac{\partial}{\partial t}(\pi R^2) + \frac{\partial}{\partial z}(\pi R^2 v) = 0 \quad (1.8.3)$$

For incompressible jets, by increasing the velocity the radius of the jet decreases. At the maximum level of the velocity, the radius of the jet reduces. The macromolecules of the polymers are compacted together closer while the jet becomes thinner as shown in Figure 1.18. When the radius of the jet reaches the minimum value and its speed becomes maximum to keep the conservation of mass equation, the jet dilates by decreasing its density which is called electrospinning dilation [161–162].

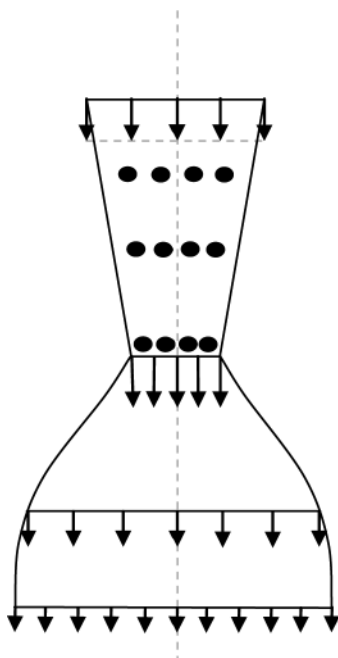


**FIGURE 1.18** Macromolecular chains are compacted during the electrospinning.

### **1.10.3 ELECTRIC CHARGE CONSERVATION**

An electric current is a flow of electric charge. Electric charge flows when there is voltage present across a conductor. In physics, charge conservation is the principle that electric charge can neither be created nor destroyed. The net quantity of electric charge, the amount of positive charge minus the amount of negative charge in the universe, is always conserved. The first written statement of the principle was by American scientist and statesman Benjamin Franklin in 1747 [163]. Charge conservation is a physical law which states that the change in the amount of electric charge in any volume of space is exactly equal to the amount of charge in a region and the flow of charge into and out of that region [164].

During the electrospinning process, the electrostatic repulsion between excess charges in the solution stretches the jet. This stretching also decreases the jet diameter that this leads to the law of charge conservation as the second governing equation [165].



In electrospinning process, the electric current that induced by electric field included two parts, conduction, and convection.

The conventional symbol for current is I:

$$I = I_{conduction} + I_{convection} \quad (1.8.4)$$

Electrical conduction is the movement of electrically charged particles through a transmission medium. The movement can form an electric current in response to an electric field. The underlying mechanism for this movement depends on the material.

$$I_{conduction} = J_{cond} \times S = KE \times \pi R^2 \quad (1.8.5)$$

$$J = \frac{I}{A(s)} \quad (1.8.6)$$

$$I = J \times S \quad (1.8.7)$$

Convection current is the flow of current with the absence of an electric field.

$$I_{convection} = J_{conv} \times S = 2\pi R(L) \times \sigma v \quad (1.8.8)$$

$$J_{conv} = \sigma v \quad (1.8.9)$$

Therefore, the total current can be calculated as:

$$\pi R^2 KE + 2\pi Rv\sigma = I \quad (1.8.10)$$

$$\frac{\partial}{\partial t}(2\pi R\sigma) + \frac{\partial}{\partial z}(\pi R^2 KE + 2\pi Rv\sigma) = 0 \quad (1.8.11)$$

### 1.10.4 MOMENTUM BALANCE

In classical mechanics, linear momentum or translational momentum is the product of the mass and velocity of an object. Like velocity, linear momentum is a vector quantity, possessing a direction as well as a magnitude:

$$P = mv \quad (1.8.12)$$

Linear momentum is also a conserved quantity, meaning that if a closed system (one that does not exchange any matter with the outside and is not acted on by outside forces) is not affected by external forces, its total linear momentum cannot change. In classical mechanics, conservation of linear momentum is implied by Newton's laws of motion; but it also holds in special relativity (with a modified formula) and, with appropriate definitions, a (generalized) linear momentum conservation law holds in electrodynamics, quantum mechanics, quantum field theory, and general relativity[163]. For example, according to the third law, the forces between two particles are equal and opposite. If the particles are numbered 1 and 2, the second law states:

$$F_1 = \frac{dP_1}{dt} \quad (1.8.13)$$

$$F_2 = \frac{dP_2}{dt} \quad (1.8.14)$$

Therefore:

$$\frac{dP_1}{dt} = -\frac{dP_2}{dt} \quad (1.8.15)$$

$$\frac{d}{dt}(P_1 + P_2) = 0 \quad (1.8.16)$$

If the velocities of the particles are  $v_{11}$  and  $v_{12}$  before the interaction, and afterwards they are  $v_{21}$  and  $v_{22}$ , then

$$m_1 v_{11} + m_2 v_{12} = m_1 v_{21} + m_2 v_{22} \tag{1.8.17}$$

This law holds no matter how complicated the force is between the particles. Similarly, if there are several particles, the momentum exchanged between each pair of particles adds up to zero; therefore; the total change in momentum is zero. This conservation law applies to all interactions, including collisions and separations caused by explosive forces. It can also be generalized to situations where Newton’s laws do not hold, for example in the theory of relativity and in electrodynamics [153, 166]. The momentum equation for the fluid can be derived as follow:

$$\rho \left( \frac{dv}{dt} + v \frac{dv}{dz} \right) = \rho g + \frac{d}{dz} [\tau_{zz} - \tau_{rr}] + \frac{\gamma}{R^2} \cdot \frac{dr}{dz} + \frac{\sigma}{\epsilon_0} \frac{d\sigma}{dz} + (\epsilon - \epsilon_0) \left( E \frac{dE}{dz} \right) + \frac{2\sigma E}{r} \tag{1.8.18}$$

But commonly, the momentum equation for electrospinning modeling is formulated by considering the forces on a short segment of the jet [153, 166].

$$\frac{d}{dz} (\pi R^2 \rho v^2) = \pi R^2 \rho g + \frac{d}{dz} [\pi R^2 (-p + \tau_{zz})] + \frac{\gamma}{R} \cdot 2\pi R R' + 2\pi R (t_i^e - t_n^e R') \tag{1.8.19}$$

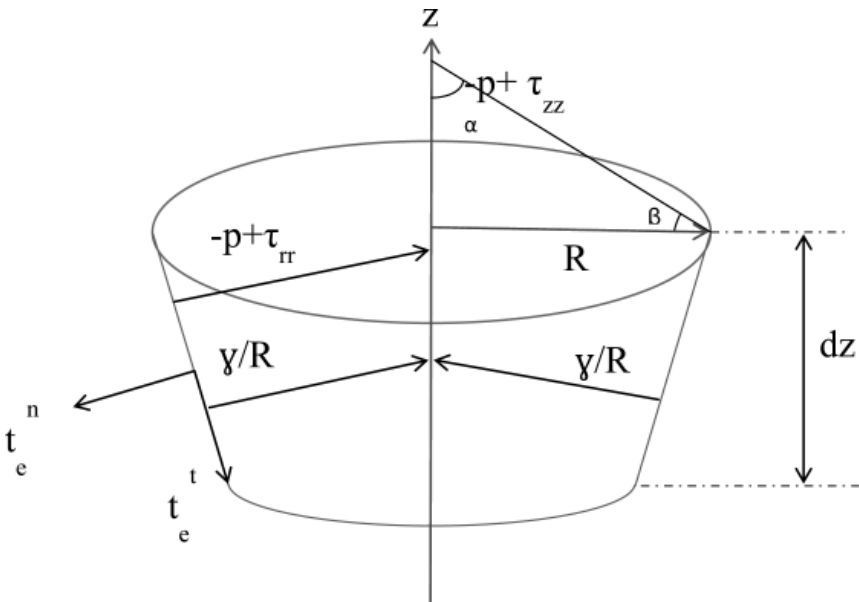


FIGURE 1.19 Momentum balance on a short section of the jet.

As shown in Figure 1.19, the element's angles could be defined as  $\alpha$  and  $\beta$ . According to the mathematical relationships, it is obvious that

$$\alpha + \beta = \frac{\pi}{2} \quad (1.8.20)$$

$$\begin{aligned} \sin \alpha &= \tan \alpha \\ \cos \alpha &= 1 \end{aligned} \quad (1.8.21)$$

Due to the figure, relationships between these electrical forces are as given below:

$$t_n^e \sin \alpha \cong t_n^e \tan \alpha \cong -t_n^e \tan \beta \cong -\frac{dR}{dz} t_n^e = -R' t_n^e \quad (1.8.22)$$

$$t_t^e \cos \alpha \cong t_t^e \quad (1.8.23)$$

Therefore, the effect of the electric forces in the momentum balance equation can be presented as follows:

$$2\pi RL(t_t^e - R' t_n^e) dz \quad (1.8.24)$$

(Notation: In the main momentum equation, final formula is obtained by dividing into  $dz$ )

In addition, the normal electric force is defined as follows:

$$t_n^e \cong \frac{1}{2} \bar{\epsilon} E_n^2 = \frac{1}{2} \bar{\epsilon} \left(\frac{\sigma}{\bar{\epsilon}}\right)^2 = \frac{\sigma^2}{2\bar{\epsilon}} \quad (1.8.25)$$

A little amount of electric forces is perished in the vicinity of the air.

$$E_n = \frac{\sigma}{\bar{\epsilon}} \quad (1.8.26)$$

The electric force can be presented by the following equation:

$$F = \frac{\Delta W e}{\Delta l} = \frac{1}{2} (\epsilon - \bar{\epsilon}) E^2 \times \Delta S \quad (1.8.27)$$

The force per surface unit is

$$\frac{F}{\Delta S} = \frac{1}{2}(\varepsilon - \bar{\varepsilon})E^2 \quad (1.8.28)$$

Generally the electric potential energy is obtained by using the following equation:

$$Ue = -We = -\int F \cdot ds \quad (1.8.29)$$

$$\Delta We = \frac{1}{2}(\varepsilon - \bar{\varepsilon})E^2 \times \Delta V = \frac{1}{2}(\varepsilon - \bar{\varepsilon})E^2 \times \Delta S \cdot \Delta l \quad (1.8.30)$$

Therefore, finally it could result in the following equation:

$$t_n^e = \frac{\sigma^2}{2\bar{\varepsilon}} - \frac{1}{2}(\varepsilon - \bar{\varepsilon})E^2 \quad (1.8.31)$$

$$t_i^e = \sigma E \quad (1.8.32)$$

### 1.10.5 COULOMB'S LAW

Coulomb's law is a mathematical description of the electric force between charged objects, which is formulated by the eighteenth-century French physicist Charles-Augustin de Coulomb. It is analogous to Isaac Newton's law of gravity. Both gravitational and electric forces decrease with the square of the distance between the objects, and both forces act along a line between them[167]. In Coulomb's law, the magnitude and sign of the electric force are determined by the electric charge, more than the mass of an object. Thus, a charge that is a basic property matter determines how electromagnetism affects the motion of charged targets [163].

Coulomb force is thought to be the main cause for the instability of the jet in the electrospinning process [168]. This statement is based on the Earnshaw's theorem, named after Samuel Earnshaw [169] which claims that "A charged body placed in an electric field of force cannot rest in stable equilibrium under the influence of the electric forces alone." This

theorem can be notably adapted to the electrospinning process [168]. The instability of charged jet influences on jet deposition and as a consequence on nanofiber formation. Therefore, some researchers applied developed models to the analysis of mechanisms of jet deposition and alignment on various collecting devices in arbitrary electric fields [66].

The equation for the potential along the centerline of the jet can be derived from Coulomb's law. Polarized charge density is obtained

$$\rho_{p'} = -\vec{\nabla} \cdot \vec{P}' \quad (1.8.33)$$

where  $P'$  is polarization:

$$\vec{P}' = (\varepsilon - \bar{\varepsilon})\vec{E} \quad (1.8.34)$$

By substituting  $P'$  in the previous equation:

$$\rho_{p'} = -(\bar{\varepsilon} - \varepsilon) \frac{dE}{dz'} \quad (1.8.35)$$

Beneficial charge per surface unit can be calculated as follows:

$$\rho_{p'} = \frac{Q_b}{\pi R^2} \quad (1.8.36)$$

$$Q_b = \rho_b \cdot \pi R^2 = -(\bar{\varepsilon} - \varepsilon) \pi R^2 \frac{dE}{dz'} \quad (1.8.37)$$

$$Q_b = -(\bar{\varepsilon} - \varepsilon) \pi \frac{d(ER^2)}{dz'} \quad (1.8.38)$$

$$\rho_{sb} = Q_b \cdot dz' = -(\bar{\varepsilon} - \varepsilon) \pi \frac{d}{dz'} (ER^2) dz' \quad (1.8.39)$$

The main equation of Coulomb's law:

$$F = \frac{1}{4\pi\varepsilon_0} \frac{qq_0}{r^2} \quad (1.8.40)$$

The electric field is:

$$E = \frac{1}{4\pi\epsilon_0} \frac{q}{r^2} \quad (1.8.41)$$

The electric potential can be measured:

$$\Delta V = -\int E \cdot dL \quad (1.8.42)$$

$$V = \frac{1}{4\pi\epsilon_0} \frac{Q_b}{r} \quad (1.8.43)$$

According to the beneficial charge equation, the electric potential could be rewritten as follows:

$$\Delta V = Q(z) - Q_\infty(z) = \frac{1}{4\pi\bar{\epsilon}} \int \frac{(q - Q_b)}{r} dz' \quad (1.8.44)$$

$$Q(z) = Q_\infty(z) + \frac{1}{4\pi\bar{\epsilon}} \int \frac{q}{r} dz' - \frac{1}{4\pi\bar{\epsilon}} \int \frac{Q_b}{r} dz' \quad (1.8.45)$$

$$Q_b = -(\bar{\epsilon} - \epsilon)\pi \frac{d(ER^2)}{dz'} \quad (1.8.46)$$

The surface charge density's equation is

$$q = \sigma \cdot 2\pi RL \quad (1.8.47)$$

$$r^2 = R^2 + (z - z')^2 \quad (1.8.48)$$

$$r = \sqrt{R^2 + (z - z')^2} \quad (1.8.49)$$

The final equation that obtained by substituting the mentioned equations is

$$Q(z) = Q_{\infty}(z) + \frac{1}{4\pi\bar{\epsilon}} \int \frac{\sigma \cdot 2\pi R}{\sqrt{(z-z')^2 + R^2}} dz' - \frac{1}{4\pi\bar{\epsilon}} \int \frac{(\bar{\epsilon} - \epsilon)\pi}{\sqrt{(z-z')^2 + R^2}} \frac{d(ER^2)}{dz'} \quad (1.8.50)$$

It is assumed that  $\beta$  is defined as follows:

$$\beta = \frac{\epsilon}{\bar{\epsilon}} - 1 = -\frac{(\bar{\epsilon} - \epsilon)}{\bar{\epsilon}} \quad (1.8.51)$$

Therefore, the potential equation becomes

$$Q(z) = Q_{\infty}(z) + \frac{1}{2\bar{\epsilon}} \int \frac{\sigma \cdot R}{\sqrt{(z-z')^2 + R^2}} dz' - \frac{\beta}{4} \int \frac{1}{\sqrt{(z-z')^2 + R^2}} \frac{d(ER^2)}{dz'} \quad (1.8.52)$$

The asymptotic approximation of  $\chi$  is used to evaluate the integrals mentioned earlier:

$$\chi = \left( -z + \xi + \sqrt{z^2 - 2z\xi + \xi^2 + R^2} \right) \quad (1.8.53)$$

where  $\chi$  is “aspect ratio” of the jet ( $L$  = length,  $R_0$  = initial radius)

This leads to the final relation to the axial electric field:

$$E(z) = E_{\infty}(z) - \ln \chi \left( \frac{1}{\bar{\epsilon}} \frac{d(\sigma R)}{dz} - \frac{\beta}{2} \frac{d^2(ER^2)}{dz^2} \right) \quad (1.8.54)$$

### 1.10.6 FORCES CONSERVATION

There exists a force, as a result of charge build-up, acting on the droplet coming out of the syringe needle pointing toward the collecting plate which can be either grounded or oppositely charged. Further, similar charges within the droplet promote jet initiation due to their repulsive forces. Nevertheless, surface tension and other hydrostatic forces inhibit the jet initiation because the total energy of a droplet is lower than that of a thin jet of equal volume upon consideration of surface energy. When the forces that aid jet initiation (such as electric field and Columbic) overcome the opposing forces (such as surface tension and gravitational), the droplet accelerates toward the collecting plate. This forms a jet of very small diameter. Other than initiating jet flow, the electric field and Columbic



forces tend to stretch the jet, thereby contributing toward the thinning effect of the resulting nanofibers.

In the flow path modeling, we recall the Newton's Second Law of motion:

$$m \frac{d^2 P}{dt^2} = \sum f \quad (1.8.55)$$

where,  $m$  (equivalent mass) and the various forces are summed as follows:

$$\sum f = f_C + f_E + f_V + f_S + f_A + f_G + \dots \quad (1.8.56)$$

In which subscripts  $C$ ,  $E$ ,  $V$ ,  $S$ ,  $A$  and  $G$  correspond to the Columbic, electric field, viscoelastic, surface tension, air drag, and gravitational forces, respectively. A description of each of these forces based on the literature [5] is summarized in Table 1.1 where

$V_0$  = applied voltage

$h$  = distance from pendent drop to ground collector

$\sigma_v$  = viscoelastic stress

$\nu$  = kinematic viscosity

**TABLE 1.1** Description of itemized forces or terms related to them

Forces	Equations
Columbic	$f_C = \frac{q^2}{l^2}$
Electric field	$f_E = -\frac{qV_0}{h}$
Viscoelastic	$f_V = \frac{d\sigma_v}{dt} = \frac{G}{l} \frac{dl}{dt} - \frac{G}{\eta} \sigma_v$
Surface tension	$f_S = \frac{\alpha\pi R^2 k}{\sqrt{x_i^2 + y_i^2}} [i x  \text{Sin}(x) + i y  \text{Sin}(y)]$

Air drag	$f_A = 0.65\pi R\rho_{air}v^2\left(\frac{2vR}{v_{air}}\right)^{-0.81}$
Gravitational	$f_G = \rho g\pi R^2$

### 1.10.7 CONSTITUTIVE EQUATIONS

In modern condensed matter physics, the constitutive equation plays a major role. In physics and engineering, a constitutive equation or relation is a relation between two physical quantities that is specific to a material or substance, and approximates the response of that material to external stimulus, usually as applied fields or forces [170]. There are a sort of mechanical equation of state, which describe how the material is constituted mechanically. With these constitutive relations, the vital role of the material is reasserted [171]. There are two groups of constitutive equations: Linear and nonlinear constitutive equations [172]. These equations are combined with other governing physical laws to solve problems; for example, in fluid mechanics the flow of a fluid in a pipe, in solid-state physics the response of a crystal to an electric field, or in structural analysis, the connection between applied stresses or forces to strains or deformations [170].

The first constitutive equation (constitutive law) was developed by Robert Hooke and is known as Hooke's law. It deals with the case of linear elastic materials. Following this discovery, this type of equation, often called a "stress-strain relation" in this example, but also called a "constitutive assumption" or an "equation of state" was commonly used [173]. Walter Noll advanced the use of constitutive equations, clarifying their classification and the role of invariance requirements, constraints, and definitions of terms such as "material," "isotropic," "aeolotropic," and so on. The class of "constitutive relations" of the form stress rate =  $f$ (velocity gradient, stress, density) was the subject of Walter Noll's dissertation in 1954 under Clifford Truesdell [170]. There are several kinds of constitutive equations that are applied commonly in electrospinning. Some of these applicable equations are discussed in the following.

### 1.10.7.1 OSTWALD–DE WAELE POWER LAW

Rheological behavior of many polymer fluids can be described by power law constitutive equations [172]. The equations that describe the dynamics in electrospinning constitute, at a minimum, those describing the conservation of mass, momentum and charge, and the electric field equation. In addition, a constitutive equation for the fluid behavior is also required [76]. A power law fluid, or the Ostwald–de Waele —relationship, is a type of generalized Newtonian fluid for which the shear stress,  $\tau$ , is given by

$$\tau = K' \left( \frac{\partial v}{\partial y} \right)^m \quad (1.8.57)$$

where  $\partial v/\partial y$  is the shear rate or the velocity gradient perpendicular to the plane of shear. The power law is only a good description of fluid behavior across the range of shear rates to which the coefficients are fitted. There are a number of other models that better describe the entire flow behavior of shear-dependent fluids, but they do so at the expense of simplicity; therefore, the power law is still used to describe fluid behavior, permit mathematical predictions, and correlate experimental data [166, 174].

Nonlinear rheological constitutive equations applicable for polymer fluids (Ostwald–de Waele power law) were applied to the electrospinning process by Spivak and Dzenis [77, 150, 175].

$$\hat{\tau}^c = \mu \left[ \text{tr} \left( \hat{\gamma}^2 \right) \right]^{(m-1)/2} \hat{\gamma} \quad (1.8.58)$$

$$\mu = K \left( \frac{\partial v}{\partial y} \right)^{m-1} \quad (1.8.59)$$

Viscous Newtonian fluids are described by a special case of equation above with the flow index  $m = 1$ . Pseudoplastic (shear thinning) fluids are described by flow indices  $0 \leq m \leq 1$ . Dilatant (shear thickening) fluids are described by the flow indices  $m > 1$  [150].

### 1.10.7.2 GIESEKUS EQUATION

In 1966, Giesekus established the concept of anisotropic forces and motions in polymer kinetic theory. With particular choices for the tensors

describing the anisotropy, one can obtain Giesekus constitutive equation from elastic dumbbell kinetic theory [176–177]. The Giesekus equation is known to predict, both qualitatively and quantitatively, material functions for steady and nonsteady shear and elongational flows.

However, the equation sustains two drawbacks: it predicts that the viscosity is inversely proportional to the shear rate in the limit of infinite shear rate and it is unable to predict any decrease in the elongational viscosity with increasing elongation rates in uniaxial elongational flow. The first one is not serious because of the retardation time that is included in the constitutive equation, but the second one is more critical because the elongational viscosity of some polymers decreases with increasing of elongation rate [178–179].

In the main Giesekus equation, the tensor of excess stresses depending on the motion of polymer units relative to their surroundings was connected to a sequence of tensors characterizing the configurational state of the different kinds of network structures present in the concentrated solution or melt. The respective set of constitutive equations indicates [180–181]:

$$S_k + \eta \frac{\partial C_k}{\partial t} = 0 \quad (1.8.60)$$

The equation below indicates the upper-convected time derivative (Oldroyd derivative):

$$\frac{\partial C_k}{\partial t} = \frac{DC_k}{Dt} - [C_k \nabla v + (\nabla v)^T C_k] \quad (1.8.61)$$

(Note: The upper convective derivative is the rate of change of any tensor property of a small parcel of fluid that is written in the coordinate system rotating and stretching with the fluid.)

$C_k$  also can be measured as follows:

$$C_k = 1 + 2E_k \quad (1.8.62)$$

According to the concept of “recoverable strain”  $S_k$  may be understood as a function of  $E_k$  and vice versa. If linear relations corresponding to Hooke’s law are adopted.

$$S_k = 2\mu_k E_k \quad (1.8.63)$$

Therefore,

$$S_k = \mu_k (C_k - 1) \quad (1.8.64)$$

Equation (1.8.60) becomes thus:

$$S_k + \lambda_k \frac{\partial S_k}{\partial t} = 2\eta D \quad (1.8.65)$$

$$\lambda_k = \frac{\eta}{\mu_k} \quad (1.8.66)$$

As a second step in order to rid the model of the shortcomings is the scalar mobility constants  $B_k$ , which are contained in the constants  $\eta$ . This mobility constant can be represented as follows:

$$\frac{1}{2}(\beta_k S_k + S_k \beta_k) + \tilde{\eta} \frac{\partial C_k}{\partial t} = 0 \quad (1.8.67)$$

The two parts of equation (1.8.67) reduces to the single constitutive equation:

$$\beta_k + \tilde{\eta} \frac{\partial C_k}{\partial t} = 0 \quad (1.8.68)$$

The excess tension tensor in the deformed network structure where the well-known constitutive equation of a so-called Neo-Hookean material is proposed [180, 182]:

Neo-Hookean equation

$$S_k = 2\mu_k E_k = \mu_k (C_k - 1) \quad (1.8.69)$$

$$\begin{aligned} \mu_k &= NKT \\ \beta_k &= 1 + \alpha(C_k - 1) = (1 - \alpha) + \alpha C_k \end{aligned} \quad (1.8.70)$$

where K is Boltzmann's constant.

By substitution Eqs (1.8.69) and (1.8.70) in the Eq. (1.8.64), it can be obtained where the condition  $0 \leq \alpha \leq 1$  must be fulfilled, the limiting case  $\alpha = 0$  corresponds to an isotropic mobility [183].

$$0 \leq \alpha \leq 1 \quad [1 + \alpha(C_k - 1)](C_k - 1) + \lambda_k \frac{\partial C_k}{\partial t} = 0 \quad (1.8.71)$$

$$\alpha = 1 \quad C_k(C_k - 1) + \lambda_k \frac{\partial C_k}{\partial t} = 0 \quad (1.8.72)$$

$$0 \leq \alpha \leq 1 \quad C_k = \frac{S_k}{\mu_k} + 1 \quad (1.8.73)$$

By substituting equations above in Eq. (1.8.64), we obtain

$$\left[ 1 + \frac{\alpha S_k}{\mu_k} \right] \frac{S_k}{\mu_k} + \lambda_k \frac{\partial C_k}{\partial t} = 0 \quad (1.8.74)$$

$$\frac{S_k}{\mu_k} + \frac{\alpha S_k^2}{\mu_k^2} + \lambda_k \frac{\partial (S_k / \mu_k + 1)}{\partial t} = 0 \quad (1.8.75)$$

$$\frac{S_k}{\mu_k} + \frac{\alpha S_k^2}{\mu_k^2} + \frac{\lambda_k}{\mu_k} \frac{\partial S_k}{\partial t} = 0 \quad (1.8.76)$$

$$S_k + \frac{\alpha S_k^2}{\mu_k} + \lambda_k \frac{\partial S_k}{\partial t} = 0 \quad (1.8.77)$$

$D$  means the rate of strain tensor of the material continuum [180].

$$D = \frac{1}{2} [\nabla v + (\nabla v)^T] \quad (1.8.78)$$

The equation of the upper convected time derivative for all fluid properties can be calculated as follows:

$$\frac{\partial \otimes}{\partial t} = \frac{D \otimes}{Dt} - [\otimes \cdot \nabla v + (\nabla v)^T \cdot \otimes] \quad (1.8.79)$$

$$\frac{D \otimes}{Dt} = \frac{\partial \otimes}{\partial t} + [(v \cdot \nabla) \cdot \otimes] \quad (1.8.80)$$

By replacing  $S_k$  instead of the symbol:

$$\lambda_k \frac{\partial S_k}{\partial t} = \lambda_k \frac{DS_k}{Dt} - \lambda_k [S_k \nabla v + (\nabla v)^T S_k] = \lambda_k \frac{DS_k}{Dt} - \lambda_k (v \cdot \nabla) S_k \quad (1.8.81)$$

By simplification the equation above, we obtain

$$S_k + \frac{\alpha S_k^2}{\mu_k} + \lambda_k \frac{DS_k}{Dt} = \lambda_k (v \cdot \nabla) S_k \quad (1.8.82)$$

$$S_k = 2\mu_k E_k \quad (1.8.83)$$

The assumption of  $E_k = 1$  would lead to the next equation:

$$S_k + \frac{\alpha \lambda_k S_k^2}{\eta} + \lambda_k \frac{DS_k}{Dt} = \frac{\eta}{\mu_k} (2\mu_k) D = 2\eta D = \eta [\nabla v + (\nabla v)^T] \quad (1.8.84)$$

In electrospinning modeling articles  $\tau$  is used commonly instead of  $S_k$  [154, 159, 161].

$$S_k \leftrightarrow \tau$$

$$\tau + \frac{\alpha \lambda_k \tau^2}{\eta} + \lambda_k \tau_{(1)} = \eta [\nabla v + (\nabla v)^T] \quad (1.8.85)$$

### 1.10.7.3 MAXWELL EQUATION

Maxwell's equations are a set of partial differential equations that, together with the Lorentz force law, form the foundation of classical electrodynamics, classical optics, and electric circuits. These fields are the bases of modern electrical and communications technologies. Maxwell's equations describe how electric and magnetic fields are generated and altered by each other and by charges and currents; they are named after the Scottish physicist and mathematician James Clerk Maxwell who published an

early form of those equations between 1861 and 1862 [184–185]. It will be discussed further in detail.

### **1.10.8 MICROSCOPIC MODELS**

One of the aims of computer simulation is to reproduce experiment to elucidate the invisible microscopic details and further explain the experiments. Physical phenomena occurring in complex materials cannot be encapsulated within a single numerical paradigm. In fact, they should be described within hierarchical, multilevel numerical models in which each submodel is responsible for different spatial-temporal behavior and passes out the averaged parameters of the model, which is next in the hierarchy. The understanding of the nonequilibrium properties of complex fluids such as the viscoelastic behavior of polymeric liquids, the rheological properties of ferrofluids and liquid crystals subjected to magnetic fields, based on the architecture of their molecular constituents is useful to get a comprehensive view of the process. The analysis of simple physical particle models for complex fluids has developed from the molecular computation of basic systems (atoms, rigid molecules) to the simulation of macromolecular “complex” system with a large number of internal degrees of freedom exposed to external forces [186–187].

The most widely used simulation methods for molecular systems are Monte Carlo, Brownian dynamics, and molecular dynamics. The microscopic approach represents the microstructural features of material by means of a large number of micromechanical elements (beads, platelet, rods) obeying stochastic differential equations. The evolution equations of the microelements arise from a balance of momentum at the elementary level. The Monte Carlo method is a stochastic strategy that relies on probabilities. The Monte Carlo sampling technique generates large numbers of configurations or microstates of equilibrated systems by stepping from one microstate to the next in a particular statistical ensemble. Random changes are made to the positions of the species present, together with their orientations and conformations where appropriate. Brownian dynamics are an efficient approach for simulations of large polymer molecules or colloidal particles in a small molecule solvent. Molecular dynamics is the most detailed molecular simulation method which computes the motions of individual molecules. Molecular dynamics efficiently evaluates



different configurational properties and dynamic quantities which cannot generally be obtained by Monte Carlo [188–189].

The first computer simulation of liquids was carried out in 1953. The model was an idealized two-dimensional representation of molecules as rigid disks. For macromolecular systems, the coarse-grained approach is widely used as the modeling process is simplified, hence becomes more efficient, and the characteristic topological features of the molecule can still be maintained. The level of detail for a coarse-grained model varies in different cases. The whole molecule can be represented by a single particle in a simulation and interactions between particles incorporate average properties of the whole molecule. With this approach, the number of degrees of freedom is greatly reduced [190].

On the contrary, a segment of a polymer molecule can also be represented by a particle (bead). The first coarse-grained model, called the “dumbbell” model, was introduced in the 1930s. Molecules are treated as a pair of beads interacting via a harmonic potential. However by using this model, it is possible to perform kinetic theory derivations and calculations for nonlinear rheological properties and solve some flow problems. The analytical results for the dumbbell models (Figure 1.20) can also be used to check computer simulation procedures in molecular dynamics and Brownian dynamics [191–192].

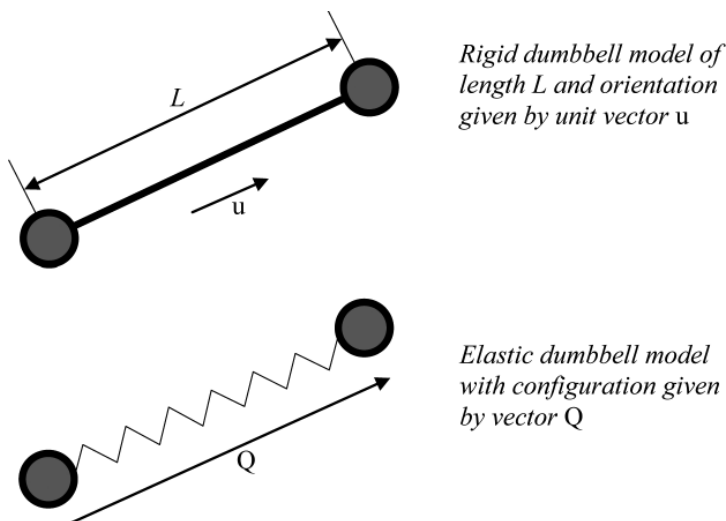


**FIGURE 1.20** The first coarse-grained models—the rigid and elastic dumbbell models.

The bead-rod and bead-spring model (Figure 1.21) were introduced to model chainlike macromolecules. Beads in the bead-rod model do not represent the atoms of the polymer chain backbone, but some portion of the chain, normally 10 to 20 monomer units. These beads are connected by rigid and massless rods. While in the bead-spring model, a portion of the chain containing several hundreds of backbone atoms are replaced by a “spring,” and the masses of the atoms are concentrated on the mass of beads [193].

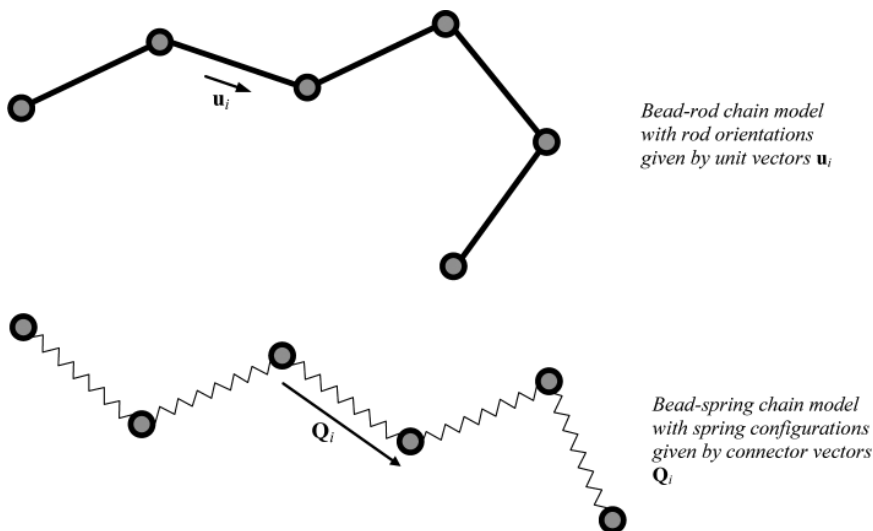


**FIGURE 1.21** The freely jointed bead-rod and bead-spring chain models.

If the springs are taken to be Hookean springs, the bead-spring chain is referred to as a Rouse chain or a Rouse–Zimm chain. This approach has been applied widely as it has a large number of internal degrees of freedom and exhibits orientability and stretchability. However the disadvantage of this model is that it does not have a constant contour length and can be stretched out to any length. Therefore, in many cases finitely extensible springs with two more parameters, the spring constant and the maximum extensibility of an individual spring, can be included so the contour length of the chain model cannot exceed a certain limit [194–195].

The understanding of the nonequilibrium properties of complex fluids such as the viscoelastic behavior of polymeric liquids, the rheological

properties of ferrofluids and liquid crystals subjected to magnetic fields, based on the architecture of their molecular constituents [186].

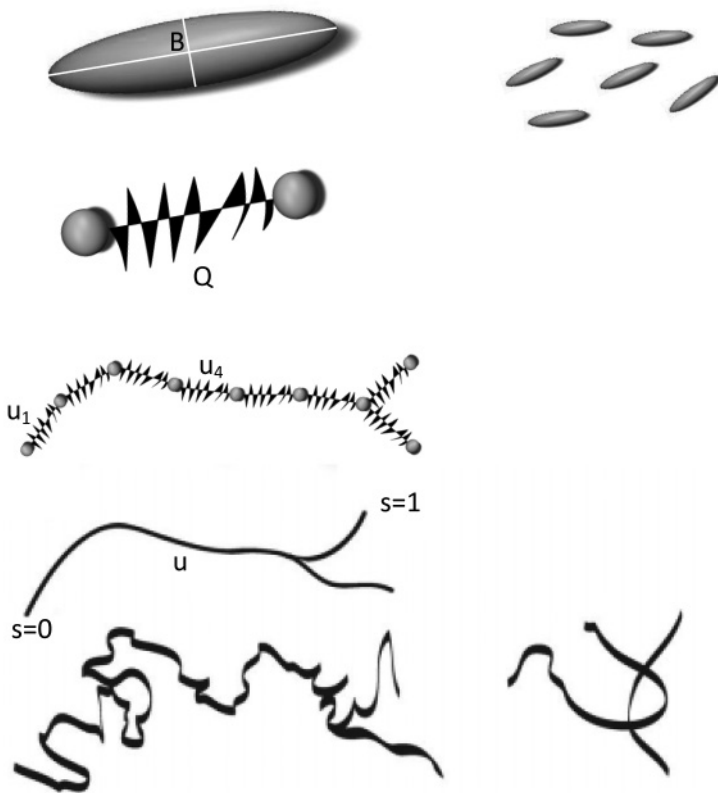


**FIGURE 1.22** Simple microscopic models for complex fluids by using dumbbell model.

Dumbbell models are very crude representations of polymer molecules. Too crude to be of much interest to a polymer chemist, since it in no way accounts for the details of the molecular architecture. It certainly does not have enough internal degrees of freedom to describe the very rapid motions that contribute, for example, to the complex viscosity at high frequencies. On the contrary, the elastic dumbbell model is orientable and stretchable, and these two properties are essential for the qualitative description of steady-state rheological properties and those involving slow changes with time. For dumbbell models, one can go through the entire program of endeavor—from molecular model for fluid dynamics—

for illustrative purposes, in order to point the way toward the task that has ultimately to be performed for more realistic models. According to the researches, dumbbell models must, to some extent then, be regarded as mechanical playthings, somewhat disconnected from the real world of polymers (Figure 1.22). However, when used intelligently, they can be useful pedagogically and very helpful in developing a qualitative understanding of rheological phenomena [186, 196].

The simplest model of flexible macromolecules in a dilute solution is the elastic dumbbell (or bead-spring) model. This has been widely used for purely mechanical theories of the stress in electrospinning modeling [197].

A Maxwell constitutive equation was first applied by Reneker et al. in 2000. Consider an electrified liquid jet in an electric field parallel to its axis. They modeled a segment of the jet by a viscoelastic dumbbell (Figure 1.23). They used a Gaussian electrostatic system of units. According to this model each particle in the electric field exerts repulsive force on another particle [66].

He had three main assumptions [66, 198]:

1. The background electric field created by the generator is considered static.
2. The fiber is a perfect insulator.
3. The polymer solution is a viscoelastic medium with constant elastic modulus, viscosity, and surface tension.

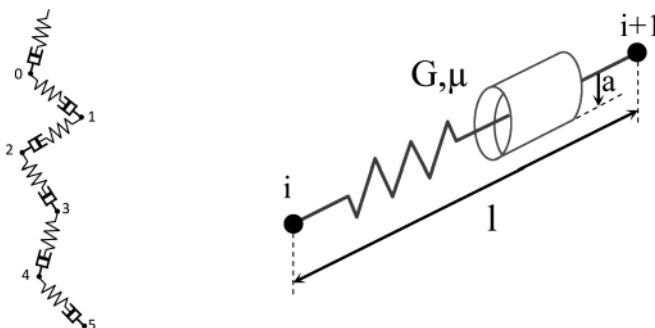


**FIGURE 1.23** A schematic of one section of the model.

The researcher considered the governing equations for each bead as follows [198]:

$$\frac{d}{dt}(\pi a^2 l) = 0 \quad (1.8.86)$$

Therefore, the stress between these particles can be measured by using the following equation [66]:

$$\frac{d\sigma}{dt} = G \frac{dl}{l dt} - \frac{G}{\eta} \sigma \quad (1.8.87)$$

The stress can be calculated by a Maxwell viscoelastic constitutive equation [199]:

$$\dot{\tau} = G \left( \varepsilon' - \frac{\tau}{\eta} \right) \quad (1.8.88)$$

where  $\varepsilon'$  is the Lagrangian axial strain [199]:

$$\varepsilon' \equiv \frac{\partial \dot{x}}{\partial \xi} \hat{t}. \quad (1.8.89)$$

Equation of motion for beads can be written as follows[200]:

$$\begin{aligned} \text{mass} \times \text{acceleration} &= \text{viscous drag} + \text{Brownian motion force} \\ &+ \text{force of one bead on another through the connector} \end{aligned} \quad (8.90)$$

The momentum balance for a bead is [198]:

$$m \frac{dv}{dt} = \underbrace{-\frac{q^2}{l^2}}_{\text{Coulomb forces}} - \underbrace{qE}_{\text{Electric force}} + \underbrace{\pi a^2 \sigma}_{\text{Mechanical forces}} \quad (1.8.91)$$

So the momentum conservation for model charges can be calculated as [201] follows:

$$m_i \frac{dv_i}{dt} = \underbrace{q_i \sum_{i \neq j} q_j K \frac{r_i - r_j}{|r_i - r_j|^3}}_{\text{Coulomb forces}} + \underbrace{q_i E}_{\text{Electric force}} + \underbrace{\pi a_{i,i+1}^2 \sigma_{i,i+1} \frac{r_{i+1} - r_i}{|r_{i+1} - r_i|} - \pi a_{i-1,i}^2 \sigma_{i-1,i} \frac{r_i - r_{i-1}}{|r_i - r_{i-1}|}}_{\text{Mechanical forces}} \quad (1.8.92)$$

Boundary condition assumptions: A small initial perturbation is added to the position of the first bead, the background electric field is axial and uniform and the first bead is described by a stationary equation. For solving

these equations, some dimensionless parameters are defined then by simplifying equations, the equations are solved by using boundary conditions [198, 201].

Now, an example for using this model for the polymer structure is mentioned. For a dumbbell consists of two that are connected with a nonlinear spring (Figure 1.24), the spring force law is given by the following equation[96]:

$$F = -\frac{HQ}{1 - Q^2/Q_0^2} \quad (1.8.93)$$

Now if we considered the model for the polymer matrix such as carbon nanotube, the rheological behavior can be obtained as follows [96, 201]:

$$\tau_{ij} = \tau_p + \tau_s \quad (1.8.94)$$

$$\tau_p = \underbrace{n_a \langle Q_a F_a \rangle}_{\text{aggregated dumbbells}} + \underbrace{n_f \langle Q_f F_f \rangle}_{\text{free dumbbells}} - nkT \delta_{ij} \quad (1.8.95)$$

$$\tau_s = \eta \dot{\gamma} \quad (1.8.96)$$

$$\lambda \langle Q \cdot Q \rangle^\nabla = \delta_{ij} - \frac{c \langle Q \cdot Q \rangle}{1 - \text{tr} \langle Q \cdot Q \rangle / b_{\max}} \quad (1.8.97)$$

The polymeric stress can be obtained from the following relation [96]:

$$\frac{\hat{\tau}_{ij}}{n_d kT} = \delta_{ij} - \frac{c \langle Q \cdot Q \rangle}{1 - \text{tr} \langle Q \cdot Q \rangle / b_{\max}} \quad (1.8.98)$$

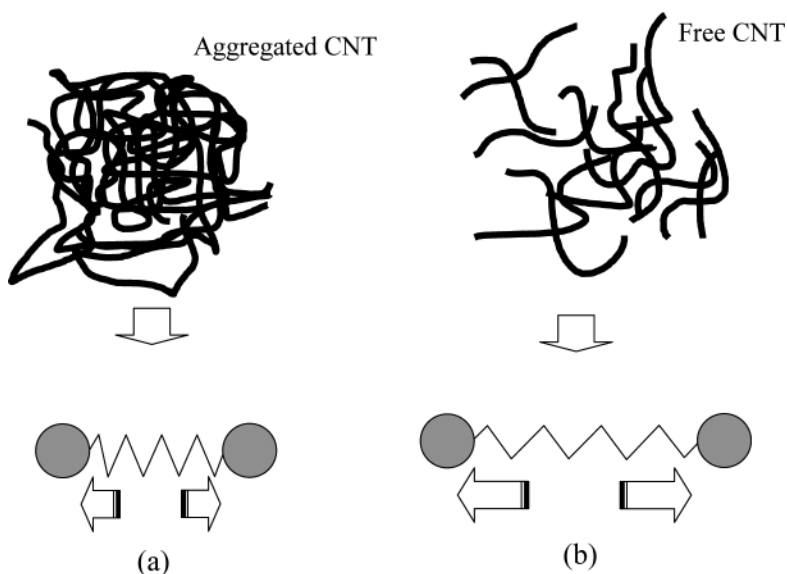


**FIGURE 1.24** Modeling of two kinds of dumbbell sets, (a) aggregate FENE dumbbell which has lower mobility and (b) free FENE dumbbell which has higher mobility.

### 1.10.9 SCALING

The physical aspect of a phenomenon can use the language of differential equation that represents the structure of the system by selecting the variables that characterize the state of it and certain mathematical constraint on the values of those variables can take on. These equations can predict the behavior of the system over a quantity such as time. For an instance, a set of continuous functions of time that describe the way the variables of the system developed over time starting from a given initial state [208]. In general, the renormalization group theory, scaling, and fractal geometry are applied to the understanding of the complex phenomena in physics, economics, and medicine [203-209].

In more recent times, in statistical mechanics, the expression “scaling laws” has referred to the homogeneity of form of the thermodynamic and correlation functions near critical points, and to the resulting relations among the exponents that occur in those functions. From the viewpoint of scaling, electrospinning modeling can be studied in two ways: allometric and dimensionless analysis. Scaling and dimensional analysis actually

started with Newton, and allometry exists everywhere in our daily life and scientific activity[209–210].

### 1.10.9.1 ALLOMETRIC SCALING

Electrospinning applies electrically generated motion to spin fibers. Therefore, it is difficult to predict the size of the produced fibers, which depends on the applied voltage in principal. Therefore, the relationship between the radius of the jet and the axial distance from the nozzle is always the subject of investigation [211–212]. It can be described as an allometric equation by using the values of the scaling exponent for the initial steady, instability, and terminal stages [213].

The relationship between  $r$  and  $z$  can be expressed as an allometric equation of the following form:

$$r \approx z^b \quad (1.8.99)$$

When the power exponent,  $b = 1$ , the relationship is isometric and when  $b \neq 1$  the relationship is allometric [211, 214]. In another view,  $b = -1/2$  is considered for the straight jet,  $b = -1/4$  for instability jet, and  $b = 0$  for final stage [172, 212].

Due to high electrical force acting on the jet, it can be illustrated [211]:

$$\frac{d}{dz} \left( \frac{v^2}{2} \right) = \frac{2\sigma E}{\rho r} \quad (1.8.100)$$

Equations of mass and charge conservations applied here as mentioned earlier [211, 214–215]

From the above equations, it can be noted that [161, 211]

$$r \approx z^b, \sigma \approx r, E \approx r^{-2}, \frac{dv^2}{dz} \approx r^{-2} \quad (1.8.101)$$

Therefore, it is obtained for the initial part of jet,  $r \approx z^{-1/4}$  for the in-stable stage and for the final stage.

The charged jet can be considered as a 1D flow as mentioned. If the conservation equations modified, they would change as follows [211]:



$$2\pi r\sigma^\alpha v + K\pi r^2 E = I \quad (1.8.102)$$

$$r \approx z^{-\alpha/(\alpha+1)} \quad (1.8.103)$$

where  $\alpha$  is a surface charge parameter; the value of  $\alpha$  depends on the surface charge in the jet. When  $\alpha = 0$  no charge in jet surface, and in  $\alpha = 1$  use for full surface charge.

Allometric scaling equations are more widely investigated by different researchers. Some of the most important allometric relationships for electrospinning are presented in Table 1.2.

**TABLE 1.2** Investigated scaling laws applied in electrospinning model

Parameters	Equation	Ref.
Conductance and polymer concentration	$g \approx c^\beta$	[161]
Fiber diameters and the solution viscosity	$d \approx \eta^\alpha$	[212]
Mechanical strength and threshold voltage	$\bar{\sigma} \approx E_{\text{threshold}}^{-\alpha}$	[216]
Threshold voltage and the solution viscosity	$E_{\text{threshold}} \approx \eta^{1/4}$	[216]
Viscosity and the oscillating frequency	$\eta \approx \omega^{-0.4}$	[216]
Volume flow rate and the current	$I \approx Q^b$	[215]
Current and the fiber radius	$I \approx r^2$	[217]
Surface charge density and the fiber radius	$\sigma \approx r^3$	[217]
Induction surface current and the fiber radius	$\phi \approx r^2$	[217]
Fiber radius and AC frequency	$r \approx \Omega^{1/4}$	[172]

Note:  $\beta$ ,  $\alpha$ , and  $b$  = scaling exponent

### 1.10.9.2 DIMENSIONLESS ANALYSIS

One of the simplest, yet most powerful, tools in the physics is dimensional analysis in which there are two kinds of quantities: dimensionless and dimensional.

In physics and all science, dimensional analysis is the analysis of the relationships between different physical quantities by identifying their dimensions. The dimension of any physical quantity is the combination of the basic physical dimensions that compose it, although the definitions of basic physical dimensions may vary. Some fundamental physical dimensions, based on the SI system of units, are length, mass, time, and electric charge. (The SI unit of electric charge is, however, defined in terms of units of length, mass and time, and, for example, the time unit and the length unit are not independent but can be linked by the speed of light  $c$ .) Other physical quantities can be expressed in terms of these fundamental physical dimensions. Dimensional analysis is based on the fact that a physical law must be independent of the units used to measure the physical variables. A straightforward practical consequence is that any meaningful equation (and any inequality and inequation) must have the same dimensions on the left and right sides. Dimensional analysis is routinely used as a check on the plausibility of derived equations and computations. It is also used to categorize types of physical quantities and units based on their relationship to or dependence on other units.

Dimensionless quantities that are without associated physical dimensions are widely used in mathematics, physics, engineering, economics, and in everyday life (such as in counting). Numerous well-known quantities, such as  $\pi$ ,  $e$ , and  $\phi$ , are dimensionless. They are “pure” numbers, and as such always have a dimension of 1 [218–219].

Dimensionless quantities are often defined as products or ratios of quantities that are not dimensionless, but whose dimensions cancel out when their powers are multiplied [220].

The basic principle of dimensional analysis was known to Isaac Newton (1686) who referred to it as the “Great Principle of Similitude.” James Clerk Maxwell played a major role in establishing modern use of dimensional analysis by distinguishing mass, length, and time as fundamental units, while referring to other units as derived. The nineteenth-century French mathematician Joseph Fourier made important contributions based on the idea that physical laws like  $F = ma$  should be independent of the units used to measure the physical variables. This led to the conclusion that

meaningful laws must be homogeneous equations in their various units of measurement, a result that was eventually formalized in the Buckingham  $\pi$  theorem. This theorem describes how every physically meaningful equation involving  $n$  variables can be equivalently rewritten as an equation of  $n-m$  dimensionless parameters, where  $m$  is the rank of the dimensional matrix. Further, and most importantly, it provides a method for computing these dimensionless parameters from the given variables.

A dimensional equation can have the dimensions reduced or eliminated through nondimensionalization, which begins with dimensional analysis, and involves scaling quantities by characteristic units of a system or natural units of nature. This gives insight into the fundamental properties of the system, as illustrated in the examples below:

In nondimensional scaling, there are two key steps:

1. Identifying a set of physically relevant dimensionless groups
2. Determining the scaling exponent for each one

Dimensional analysis will help you with step (a), but it cannot be applicable possibly for step (b).

A good approach to systematically getting to grips with such problems is through the tools of dimensional analysis (Bridgman, 1963). The dominant balance of forces controlling the dynamics of any process depends on the relative magnitudes of each underlying physical effect entering the set of governing equations [221]. Now, the most general characteristics parameters that are used in dimensionless analysis in electrospinning are introduced in Table 1.3.

**TABLE 1.3** Characteristics parameters employed and their definitions

Parameter	Definition
Length	$R_0$
Velocity	$v_0 = \frac{Q}{\pi R_0^2 K}$
Electric field	$E_0 = \frac{I}{\pi R_0^2 K}$
Surface charge density	$\sigma_0 = \bar{\epsilon} E_0$
Viscous stress	$\tau_0 = \frac{\eta_0 v_0}{R_0}$

For achievement of a simplified form of equations and reduction of a number of unknown variables, the parameters should be subdivided into characteristic scales to become dimensionless. Electrospinning dimensionless groups are shown in Table 1.4 [222].

**TABLE 1.4** Dimensionless groups employed and their definitions

Name	Definition	Field of application
Froude number	$Fr = \frac{v_0^2}{gR_0}$	The ratio of inertial to gravitational forces
Reynolds number	$Re = \frac{\rho v_0 R_0}{\eta_0}$	The ratio of the inertia forces of the viscous forces
Weber number	$We = \frac{\rho v_0^2 R_0}{\gamma}$	The ratio of the surface tension forces to the inertia forces
Deborah number	$De = \frac{\lambda v_0}{R_0}$	The ratio of the fluid relaxation time to the instability growth time
Electric Peclet number	$Pe = \frac{2\bar{\epsilon}v_0}{KR_0}$	The ratio of the characteristic time for flow to that for electrical conduction
Euler number	$Eu = \frac{\epsilon_0 E^2}{\rho v_0^2}$	The ratio of electrostatic forces to inertia forces
Capillary number	$Ca = \frac{\eta v_0}{\gamma}$	The ratio of inertia forces of viscous forces
Ohnesorge number	$oh = \frac{\eta}{(\rho\gamma R_0)^{1/2}}$	The ratio of viscous force to surface force
Viscosity ratio	$r_\eta = \frac{\eta_p}{\eta_0}$	The Ratio of the Polymer Viscosity to Total Viscosity
Aspect ratio	$\chi = \frac{L}{R_0}$	The ratio of the length of the primary radius of jet

**TABLE 1.4** (Continued)

Name	Definition	Field of application
Electrostatic force parameter	$\varepsilon = \frac{\bar{\varepsilon} E_0^2}{\rho v_0^2}$	The relative importance of the electrostatic and hydrodynamic forces
Dielectric constant ratio	$\beta = \frac{\varepsilon}{\bar{\varepsilon}} - 1$	The ratio of the field without the dielectric to the net field with the dielectric

The governing and constitutive equations can be transformed into a dimensionless form using the dimensionless parameters and groups.

### 1.10.10 SOME OF ELECTROSPINNING MODELS

The most important mathematical models for electrospinning process are classified in the Table 1.5 according to the year, advantages, and disadvantages of the models.

**TABLE 1.5** The most important mathematical models for electrospinning

Researchers	Model	Year	Ref.
Taylor, G. I. Melcher, J. R.	Leaky dielectric model <ul style="list-style-type: none"> <li>✓ Dielectric fluid</li> <li>✓ Bulk charge in the fluid jet considered to be zero</li> <li>✓ Only axial motion</li> <li>✓ Steady-state part of jet</li> </ul>	1969	[223]
Ramos	Slender body <ul style="list-style-type: none"> <li>✓ Incompressible and axisymmetric and viscous jet under gravity force</li> <li>✓ No electrical force</li> <li>✓ Jet radius decreases near zero</li> <li>✓ Velocity and pressure of jet only change during axial direction</li> <li>✓ Mass and volume control equations and Taylor expansion were applied to predict jet radius.</li> </ul>	1996	[224]

**TABLE 1.5** (Continued)

Researchers	Model	Year	Ref.
Saville, D. A.	Electrohydrodynamic model <ul style="list-style-type: none"> <li>✓ The hydrodynamic equations of dielectric model were modified.</li> <li>✓ Using dielectric assumption</li> <li>✓ This model can predict drop formation</li> <li>✓ Considering jet as a cylinder (ignoring the diameter reduction)</li> <li>✓ Only for steady-state part of the jet</li> </ul>	1997	[225]
Spivak, A. Dzenis, Y.	Spivak and Dzenis model <ul style="list-style-type: none"> <li>✓ The motions of a viscose fluid jet with lower conductivity were surveyed in an external electric field.</li> <li>✓ Single Newtonian fluid jet</li> <li>✓ The electric field assumed to be uniform and constant, unaffected by the charges carried by the jet</li> <li>✓ Use asymptotic approximation was applied in a long distance from the nozzle.</li> <li>✓ Tangential electric force assumed to be zero.</li> <li>✓ Using nonlinear rheological constitutive equation (Ostwald–de Waele law), nonlinear behavior of fluid jet were investigated.</li> </ul>	1998	[150]
Jong Wook	Droplet formation model <ul style="list-style-type: none"> <li>✓ Droplet formation of charged fluid jet was studied in this model.</li> <li>✓ The ratio of mass, energy and electric charge transition are the most important parameters on droplet formation.</li> <li>✓ Deformation and breakup of droplets were investigated too.</li> <li>✓ Newtonian and non-Newtonian fluids</li> <li>✓ Only for high conductivity and viscose fluids</li> </ul>	2000	[226]

**TABLE 1.5** (Continued)

Researchers	Model	Year	Ref.
Reneker, D. H.	Reneker model	2000	[227]
Yarin, A. L.	<ul style="list-style-type: none"> <li>✓ For description of instabilities in viscoelastic jets.</li> <li>✓ Using molecular chain theory, behavior of polymer chain of spring-bead model in electric field was studied.</li> <li>✓ Electric force based on electric field cause instability of fluid jet while repulsion force between surface charges make perturbation and bending instability.</li> <li>✓ The motion paths of these two cases were studied</li> <li>✓ Governing equations: momentum balance, motion equations for each bead, Maxwell tension and Columbic equations</li> </ul>		
Hohman, M. Shin, M.	Stability Theory <ul style="list-style-type: none"> <li>✓ This model is based on a dielectric model with some modification for Newtonian fluids.</li> <li>✓ This model can describe whipping, bending and Rayleigh instabilities and introduced new ballooning instability.</li> <li>✓ Four motion regions were introduced: dipping mode, spindle mode, oscillating mode, precession mode.</li> <li>✓ Surface charge density introduced as the most effective parameter on instability formation.</li> <li>✓ Effect of fluid conductivity and viscosity on nanofibers diameter were discussed.</li> <li>✓ Steady solutions may be obtained only if the surface charge density at the nozzle is set to zero or a very low value.</li> </ul>	2001	[60]

**TABLE 1.5** (Continued)

Researchers	Model	Year	Ref.
Feng, J. J	<ul style="list-style-type: none"> <li>✓ Modifying Hohman model</li> <li>✓ For both Newtonian and non-Newtonian fluids</li> <li>✓ Unlike Hohman model, the initial surface charge density was not zero, so the “ballooning instability” did not accrue.</li> <li>✓ Only for steady-state part of the jet</li> <li>✓ Simplifying the electric field equation which Hohman used in order to eliminate ballooning instability.</li> </ul>	2002	[153]
Wan–Guo–Pan	<p>Wan–Guo–Pan model</p> <ul style="list-style-type: none"> <li>✓ They introduced thermo-electro-hydro dynamics model in electrospinning process</li> <li>✓ This model is a modification on Spivak model which mentioned before</li> <li>✓ The governing equations in this model: Modified Maxwell equation, Navier–Stocks equations, and several rheological constitutive equations.</li> </ul>	2004	[175]
Ji-Haun	<p>AC-electrospinning model</p> <ul style="list-style-type: none"> <li>✓ Whipping instability in this model was distinguished as the most effective parameter on uncontrollable deposition of nanofibers.</li> <li>✓ Applying AC current can reduce this instability so make oriented nanofibers.</li> <li>✓ This model found a relationship between axial distance from nozzle and jet diameter.</li> <li>✓ This model also connected ac frequency and jet diameter.</li> </ul>	2005	[172]



**TABLE 1.5** (Continued)

Researchers	Model	Year	Ref.
Roozmond (Eindhoven University and Technology)	Combination of slender body and dielectric model In this model, a new model for viscoelastic jets in electrospinning was presented by combining these two models. All variables were assumed uniform in cross-section of the jet, but they changed in during $z$ direction. Nanofiber diameter can be predicted.	2007	[228]
Wan	Electromagnetic model ✓ Results indicated that the electromagnetic field which made because of electrical field in charged polymeric jet is the most important reason of helix motion of jet during the process.	2012	[229]
Dasri	Dasri model ✓ This model was presented for description of unstable behavior of fluid jet during electrospinning. ✓ This instability causes random deposition of nanofiber on surface of the collector. ✓ This model described dynamic behavior of fluid by combining assumption of Reneker and Spivak models.	2012	[230]

The most frequent numeric mathematical methods which were used in different models are listed in Table 1.6:

**TABLE 1.6** Applied numerical methods for electrospinning

Method	Ref.
Relaxation method	[153, 159, 231]
Boundary integral method (boundary element method)	[199, 226]
Semi-inverse method	[159, 172]
(Integral) control-volume formulation	[224]

**TABLE 1.6** (Continued)

<b>Method</b>	<b>Ref.</b>
Finite element method	[223]
Kutta–Merson method	[232]
Lattice Boltzmann method with finite difference method	[233]

## 1.11 ELECTROSPINNING SIMULATION

Electrospun polymer nanofibers demonstrate outstanding mechanical and thermodynamic properties as compared with macroscopic-scale structures. These features are attributed to nanofiber microstructure [234–254]. Theoretical modeling predicts the nanostructure formations during electrospinning. This prediction could be verified by various experimental condition and analysis methods that called are simulation. Numerical simulations can be compared with experimental observations as the last evidence [149, 236].

Parametric analysis and accounting complex geometries in simulation of electrospinning are extremely difficult due to the nonlinearity nature in the problem. Therefore, a lot of researches have done to develop an existing electrospinning simulation of viscoelastic liquids [231].

## KEYWORDS

- **Electrospinning**
- **Freeze-drying**
- **Laser-based techniques**
- **Molecular dynamics**
- **Momentum balance**
- **Nanocoatings**
- **Nanoparticles**
- **Nanostructures**
- **Proton exchange mat**
- **Quantum dots**

## REFERENCES

1. Poole, C. P.; and Owens, F. J.; Introduction to Nanotechnology. New Jersey, Hoboken: Wiley; **2003**, 400 p.
2. Nalwa, H. S.; Nanostructured Materials and Nanotechnology: Concise Edition. Gulf Professional Publishing; **2001**, 324 p.
3. Gleiter, H.; Nanostructured materials: state of the art and perspectives. *Nanostruct. Mater.* **1995**, *6(1)*, 3–14.
4. Wong, Y.; et al. Selected applications of nanotechnology in textiles. *AUTEX Res. J.* **2006**, *6(1)*, 1–8.
5. Yu, B.; and Meyyappan, M.; Nanotechnology: role in emerging nanoelectronics. *Solid-State Electron.* **2006**, *50(4)*, 536–544.
6. Farokhzad, O. C.; and Langer, R.; Impact of nanotechnology on drug delivery. *ACS Nano.* **2009**, *3(1)*, 16–20.
7. Serrano, E.; Rus, G.; and Garcia-Martinez, J.; Nanotechnology for sustainable energy. *Renew. Sust. Energ. Rev.* **2009**, *13(9)*, 2373–2384.
8. Dreher, K. L.; Health and environmental impact of nanotechnology: toxicological assessment of manufactured nanoparticles. *Toxicol. Sci.* **2004**, *77(1)*, 3–5.
9. Bhushan, B.; Introduction to nanotechnology. In: Springer Handbook of Nanotechnology. Springer; **2010**, 1–13.
10. Ratner, D.; and Ratner, M. A.; Nanotechnology and Homeland Security: New Weapons for New Wars. Prentice Hall Professional; **2004**, 145 p.
11. Aricò, A. S.; et al. Nanostructured materials for advanced energy conversion and storage devices. *Nat. Mater.* **2005**, *4(5)*, 366–377.
12. Wang, Z. L.; Nanomaterials for nanoscience and nanotechnology. *Charact. Nanophase Mater.* **2000**, 1–12.
13. Gleiter, H.; Nanostructured materials: basic concepts and microstructure. *Acta Mater.* **2000**, *48(1)*, 1–29.
14. Wang, X.; et al. A general strategy for nanocrystal synthesis. *Nature.* **2005**, *437(7055)*, 121–124.
15. Kelsall, R. W.; et al. Nanoscale Science and Technology. New York: Wiley Online Library; **2005**, 455.
16. Engel, E.; et al. Nanotechnology in regenerative medicine: the materials side. *Trends in Biotechnol.* **2008**, *26(1)*, 39–47.
17. Beachley, V.; and Wen, X.; Polymer nanofibrous structures: fabrication, biofunctionalization, and cell interactions. *Prog. Polym. Sci.* **2010**, *35(7)*, 868–892.
18. Gogotsi, Y.; Nanomaterials Handbook. New York: CRC Press; **2006**, 779.
19. Li, C.; and Chou, T.; A structural mechanics approach for the analysis of carbon nanotubes. *Int. J. Solids Struct.* **2003**, *40(10)*, 2487–2499.
20. Delerue, C.; and Lannoo, M.; Nanostructures: Theory and Modelling. Springer; **2004**, 304 p.
21. Pokropivny, V.; and Skorokhod, V.; Classification of nanostructures by dimensionality and concept of surface forms engineering in nanomaterial science. *Mater. Sci. Eng. C.* **2007**, *27(5)*, 990–993.

22. Balbuena, P.; and Seminario, J. M.; Nanomaterials: Design and Simulation: Design and Simulation. Elsevier; **2006**, *18*, 523.
23. Kawaguchi, T.; and Matsukawa, H.; Numerical study of nanoscale lubrication and friction at solid interfaces. *Mol. Phys.* **2002**, *100(19)*, 3161–3166.
24. Ponomarev, S. Y.; Thayer, K. M.; and Beveridge, D. L.; Ion Motions in Molecular Dynamics Simulations on DNA. Proceedings of the National Academy of Sciences of the United States of America. **2004**, *101(41)*, 14771–14775.
25. Loss, D.; and DiVincenzo, D. P.; Quantum computation with quantum dots. *Phys. Rev. A.* **1998**, *57(1)*, 120–125.
26. Theodosiou, T. C.; and Saravanos, D. A.; Molecular mechanics based finite element for carbon nanotube modeling. *Comput. Model. Eng. Sci.* **2007**, *19(2)*, 19–24.
27. Pokropivny, V.; and Skorokhod, V.; New dimensionality classifications of nanostructures. *Phys. E: Low-Dimens. Syst. Nanostruct.* **2008**, *40(7)*, 2521–2525.
28. Lieber, C. M.; One-dimensional nanostructures: chemistry, physics & applications. *Solid State Commun.* **1998**, *107(11)*, 607–616.
29. Emary, C.; Theory of Nanostructures. New York: Wiley; **2009**, 141.
30. Edelstein, A. S.; and Cammarata, R. C.; Nanomaterials: Synthesis, Properties and Applications. CRC Press; **1998**.
31. Grzelczak, M.; et al. Directed self-assembly of nanoparticles. *ACS Nano.* **2010**, *4(7)*, 3591–3605.
32. Hung, C.; et al. Strain directed assembly of nanoparticle arrays within a semiconductor. *J. Nanopart. Res.* **1999**, *1(3)*, 329–347.
33. Wang, L.; and Hong, R.; Synthesis, surface modification and characterisation of nanoparticles. *Polym. Compos.* **2001**, *2*, 13–51.
34. Lai, W.; et al. Synthesis of nanostructured materials by hot and cold plasma. In: *Int. Plasma Chem. Soc.* Orleans, France; **2012**, 5 p.
35. Petermann, N.; et al. Plasma synthesis of nanostructures for improved thermoelectric properties. *J. Phys. D: Appl. Phys.* **2011**, *44(17)*, 174034.
36. Ye, Y.; et al. RF Plasma Method. Google Patents: USA; **2001**.
37. Hyeon, T.; Chemical synthesis of magnetic nanoparticles. *Chem. Commun.* **2003**, *8*, 927–934.
38. Galvez, A.; et al. Carbon nanoparticles from laser pyrolysis. *Carbon.* **2002**, *40(15)*, 2775–2789.
39. Porterat, D.; Synthesis of Nanoparticles by Laser Pyrolysis. Google Patents: USA; **2012**.
40. Tiwari, J. N.; Tiwari, R. N.; and Kim, K. S.; Zero-dimensional, one-dimensional, two-dimensional and three-dimensional nanostructured materials for advanced electrochemical energy devices. *Prog. Mater. Sci.* **2012**, *57(4)*, 724–803.
41. Murray, P. T.; et al. Nanomaterials produced by laser ablation techniques Part I: synthesis and passivation of nanoparticles, in nondestructive evaluation for health monitoring and diagnostics. *Int. Soc. Opt. Phot.* **2006**, 61750–61750.
42. Dolgaev, S. I.; et al. Nanoparticles produced by laser ablation of solids in liquid environment. *Appl. Surf. Sci.* **2002**, *186(1)*, 546–551.
43. Becker, M. F.; et al. Metal nanoparticles generated by laser ablation. *Nanostruct. Mater.* **1998**, *10(5)*, 853–863.

44. Bonneau, F.; et al. Numerical simulations for description of UV laser interaction with gold nanoparticles embedded in silica. *Appl. Phys. B*. **2004**, *78*(3–4), 447–452.
45. Chen, Y. H.; and Yeh, C. S.; Laser ablation method: use of surfactants to form the dispersed Ag nanoparticles. *Colloids Surf. A: Physicochem. Eng. Asp.* **2002**, *197*(1), 133–139.
46. Andrady, A. L.; Science and Technology of Polymer Nanofibers. Hoboken: John Wiley & Sons Inc.; **2008**, 404 p.
47. Wang, H. S.; Fu, G. D.; and Li, X. S.; Functional polymeric nanofibers from electrospinning. *Recent Patents Nanotechnol.* **2009**, *3*(1), 21–31.
48. Ramakrishna, S.; An Introduction to Electrospinning and Nanofibers. World Scientific Publishing Company; **2005**, 396 p.
49. Reneker, D. H.; and Chun, I.; Nanometer diameter fibres of polymer, produced by electrospinning. *Nanotechnol.* **1996**, *7*(3), 216.
50. Doshi, J.; and Reneker, D. H.; Electrospinning process and applications of electrospun fibers. *J. Electrostat.* **1995**, *35*(2), 151–160.
51. Burger, C.; Hsiao, B.; and Chu, B.; Nanofibrous materials and their applications. *Ann. Rev. Mater. Res.* **2006**, *36*, 333–368.
52. Fang, J.; et al. Applications of electrospun nanofibers. *Chin. Sci. Bull.* **2008**, *53*(15), 2265–2286.
53. Ondarcuhu, T.; and Joachim, C.; Drawing a single nanofibre over hundreds of microns. *EPL (Europhys. Lett.)* **1998**, *42*(2), 215.
54. Nain, A. S.; et al. Drawing suspended polymer micro/nanofibers using glass micropipettes. *Appl. Phys. Lett.* **2006**, *89*(18), 183105–183105–3.
55. Bajakova, J.; et al. “Drawing”-the production of individual nanofibers by experimental method. In: *Nanocconf.* Brno, Czech Republic, EU; **2011**.
56. Feng, L.; et al. Super hydrophobic surface of aligned polyacrylonitrile nanofibers. *Angew. Chemie.* **2002**, *114*(7), 1269–1271.
57. Delvaux, M.; et al. Chemical and electrochemical synthesis of polyaniline micro-and nano-tubules. *Synthetic Met.* **2000**, *113*(3), 275–280.
58. Barnes, C. P.; et al. Nanofiber technology: designing the next generation of tissue engineering scaffolds. *Adv. Drug Deliv. Rev.* **2007**, *59*(14), 1413–1433.
59. Palmer, L. C.; and Stupp, S. I.; Molecular self-assembly into one-dimensional nanostructures. *Acc. Chem. Res.* **2008**, *41*(12), 1674–1684.
60. Hohman, M. M.; et al. Electrospinning and electrically forced jets. I. Stability theory. *Phys. Fluids.* **2001**, *13*, 2201–2220.
61. Hohman, M. M.; et al. Electrospinning and electrically forced jets. II. Applications. *Phys. Fluids.* **2001**, *13*, 2221.
62. Shin, Y. M.; et al. Experimental characterization of electrospinning: the electrically forced jet and instabilities. *Polym.* **2001**, *42*(25), 9955–9967.
63. Fridrikh, S. V.; et al. Controlling the fiber diameter during electrospinning. *Phys. Rev. Lett.* **2003**, *90*(14), 144502–144502.
64. Yarin, A. L.; Koombhongse, S.; and Reneker, D. H.; Taylor cone and jetting from liquid droplets in electrospinning of nanofibers. *J. Appl. Phys.* **2001**, *90*(9), 4836–4846.
65. Zeleny, J.; The electrical discharge from liquid points, and a hydrostatic method of measuring the electric intensity at their surfaces. *Phys. Rev.* **1914**, *3*(2), 69–91.

66. Reneker, D. H.; et al. Bending instability of electrically charged liquid jets of polymer solutions in electrospinning. *J. Appl. Phys.* **2000**, *87*, 4531–4547.
67. Frenot, A.; and Chronakis, I. S.; Polymer nanofibers assembled by electrospinning. *Current Opinion Colloid Interf. Sci.* **2003**, *8(1)*, 64–75.
68. Gilbert, W.; De Magne Transl. PF Mottelay, Dover, UK. New York: Dover Publications Inc.; **1958**, 366 p.
69. Tucker, N.; et al. The history of the science and technology of electrospinning from 1600 to 1995. *J. Eng. Fibers Fabrics.* **2012**, *7*, 63–73.
70. Hassounah, I.; Melt Electrospinning of Thermoplastic Polymers. Aachen: Hochschulbibliothek Rheinisch-Westfälische Technischen Hochschule Aachen; **2012**, 650 p.
71. Taylor, G. I.; The scientific papers of sir geoffrey ingram taylor. *Mech. Fluids.* **1971**, *4*.
72. Yeo, L. Y.; and Friend, J. R.; Electrospinning carbon nanotube polymer composite nanofibers. *J. Exp. Nanosci.* **2006**, *1(2)*, 177–209.
73. Bhardwaj, N.; and Kundu, S. C.; Electrospinning: a fascinating fiber fabrication technique. *Biotechnol. Adv.* **2010**, *28(3)*, 325–347.
74. Huang, Z. M.; et al. A review on polymer nanofibers by electrospinning and their applications in nanocomposites. *Compos. Sci. Technol.* **2003**, *63(15)*, 2223–2253.
75. Haghi, A. K.; Electrospinning of Nanofibers in Textiles. North Carolina: Apple Academic Press Inc; **2011**, 132.
76. Bhattacharjee, P.; Clayton, V.; and Rutledge, A. G.; Electrospinning and Polymer Nanofibers: Process Fundamentals. In: Comprehensive Biomaterials. Elsevier. **2011**, 497–512 p.
77. Garg, K.; and Bowlin, G. L.; Electrospinning jets and nanofibrous structures. *Biomecrofluidics.* **2011**, *5*, 13403–13421.
78. Angammana, C. J.; and Jayaram, S. H.; A Theoretical Understanding of the Physical Mechanisms of Electrospinning. In: Proc. ESA Annual Meeting on Electrostatics. Cleveland OH: Case Western Reserve University; **2011**, 1–9 p.
79. Reneker, D. H.; and Yarin, A. L.; Electrospinning jets and polymer nanofibers. *Polym.* **2008**, *49(10)*, 2387–2425.
80. Deitzel, J.; et al. The effect of processing variables on the morphology of electrospun nanofibers and textiles. *Polym.* **2001**, *42(1)*, 261–272.
81. Rutledge, G. C.; and Fridrikh, S. V.; Formation of fibers by electrospinning. *Adv. Drug Deliv. Rev.* **2007**, *59(14)*, 1384–1391.
82. De Vrieze, S.; et al. The effect of temperature and humidity on electrospinning. *J. Mater. Sci.* **2009**, *44(5)*, 1357–1362.
83. Kumar, P.; Effect of collector on electrospinning to fabricate aligned nanofiber. In: Department of Biotechnology and Medical Engineering. Rourkela: National Institute of Technology Rourkela; **2012**, 88 p.
84. Sanchez, C.; Arribart, H.; and Guille, M.; Biomimetism and bioinspiration as tools for the design of innovative materials and systems. *Nat. Mater.* **2005**, *4(4)*, 277–288.
85. Ko, F.; et al. Electrospinning of continuous carbon nanotube-filled nanofiber yarns. *Adv. Mater.* **2003**, *15(14)*, 1161–1165.
86. Stuart, M.; et al. Emerging applications of stimuli-responsive polymer materials. *Nat. Mater.* **2010**, *9(2)*, 101–113.

87. Gao, W.; Chan, J.; and Farokhzad, O.; pH-responsive nanoparticles for drug delivery. *Mol. Pharmaceutics*. **2010**, *7(6)*, 1913–1920.
88. Li, Y.; et al. Stimulus-responsive polymeric nanoparticles for biomedical applications. *Sci. China Chem.* **2010**, *53(3)*, 447–457.
89. Tirelli, N.; (Bio) Responsive nanoparticles. *Current Opinion Colloid Interf. Sci.* **2006**, *11(4)*, 210–216.
90. Bonini, M.; et al. A new way to prepare nanostructured materials: flame spraying of microemulsions. *J. Phys. Chem. B.* **2002**, *106(24)*, 6178–6183.
91. Thierry, B.; et al. Nanocoatings onto arteries via layer-by-layer deposition: toward the in vivo repair of damaged blood vessels. *J. Am. Chem. Soc.* **2003**, *125(25)*, 7494–7495.
92. Andradý, A.; Science and Technology of Polymer Nanofibers. Wiley. com. **2008**.
93. Carroll, C. P.; et al. Nanofibers from electrically driven viscoelastic jets: modeling and experiments. *Korea-Aust. Rheol. J.* **2008**, *20(3)*, 153–164.
94. Zhao, Y.; and Jiang, L.; Hollow micro/nanomaterials with multilevel interior structures. *Adv. Mater.* **2009**, *21(36)*, 3621–3638.
95. Carroll, C. P.; The development of a comprehensive simulation model for electrospinning. Cornell University; **2009**, *70*, 300 p.
96. Song, Y. S.; and Youn, J. R.; Modeling of rheological behavior of nanocomposites by Brownian dynamics simulation. *Korea-Aust. Rheol. J.* **2004**, *16(4)*, 201–212.
97. Dror, Y.; et al. Carbon nanotubes embedded in oriented polymer nanofibers by electrospinning. *Langmuir*. **2003**, *19(17)*, 7012–7020.
98. Gates, T.; et al. Computational materials: multi-scale modeling and simulation of nanostructured materials. *Compos. Sci. Technol.* **2005**, *65(15)*, 2416–2434.
99. Agic, A.; Multiscale mechanical phenomena in electrospun carbon nanotube composites. *J. Appl. Polym. Sci.* **2008**, *108(2)*, 1191–1200.
100. Teo, W.; and Ramakrishna, S.; Electrospun nanofibers as a platform for multifunctional, hierarchically organized nanocomposite. *Compos. Sci. Technol.* **2009**, *69(11)*, 1804–1817.
101. Silling, S.; and Bobaru, F.; Peridynamic modeling of membranes and fibers. *Int. J. Non-Linear Mech.* **2005**, *40(2)*, 395–409.
102. Berhan, L.; et al. Mechanical properties of nanotube sheets: alterations in joint morphology and achievable moduli in manufacturable materials. *J. Appl. Phys.* **2004**, *95(8)*, 4335–4345.
103. Heyden, S.; Network Modelling for the Evaluation of Mechanical Properties of Cellulose Fibre Fluff. Lund University; **2000**.
104. Collins, A. J.; et al. The value of modeling and simulation standards. Virginia Modeling, Analysis and Simulation Center. Virginia: Old Dominion University; **2011**, 1–8 p.
105. Kuwabara, S.; The forces experienced by randomly distributed parallel circular cylinders or spheres in a viscous flow at small Reynolds numbers. *J. Phys. Soc. Jpn.* **1959**, *14*, 527.
106. Brown, R.; Air Filtration: An Integrated Approach to the Theory and Applications of Fibrous Filters. New York: Pergamon Press New York; **1993**.

107. Buysse, W. M.; et al. A 2D model for the electrospinning process. In: Department of Mechanical Engineering. Eindhoven: Eindhoven University of Technology; **2008**, 75.
108. Ante, A.; and Budimir, M.; Design Multifunctional Product by Nanostructures. *Sciyo. com.* **2010**, 27.
109. Jackson, G.; and James, D.; The permeability of fibrous porous media. *Can. J. Chem. Eng.* **1986**, *64*(3), 364–374.
110. Sundmacher, K.; Fuel cell engineering: toward the design of efficient electrochemical power plants. *Ind. Eng. Chem. Res.* **2010**, *49*(21), 10159–10182.
111. Kim, Y.; et al. Electrospun bimetallic nanowires of PtRh and PtRu with compositional variation for methanol electrooxidation. *Electrochem. Commun.* **2008**, *10*(7), 1016–1019.
112. Kim, H.; et al. Pt and PtRh nanowire electrocatalysts for cyclohexane-fueled polymer electrolyte membrane fuel cell. *Electrochem. Commun.* **2009**, *11*(2), 446–449.
113. Formo, E.; et al. Functionalization of electrospun TiO<sub>2</sub> nanofibers with Pt nanoparticles and nanowires for catalytic applications. *Nano Lett.* **2008**, *8*(2), 668–672.
114. Xuyen, N.; et al. Hydrolysis-induced immobilization of Pt (acac)<sub>2</sub> on polyimide-based carbon nanofiber mat and formation of Pt nanoparticles. *J. Mater. Chem.* **2009**, *19*(9), 1283–1288.
115. Lee, K.; et al. Nafion nanofiber membranes. *ECS Transact.* **2009**, *25*(1), 1451–1458.
116. Qu, H.; Wei, S.; and Guo, Z.; Coaxial electrospun nanostructures and their applications. *J. Mater. Chem. A.* **2013**, *1*(38), 11513–11528.
117. Thavasi, V.; Singh, G.; and Ramakrishna, S.; Electrospun nanofibers in energy and environmental applications. *Energ. Environ. Sci.* **2008**, *1*(2), 205–221.
118. Dersch, R.; et al. Nanoprocessing of polymers: applications in medicine, sensors, catalysis, photonics. *Polym. Adv. Technol.* **2005**, *16*(2–3), 276–282.
119. Yih, T.; and Al-Fandi, M.; Engineered nanoparticles as precise drug delivery systems. *J. Cell. Biochem.* **2006**, *97*(6), 1184–1190.
120. Kenawy, E.; et al. Release of tetracycline hydrochloride from electrospun poly (ethylene-co-vinylacetate), poly (lactic acid), and a blend. *J. Controlled Release.* **2002**, *81*(1), 57–64.
121. Verreck, G.; et al. Incorporation of drugs in an amorphous state into electrospun nanofibers composed of a water-insoluble, nonbiodegradable polymer. *J. Controlled Release.* **2003**, *92*(3), 349–360.
122. Zeng, J.; et al. Biodegradable electrospun fibers for drug delivery. *J. Controlled Release.* **2003**, *92*(3), 227–231.
123. Luu, Y.; et al. Development of a nanostructured DNA delivery scaffold via electrospinning of PLGA and PLA–PEG block copolymers. *J. Controlled Release.* **2003**, *89*(2), 341–353.
124. Zong, X.; et al. Structure and process relationship of electrospun bioabsorbable nanofiber membranes. *Polym.* **2002**, *43*(16), 4403–4412.
125. Yu, D.; et al. PVP nanofibers prepared using co-axial electrospinning with salt solution as sheath fluid. *Mater. Lett.* **2012**, *67*(1), 78–80.
126. Verreck, G.; et al. Preparation and characterization of nanofibers containing amorphous drug dispersions generated by electrostatic spinning. *Pharm. Res.* **2003**, *20*(5), 810–817.



127. Jiang, H.; et al. Preparation and characterization of ibuprofen-loaded poly (lactide-co-glycolide)/poly (ethylene glycol)-g-chitosan electrospun membranes. *J. Biomater. Sci. Polym. Edn.* **2004**, *15*(3), 279–296.
128. Yang, D.; Li, Y.; and Nie, J.; Preparation of gelatin/PVA nanofibers and their potential application in controlled release of drugs. *Carbohydr. Polym.* **2007**, *69*(3), 538–543.
129. Kim, K.; et al. Incorporation and controlled release of a hydrophilic antibiotic using poly (lactide-co-glycolide)-based electrospun nanofibrous scaffolds. *J. Controlled Release.* **2004**, *98*(1), 47–56.
130. Xu, X.; et al. Ultrafine medicated fibers electrospun from W/O emulsions. *J. Controlled Release.* **2005**, *108*(1), 33–42.
131. Zeng, J.; et al. Poly (vinyl alcohol) nanofibers by electrospinning as a protein delivery system and the retardation of enzyme release by additional polymer coatings. *Biomacromol.* **2005**, *6*(3), 1484–1488.
132. Yun, J.; et al. Effect of oxyfluorination on electromagnetic interference shielding behavior of MWCNT/PVA/PAAc composite microcapsules. *Euro. Polym. J.* **2010**, *46*(5), 900–909.
133. Jiang, H.; et al. A facile technique to prepare biodegradable coaxial electrospun nanofibers for controlled release of bioactive agents. *J. Controlled Release.* **2005**, *108*(2), 237–243.
134. He, C.; Huang, Z.; and Han, X.; Fabrication of drug-loaded electrospun aligned fibrous threads for suture applications. *J. Biomed. Mater. Res. Part A.* **2009**, *89*(1), 80–95.
135. Qi, R.; et al. Electrospun poly (lactic-co-glycolic acid)/halloysite nanotube composite nanofibers for drug encapsulation and sustained release. *J. Mater. Chem.* **2010**, *20*(47), 10622–10629.
136. Reneker, D. H.; et al. Electrospinning of nanofibers from polymer solutions and melts. *Adv. Appl. Mech.* **2007**, *41*, 343–346.
137. Haghi, A. K.; and Zaikov, G.; Advances in Nanofibre Research. Smithers Rapra Technology; **2012**, 194 p.
138. Maghsoodloo, S.; et al. A detailed review on mathematical modeling of electrospun nanofibers. *Polym. Res. J.* **2012**, *6*, 361–379.
139. Fritzson, P.; Principles of object-oriented modeling and simulation with Modelica 2.1. Wiley-IEEE Press; **2010**.
140. Robinson, S.; Simulation: The Practice of Model Development and Use. Wiley; **2004**, 722 p.
141. Carson, I. I.; and John, S.; Introduction to modeling and simulation. In: Proceedings of the 36th Conference on Winter Simulation. Washington, DC: Winter Simulation Conference; **2004**, 9–16 p.
142. Banks, J.; Handbook of Simulation. Wiley Online Library; **1998**, 342 p.
143. Pritsker, A. B.; and Alan, B.; Principles of Simulation Modeling. New York: Wiley; **1998**, 426 p.
144. Yu, J. H.; Fridrikh, S. V.; and Rutledge, G. C.; The role of elasticity in the formation of electrospun fibers. *Polym.* **2006**, *47*(13), 4789–4797.
145. Han, T.; Yarin, A. L.; and Reneker, D. H.; Viscoelastic electrospun jets: initial stresses and elongational rheometry. *Polym.* **2008**, *49*(6), 1651–1658.

146. Bhattacharjee, P. K.; et al. Extensional stress growth and stress relaxation in entangled polymer solutions. *J. Rheol.* **2003**, *47*, 269–290.
147. Paruchuri, S.; and Brenner, M. P.; Splitting of a liquid jet. *Phys. Rev. Lett.* **2007**, *98*(13), 134502–134504.
148. Ganan-Calvo, A. M.; On the theory of electrohydrodynamically driven capillary jets. *J. Fluid Mech.* **1997**, *335*, 165–188.
149. Liu, L.; and Dzenis, Y. A.; Simulation of electrospun nanofibre deposition on stationary and moving substrates. *Micro Nano Lett.* **2011**, *6*(6), 408–411.
150. Spivak, A. F.; and Dzenis, Y. A.; Asymptotic decay of radius of a weakly conductive viscous jet in an external electric field. *Appl. Phys. Lett.* **1998**, *73*(21), 3067–3069.
151. Jaworek, A.; and Krupa, A.; Classification of the modes of EHD spraying. *J. Aerosol Sci.* **1999**, *30*(7), 873–893.
152. Senador, A. E., Shaw, M. T.; and Mather, P. T.; Electrospinning of polymeric nanofibers: analysis of jet formation. In: *Mater. Res. Soc.* California, USA: Cambridge Univ Press; **2000**, 11 p.
153. Feng, J. J.; The stretching of an electrified non-Newtonian jet: a model for electrospinning. *Phys. Fluids.* **2002**, *14*(11), 3912–3927.
154. Feng, J. J.; Stretching of a straight electrically charged viscoelastic jet. *J. Non-Newtonian Fluid Mech.* **2003**, *116*(1), 55–70.
155. Spivak, A. F.; Dzenis, Y. A.; and Reneker, D. H.; A model of steady state jet in the electrospinning process. *Mech. Res. Commun.* **2000**, *27*(1), 37–42.
156. Yarin, A. L.; Koombhongse, S.; and Reneker, D. H.; Bending instability in electrospinning of nanofibers. *J. Appl. Phys.* **2001**, *89*, 3018.
157. Gradoń, L.; Principles of momentum, mass and energy balances. *Chem. Eng. Chem. Process Technol.* *1*, 1–6.
158. Bird, R. B.; Stewart, W. E.; and Lightfoot, E. N.; Transport Phenomena. New York: Wiley & Sons, Incorporated, John; **1960**, 2, 808.
159. Peters, G. W. M.; Hulsen, M. A.; and Solberg, R. H. M.; A Model for Electrospinning Viscoelastic Fluids, in Department of Mechanical Engineering. Eindhoven: Eindhoven University of Technology; **2007**, 26 p.
160. Whitaker, R. D.; An historical note on the conservation of mass. *J. Chem. Educ.* **1975**, *52*(10), 658.
161. He, J. H.; et al. Mathematical models for continuous electrospun nanofibers and electrospun nanoporous microspheres. *Polym. Int.* **2007**, *56*(11), 1323–1329.
162. Xu, L.; Liu, F.; and Faraz, N.; Theoretical model for the electrospinning nanoporous materials process. *Comput. Math. Appl.* **2012**, *64*(5), 1017–1021.
163. Heilbron, J. L.; Electricity in the 17th and 18th Century: A Study of Early Modern Physics. University of California Press; **1979**, 437 p.
164. Orito, S.; and Yoshimura, M.; Can the universe be charged? *Phys. Rev. Lett.* **1985**, *54*(22), 2457–2460.
165. Karra, S.; Modeling electrospinning process and a numerical scheme using Lattice Boltzmann method to simulate viscoelastic fluid flows. In: Indian Institute of Technology. Chennai: Texas A & M University; **2007**, 60 p.
166. Hou, S. H.; and Chan, C. K.; Momentum equation for straight electrically charged jet. *Appl. Math. Mech.* **2011**, *32*(12), 1515–1524.

167. Maxwell, J. C.; Electrical Research of the Honorable Henry Cavendish, 426, in Cambridge University Press, Cambridge, Editor. Cambridge, UK: Cambridge University Press; **1878**.
168. Vught, R. V.; Simulating the dynamical behaviour of electrospinning processes. In: Department of Mechanical Engineering. Eindhoven: Eindhoven University of Technology; **2010**, 68.
169. Jeans, J. H.; The Mathematical Theory of Electricity and Magnetism. London: Cambridge University Press; **1927**, 536.
170. Truesdell, C.; and Noll, W.; The Non-Linear Field Theories of Mechanics. Springer; **2004**, 579 p.
171. Roylance, D.; Constitutive equations. In: Lecture Notes. Department of Materials Science and Engineering. Cambridge: Massachusetts Institute of Technology; **2000**, 10 p.
172. He, J. H.; Wu, Y.; and Pang, N.; A mathematical model for preparation by AC-electrospinning process. *Int. J. Nonlinear Sci. Numer. Simul.* **2005**, 6(3), 243–248.
173. Little, R. W.; Elasticity. Courier Dover Publications; **1999**, 431.
174. Clauset, A.; Shalizi, C. R.; and Newman, M. E. J.; Power-law distributions in empirical data. *SIAM Rev.* **2009**, 51(4), 661–703.
175. Wan, Y.; Guo, Q.; and Pan, N.; Thermo-electro-hydrodynamic model for electrospinning process. *Int. J. Nonlinear Sci. Numer. Simul.* **2004**, 5(1), 5–8.
176. Giesekus, H.; Die elastizität von flüssigkeiten. *Rheol. Acta.* **1966**, 5(1), 29–35.
177. Giesekus, H.; The physical meaning of Weissenberg's hypothesis with regard to the second normal-stress difference. In: The Karl Weissenberg 80th Birthday Celebration Essays. Eds. Harris, J.; and Weissenberg, K.; East African Literature Bureau; **1973**, 103–112 p.
178. Wiest, J. M.; A differential constitutive equation for polymer melts. *Rheol. Acta.* **1989**, 28(1), 4–12.
179. Bird, R. B.; and Wiest, J. M.; Constitutive equations for polymeric liquids. *Ann. Rev. Fluid Mech.* **1995**, 27(1), 169–193.
180. Giesekus, H.; A simple constitutive equation for polymer fluids based on the concept of deformation-dependent tensorial mobility. *J. Non-Newtonian Fluid Mech.* **1982**, 11(1), 69–109.
181. Oliveira, P. J.; On the numerical implementation of nonlinear viscoelastic models in a finite-volume method. *Numer. Heat Transfer: Part B: Fundam.* **2001**, 40(4), 283–301.
182. Simhambhatla, M.; and Leonov, A. I.; On the rheological modeling of viscoelastic polymer liquids with stable constitutive equations. *Rheol. Acta.* **1995**, 34(3), 259–273.
183. Giesekus, H.; A unified approach to a variety of constitutive models for polymer fluids based on the concept of configuration-dependent molecular mobility. *Rheol. Acta.* **1982**, 21(4–5), 366–375.
184. Eringen, A. C.; and Maugin, G. A.; Electrohydrodynamics. In: *Electrodynamics of Continua II*. Springer; **1990**, 551–573 p.
185. Hutter, K.; Electrohydrodynamics of continua (A. Cemal Eringen and Gerard A. Maugin). *SIAM Rev.* **1991**, 33(2), 315–320.

186. Kröger, M.; Simple models for complex nonequilibrium fluids. *Phys. Rep.* **2004**, *390(6)*, 453–551.
187. Denn, M. M.; Issues in viscoelastic fluid mechanics. *Ann. Rev. Fluid Mech.* **1990**, *22(1)*, 13–32.
188. Rosicky, P. J.; Doll, J. D.; and Friedman, H. L.; Brownian dynamics as smart monte carlo simulation. *J. Chem. Phys.* **1978**, *69*, 4628–4633.
189. Chen, J. C.; and Kim, A. S.; Brownian dynamics, molecular dynamics, and monte carlo modeling of colloidal systems. *Adv. Colloid Interf. Sci.* **2004**, *112(1)*, 159–173.
190. Pasini, P.; and Zannoni, C.; Computer Simulations of Liquid Crystals and Polymers. Erice: Springer; **2005**, *177*, 380 p.
191. Zhang, H.; and Zhang, P.; Local existence for the FENE-dumbbell model of polymeric fluids. *Arch. Rat. Mech. Anal.* **2006**, *181(2)*, 373–400.
192. Isihara, A.; Theory of high polymer solutions (the dumbbell model). *J. Chem. Phys.* **1951**, *19*, 397–343.
193. Masmoudi, N.; Well-posedness for the FENE dumbbell model of polymeric flows. *Commun. Pure Appl. Math.* **2008**, *61(12)*, 1685–1714.
194. Stockmayer, W. H.; et al. Dynamic properties of solutions. Models for chain molecule dynamics in dilute solution. *Discuss. Faraday Soc.* **1970**, *49*, 182–192.
195. Graham, R. S.; et al. Microscopic theory of linear, entangled polymer chains under rapid deformation including chain stretch and convective constraint release. *J. Rheol.* **2003**, *47*, 1171–1200.
196. Gupta, R. K.; Kennel, E.; and Kim, K. S.; Polymer Nanocomposites Handbook. CRC Press; **2010**.
197. Marrucci, G.; The free energy constitutive equation for polymer solutions from the dumbbell model. *J. Rheol.* **1972**, *16*, 321–331.
198. Reneker, D. H.; et al. Electrospinning of nanofibers from polymer solutions and melts. *Adv. Appl. Mech.* **2007**, *41*, 43–195.
199. Kowalewski, T. A.; Barral, S.; and Kowalczyk, T.; Modeling electrospinning of nanofibers. In: IUTAM Symposium on Modelling Nanomaterials and Nanosystems. Aalborg, Denmark: Springer; **2009**, 279–292 p.
200. Macosko, C. W.; Rheology: principles, measurements, and applications. Poughkeepsie. Newyork: Wiley-VCH; **1994**, 578 p.
201. Kowalewski, T. A.; Blonski, S.; and Barral, S.; Experiments and modelling of electrospinning process. *Tech. Sci.* **2005**, *53(4)*, 385–394.
202. Ma, W. K. A.; et al. Rheological modeling of carbon nanotube aggregate suspensions. *J. Rheol.* **2008**, *52*, 1311–1330.
203. Buysse, W. M.; A 2D Model for the Electrospinning Process, in Department of Mechanical Engineering. Eindhoven: Eindhoven University of Technology; **2008**, 71 p.
204. Silling, S. A.; and Bobaru, F.; Peridynamic modeling of membranes and fibers. *Int. J. Non-Linear Mech.* **2005**, *40(2)*, 395–409.
205. Teo, W. E.; and Ramakrishna, S.; Electrospun nanofibers as a platform for multifunctional, hierarchically organized nanocomposite. *Compos. Sci. Technol.* **2009**, *69(11)*, 1804–1817.
206. Wu, X.; and Dzenis, Y. A.; Elasticity of planar fiber networks. *J. Appl. Phys.* **2005**, *98(9)*, 93501.

207. Tatlier, M.; and Berhan, L.; Modelling the negative poisson's ratio of compressed fused fibre networks. *Phys. Status Solidi (b)*. **2009**, *246(9)*, 2018–2024.
208. Kuipers, B.; Qualitative Reasoning: Modeling and Simulation with Incomplete Knowledge. The MIT Press; **1994**, 554 p.
209. West, B. J.; Comments on the renormalization group, scaling and measures of complexity. *Chaos Solitons Fractals*. **2004**, *20(1)*, 33–44.
210. De Gennes, P. G.; and Witten, T. A.; Scaling Concepts in Polymer Physics. Cornell University Press; **1980**, 324 p.
211. He, J. H.; and Liu, H. M.; Variational approach to nonlinear problems and a review on mathematical model of electrospinning. *Nonlinear Anal.* **2005**, *63*, e919–e929.
212. He, J. H.; Wan, Y. Q.; and Yu, J. Y.; Allometric scaling and instability in electrospinning. *Int. J. Nonlinear Sci. Numer. Simul.* **2004**, *5(3)*, 243–252.
213. He, J. H.; Wan, Y. Q.; and Yu, J. Y.; Allometric scaling and instability in electrospinning. *Int. J. Nonlinear Sci. Numer. Simul.* **2004**, *5*, 243–252.
214. He, J. H.; and Wan, Y. Q.; Allometric scaling for voltage and current in electrospinning. *Polym.* **2004**, *45*, 6731–6734.
215. He, J. H.; Wan, Y. Q.; and Yu, J. Y.; Scaling law in electrospinning: relationship between electric current and solution flow rate. *Polym.* **2005**, *46*, 2799–2801.
216. He, J. H.; Wanc, Y. Q.; and Yuc, J. Y.; Application of vibration technology to polymer electrospinning. *Int. J. Nonlinear Sci. Numer. Simul.* **2004**, *5(3)*, 253–262.
217. Kessick, R.; Fenn, J.; and Tepper, G.; The use of AC potentials in electro spraying and electrospinning processes. *Polym.* **2004**, *45(9)*, 2981–2984.
218. Boucher, D. F.; and Alves, G. E.; Dimensionless Numbers. Part 1 and 2. **1959**.
219. Ipsen, D. C.; Units Dimensions and Dimensionless Numbers. New York: McGraw Hill Book Company Inc; **1960**, 466 p.
220. Langhaar, H. L.; Dimensional Analysis and Theory of Models. New York: Wiley; **1951**, *2*, 166
221. McKinley, G. H.; Dimensionless groups for understanding free surface flows of complex fluids. *Bull. Soc. Rheol.* **2005**, *2005*, 6–9.
222. Carroll, C. P.; et al. Nanofibers from electrically driven viscoelastic jets: modeling and experiments. *Korea-Aust. Rheol. J.* **2008**, *20(3)*, 153–164.
223. Saville, D.; Electrohydrodynamics: the Taylor-Melcher leaky dielectric model. *Ann. Rev. Fluid Mech.* **1997**, *29(1)*, 27–64.
224. Ramos, J. I.; Force fields on inviscid, slender, annular liquid. *Int. J. Numer. Methods Fluids.* **1996**, *23*, 221–239.
225. Saville, D. A.; Electrohydrodynamics: the Taylor-Melcher leaky dielectric model. *Ann. Rev. Fluid Mech.* **1997**, *29(1)*, 27–64.
226. Senador, A. E.; Shaw, M. T.; and Mather, P. T.; Electrospinning of polymeric nanofibers: analysis of jet formation. In: MRS Proceedings. Cambridge Univ Press; **2000**.
227. Reneker, D. H.; et al. Bending instability of electrically charged liquid jets of polymer solutions in electrospinning. *J. Appl. Phys.* **2000**, *87*, 4531.
228. Peters, G.; Hulslen, M.; and Solberg, R.; A Model for Electrospinning Viscoelastic Fluids.
229. Wan, Y.; et al. Modeling and simulation of the electrospinning jet with archimedean spiral. *Adv. Sci. Lett.* **2012**, *10(1)*, 590–592.

230. Dasri, T.; Mathematical models of bead-spring jets during electrospinning for fabrication of nanofibers. *Walailak J. Sci. Technol.* **2012**, *9*.
231. Solberg, R. H. M.; Position-Controlled Deposition for Electrospinning. Eindhoven: Eindhoven University of Technology; **2007**, 75 p.
232. Holzmeister, A.; Yarin, A. L.; and Wendorff, J. H.; Barb formation in electrospinning: experimental and theoretical investigations. *Polym.* **2010**, *51(12)*, 2769–2778.
233. Karra, S.; Modeling electrospinning process and a numerical scheme using Lattice Boltzmann method to simulate viscoelastic fluid flows. **2012**.
234. Arinstein, A.; et al. Effect of supramolecular structure on polymer nanofibre elasticity. *Nat. Nanotechnol.* **2007**, *2(1)*, 59–62.
235. Lu, C.; et al. Computer simulation of electrospinning. Part I. Effect of solvent in electrospinning. *Polym.* **2006**, *47(3)*, 915–921.
236. Greenfeld, I.; et al. Polymer dynamics in semidilute solution during electrospinning: a simple model and experimental observations. *Phys. Rev.* **2011**, *84(4)*, 41806–41815.
237. Ly, H. V.; and Tran, H. T.; Modeling and control of physical processes using proper orthogonal decomposition. *Math. Comput. Modell.* **2001**, *33(1)*, 223–236.
238. Peiró, J.; and Sherwin, S.; Finite difference, finite element and finite volume methods for partial differential equations. In: *Handbook of Materials Modeling*. London: Springer; **2005**, 2415–2446 p.
239. Kitano, H.; Computational systems biology. *Nature.* **2002**, *420(6912)*, 206–210.
240. Gerald, C. F.; and Wheatley, P. O.; *Applied Numerical Analysis*. Ed. 7th. Addison-Wesley; **2007**, 624 p.
241. Burden, R. L.; and Faires, J. D.; *Numerical Analysis*. Thomson Brooks/Cole; **2005**, *8*, 850 p.
242. Lawrence, C. E.; *Partial Differential Equations*. American Mathematical Society; **2010**, 749 p.
243. Quarteroni, A.; Quarteroni, A. M.; and Valli, A.; *Numerical Approximation of Partial Differential Equations*. Springer; **2008**, *23*, 544 p.
244. Butcher, J. C.; A history of Runge-Kutta methods. *Appl. Numer. Math.* **1996**, *20(3)*, 247–260.
245. Cartwright, J. H. E.; and Piro, O.; The dynamics of Runge–Kutta methods. *Int. J. Bifurcat. Chaos.* **1992**, *2(03)*, 427–449.
246. Zingg, D. W.; and Chisholm, T. T.; Runge–Kutta methods for linear ordinary differential equations. *Appl. Numer. Math.* **1999**, *31(2)*, 227–238.
247. Butcher, J. C.; *The Numerical Analysis of Ordinary Differential Equations: Runge-Kutta and General Linear Methods*. Wiley-Interscience; **1987**, 512 p.
248. Reznik, S. N.; et al. Evolution of a compound droplet attached to a core-shell nozzle under the action of a strong electric field. *Phys. Fluids.* **2006**, *18(6)*, 062101–062101–13.
249. Reznik, S. N.; et al. Transient and steady shapes of droplets attached to a surface in a strong electric field. *J. Fluid Mech.* **2004**, *516*, 349–377.
250. Donea, J.; and Huerta, A.; *Finite Element Methods for Flow Problems*. Wiley. com. **2003**, 362 p.
251. Zienkiewicz, O. C.; and Taylor, R. L.; *The Finite Element Method: Solid Mechanics*. Butterworth-Heinemann; **2000**, *2*, 459 p.

252. Brenner, S. C.; and Scott, L. R.; The Mathematical Theory of Finite Element Methods. Springer; **2008**, *15*, 397 p.
253. Bathe, K. J.; Finite Element Procedures. Prentice Hall Englewood Cliffs; **1996**, *2*, 1037 p.
254. Reddy, J. N.; An Introduction to the Finite Element Method. New York: McGraw-Hill; **2006**, *2*, 912 p.

# References

## 1 1. Electrospinning Process: A Comprehensive Review and Update

1. Poole, C. P.; and Owens, F. J.; Introduction to Nanotechnology. New Jersey, Hoboken: Wiley; 2003, 400 p.
2. Nalwa, H. S.; Nanostructured Materials and Nanotechnology: Concise Edition. Gulf Professional Publishing; 2001, 324 p.
3. Gleiter, H.; Nanostructured materials: state of the art and perspectives. *Nanostruct. Mater.* 1995, 6(1), 3-14.
4. Wong, Y.; et al. Selected applications of nanotechnology in textiles. *AUTEX Res. J.* 2006, 6(1), 1-8.
5. Yu, B.; and Meyyappan, M.; Nanotechnology: role in emerging nanoelectronics. *Solid-State Electron.* 2006, 50(4), 536-544.
6. Farokhzad, O. C.; and Langer, R.; Impact of nanotechnology on drug delivery. *ACS Nano.* 2009, 3(1), 16-20.
7. Serrano, E.; Rus, G.; and Garcia-Martinez, J.; Nanotechnology for sustainable energy. *Renew. Sust. Energ. Rev.* 2009, 13(9), 2373-2384.
8. Dreher, K. L.; Health and environmental impact of nanotechnology: toxicological assessment of manufactured nanoparticles. *Toxicol. Sci.* 2004, 77(1), 3-5.
9. Bhushan, B.; Introduction to nanotechnology. In: *Springer Handbook of Nanotechnology.* Springer; 2010, 1-13.
10. Ratner, D.; and Ratner, M. A.; Nanotechnology and Homeland Security: New Weapons for New Wars. Prentice Hall Professional; 2004, 145 p.
11. Aricò, A. S.; et al. Nanostructured materials for advanced energy conversion and storage devices. *Nat. Mater.* 2005, 4(5), 366-377.
12. Wang, Z. L.; Nanomaterials for nanoscience and nanotechnology. *Charact. Nanophase Mater.* 2000, 1-12.
13. Gleiter, H.; Nanostructured materials: basic concepts and microstructure. *Acta Mater.* 2000, 48(1), 1-29.



14. Wang, X.; et al. A general strategy for nanocrystal synthesis. *Nature*. 2005, 437(7055), 121-124.
15. Kelsall, R. W.; et al. *Nanoscale Science and Technology*. New York: Wiley Online Library; 2005, 455.
16. Engel, E.; et al. Nanotechnology in regenerative medicine: the materials side. *Trends in Biotechnol.* 2008, 26(1), 39-47.
17. Beachley, V.; and Wen, X.; Polymer nanofibrous structures: fabrication, biofunctionalization, and cell interactions. *Prog. Polym. Sci.* 2010, 35(7), 868-892.
18. Gogotsi, Y.; *Nanomaterials Handbook*. New York: CRC Press; 2006, 779.
19. Li, C.; and Chou, T.; A structural mechanics approach for the analysis of carbon nanotubes. *Int. J. Solids Struct.* 2003, 40(10), 2487-2499.
20. Delerue, C.; and Lannoo, M.; *Nanostructures: Theory and Modelling*. Springer; 2004, 304 p.
21. Pokropivny, V.; and Skorokhod, V.; Classification of nanostructures by dimensionality and concept of surface forms engineering in nanomaterial science. *Mater. Sci. Eng. C.* 2007, 27(5), 990-993.
22. Balbuena, P.; and Seminario, J. M.; *Nanomaterials: Design and Simulation: Design and Simulation*. Elsevier; 2006, 18, 523.
23. Kawaguchi, T.; and Matsukawa, H.; Numerical study of nanoscale lubrication and friction at solid interfaces. *Mol. Phys.* 2002, 100(19), 3161-3166.
24. Ponomarev, S. Y.; Thayer, K. M.; and Beveridge, D. L.; Ion Motions in Molecular Dynamics Simulations on DNA. *Proceedings of the National Academy of Sciences of the United States of America.* 2004, 101(41), 14771-14775.
25. Loss, D.; and DiVincenzo, D. P.; Quantum computation with quantum dots. *Phys. Rev. A.* 1998, 57(1), 120-125.
26. Theodosiou, T. C.; and Saravanos, D. A.; Molecular mechanics based finite element for carbon nanotube modeling. *Comput. Model. Eng. Sci.* 2007, 19(2), 19-24.

27. Pokropivny, V.; and Skorokhod, V.; New dimensionality classifications of nanostructures. *Phys. E: Low-Dimens. Syst. Nanostruct.* 2008, 40(7), 2521-2525.
28. Lieber, C. M.; One-dimensional nanostructures: chemistry, physics & applications. *Solid State Commun.* 1998, 107(11), 607-616.
29. Emary, C.; *Theory of Nanostructures.* New York: Wiley; 2009, 141.
30. Edelstein, A. S.; and Cammarata, R. C.; *Nanomaterials: Synthesis, Properties and Applications.* CRC Press; 1998.
31. Grzelczak, M.; et al. Directed self-assembly of nanoparticles. *ACS Nano.* 2010, 4(7), 3591-3605.
32. Hung, C.; et al. Strain directed assembly of nanoparticle arrays within a semiconductor. *J. Nanopart. Res.* 1999, 1(3), 329-347.
33. Wang, L.; and Hong, R.; Synthesis, surface modification and characterisation of nanoparticles. *Polym. Compos.* 2001, 2, 13-51.
34. Lai, W.; et al. Synthesis of nanostructured materials by hot and cold plasma. In: *Int. Plasma Chem. Soc. Orleans, France; 2012, 5 p.*
35. Petermann, N.; et al. Plasma synthesis of nanostructures for improved thermoelectric properties. *J. Phys. D: Appl. Phys.* 2011, 44(17), 174034.
36. Ye, Y.; et al. RF Plasma Method. *Google Patents: USA; 2001.*
37. Hyeon, T.; Chemical synthesis of magnetic nanoparticles. *Chem. Commun.* 2003, 8, 927-934.
38. Galvez, A.; et al. Carbon nanoparticles from laser pyrolysis. *Carbon.* 2002, 40(15), 2775-2789.
39. Porterat, D.; *Synthesis of Nanoparticles by Laser Pyrolysis.* *Google Patents: USA; 2012.*
40. Tiwari, J. N.; Tiwari, R. N.; and Kim, K. S.; Zero-dimensional, one-dimensional, two-dimensional and three-dimensional nanostructured materials for advanced electrochemical energy devices. *Prog. Mater. Sci.* 2012, 57(4), 724-803.

41. Murray, P. T.; et al. Nanomaterials produced by laser ablation techniques Part I: synthesis and passivation of nanoparticles, in nondestructive evaluation for health monitoring and diagnostics. *Int. Soc. Opt. Phot.* 2006, 61750-61750.
42. Dolgaev, S. I.; et al. Nanoparticles produced by laser ablation of solids in liquid environment. *Appl. Surf. Sci.* 2002, 186(1), 546-551.
43. Becker, M. F.; et al. Metal nanoparticles generated by laser ablation. *Nanostruct. Mater.* 1998, 10(5), 853-863.
44. Bonneau, F.; et al. Numerical simulations for description of UV laser interaction with gold nanoparticles embedded in silica. *Appl. Phys. B.* 2004, 78(3-4), 447-452.
45. Chen, Y. H.; and Yeh, C. S.; Laser ablation method: use of surfactants to form the dispersed Ag nanoparticles. *Colloids Surf. A: Physicochem. Eng. Asp.* 2002, 197(1), 133-139.
46. Andradý, A. L.; *Science and Technology of Polymer Nanofibers.* Hoboken: John Wiley & Sons Inc.; 2008, 404 p.
47. Wang, H. S.; Fu, G. D.; and Li, X. S.; Functional polymeric nanofibers from electrospinning. *Recent Patents Nanotechnol.* 2009, 3(1), 21-31.
48. Ramakrishna, S.; *An Introduction to Electrospinning and Nanofibers.* World Scientific Publishing Company; 2005, 396 p.
49. Reneker, D. H.; and Chun, I.; Nanometer diameter fibres of polymer, produced by electrospinning. *Nanotechnol.* 1996, 7(3), 216.
50. Doshi, J.; and Reneker, D. H.; Electrospinning process and applications of electrospun fibers. *J. Electrostat.* 1995, 35(2), 151-160.
51. Burger, C.; Hsiao, B.; and Chu, B.; Nanofibrous materials and their applications. *Ann. Rev. Mater. Res.* 2006, 36, 333-368.
52. Fang, J.; et al. Applications of electrospun nanofibers. *Chin. Sci. Bull.* 2008, 53(15), 2265-2286.

53. Ondarcuhu, T.; and Joachim, C.; Drawing a single nanofibre over hundreds of microns. *EPL (Europhys. Lett.)* 1998, 42(2), 215.
54. Nain, A. S.; et al. Drawing suspended polymer micro/nanofibers using glass micropipettes. *Appl. Phys. Lett.* 2006, 89(18), 183105-183105-3.
55. Bajakova, J.; et al. "Drawing"-the production of individual nanofibers by experimental method. In: *Nanoconf. Brno, Czech Republic, EU; 2011.*
56. Feng, L.; et al. Super hydrophobic surface of aligned polyacrylonitrile nanofibers. *Angew. Chemie.* 2002, 114(7), 1269-1271.
57. Delvaux, M.; et al. Chemical and electrochemical synthesis of polyaniline micro-and nano-tubules. *Synthetic Met.* 2000, 113(3), 275-280.
58. Barnes, C. P.; et al. Nanofiber technology: designing the next generation of tissue engineering scaffolds. *Adv. Drug Deliv. Rev.* 2007, 59(14), 1413-1433.
59. Palmer, L. C.; and Stupp, S. I.; Molecular self-assembly into one-dimensional nanostructures. *Acc. Chem. Res.* 2008, 41(12), 1674-1684.
60. Hohman, M. M.; et al. Electrospinning and electrically forced jets. I. Stability theory. *Phys. Fluids.* 2001, 13, 2201-2220.
61. Hohman, M. M.; et al. Electrospinning and electrically forced jets. II. Applications. *Phys. Fluids.* 2001, 13, 2221.
62. Shin, Y. M.; et al. Experimental characterization of electrospinning: the electrically forced jet and instabilities. *Polym.* 2001, 42(25), 9955-9967.
63. Fridrikh, S. V.; et al. Controlling the fiber diameter during electrospinning. *Phys. Rev. Lett.* 2003, 90(14), 144502-144502.
64. Yarin, A. L.; Koombhongse, S.; and Reneker, D. H.; Taylor cone and jetting from liquid droplets in electrospinning of nanofibers. *J. Appl. Phys.* 2001, 90(9), 4836-4846.
65. Zeleny, J.; The electrical discharge from liquid

points, and a hydrostatic method of measuring the electric intensity at their surfaces. *Phys. Rev.* 1914, 3(2), 69-91.

66. Reneker, D. H.; et al. Bending instability of electrically charged liquid jets of polymer solutions in electrospinning. *J. Appl. Phys.* 2000, 87, 4531-4547.

67. Frenot, A.; and Chronakis, I. S.; Polymer nanofibers assembled by electrospinning. *Current Opinion Colloid Interf. Sci.* 2003, 8(1), 64-75.

68. Gilbert, W.; *De Magnete Transl.* PF Mottelay, Dover, UK. New York: Dover Publications Inc.; 1958, 366 p.

69. Tucker, N.; et al. The history of the science and technology of electrospinning from 1600 to 1995. *J. Eng. Fibers Fabrics.* 2012, 7, 63-73.

70. Hassounah, I.; *Melt Electrospinning of Thermoplastic Polymers.* Aachen: Hochschulbibliothek Rheinisch-Westfälische Technischen Hochschule Aachen; 2012, 650 p.

71. Taylor, G. I.; *The scientific papers of sir geoffrey ingram taylor.* *Mech. Fluids.* 1971, 4.

72. Yeo, L. Y.; and Friend, J. R.; Electrospinning carbon nanotube polymer composite nanofibers. *J. Exp. Nanosci.* 2006, 1(2), 177-209.

73. Bhardwaj, N.; and Kundu, S. C.; Electrospinning: a fascinating fiber fabrication technique. *Biotechnol. Adv.* 2010, 28(3), 325-347.

74. Huang, Z. M.; et al. A review on polymer nanofibers by electrospinning and their applications in nanocomposites. *Compos. Sci. Technol.* 2003, 63(15), 2223-2253.

75. Haghi, A. K.; *Electrospinning of Nanofibers in Textiles.* North Carolina: Apple Academic Press Inc; 2011, 132.

76. Bhattacharjee, P.; Clayton, V.; and Rutledge, A. G.; *Electrospinning and Polymer Nanofibers: Process Fundamentals.* In: *Comprehensive Biomaterials.* Elsevier. 2011, 497-512 p.

77. Garg, K.; and Bowlin, G. L.; Electrospinning jets and nanofibrous structures. *Biomicrofluidics.* 2011, 5, 13403-13421.

78. Angammana, C. J.; and Jayaram, S. H.; A Theoretical Understanding of the Physical Mechanisms of Electrospinning. In: Proc. ESA Annual Meeting on Electrostatics. Cleveland OH: Case Western Reserve University; 2011, 1-9 p.
79. Reneker, D. H.; and Yarin, A. L.; Electrospinning jets and polymer nanofibers. *Polym.* 2008, 49(10), 2387-2425.
80. Deitzel, J.; et al. The effect of processing variables on the morphology of electrospun nanofibers and textiles. *Polym.* 2001, 42(1), 261-272.
81. Rutledge, G. C.; and Fridrikh, S. V.; Formation of fibers by electrospinning. *Adv. Drug Deliv. Rev.* 2007, 59(14), 1384-1391.
82. De Vrieze, S.; et al. The effect of temperature and humidity on electrospinning. *J. Mater. Sci.* 2009, 44(5), 1357-1362.
83. Kumar, P.; Effect of collector on electrospinning to fabricate aligned nanofiber. In: Department of Biotechnology and Medical Engineering. Rourkela: National Institute of Technology Rourkela; 2012, 88 p.
84. Sanchez, C.; Arribart, H.; and Guille, M.; Biomimetism and bioinspiration as tools for the design of innovative materials and systems. *Nat. Mater.* 2005, 4(4), 277-288.
85. Ko, F.; et al. Electrospinning of continuous carbon nanotube-filled nanofiber yarns. *Adv. Mater.* 2003, 15(14), 1161-1165.
86. Stuart, M.; et al. Emerging applications of stimuli-responsive polymer materials. *Nat. Mater.* 2010, 9(2), 101-113.
87. Gao, W.; Chan, J.; and Farokhzad, O.; pH-responsive nanoparticles for drug delivery. *Mol. Pharmaceutics.* 2010, 7(6), 1913-1920.
88. Li, Y.; et al. Stimulus-responsive polymeric nanoparticles for biomedical applications. *Sci. China Chem.* 2010, 53(3), 447-457.
89. Tirelli, N.; (Bio) Responsive nanoparticles. *Current Opinion Colloid Interf. Sci.* 2006, 11(4), 210-216.

90. Bonini, M.; et al. A new way to prepare nanostructured materials: flame spraying of microemulsions. *J. Phys. Chem. B.* 2002, 106(24), 6178-6183.
91. Thierry, B.; et al. Nanocoatings onto arteries via layer-by-layer deposition: toward the in vivo repair of damaged blood vessels. *J. Am. Chem. Soc.* 2003, 125(25), 7494- 7495.
92. Andradý, A.; *Science and Technology of Polymer Nanofibers.* Wiley. com. 2008.
93. Carroll, C. P.; et al. Nanofibers from electrically driven viscoelastic jets: modeling and experiments. *Korea-Aust. Rheol. J.* 2008, 20(3), 153-164.
94. Zhao, Y.; and Jiang, L.; Hollow micro/nanomaterials with multilevel interior structures. *Adv. Mater.* 2009, 21(36), 3621-3638.
95. Carroll, C. P.; The development of a comprehensive simulation model for electrospinning. Cornell University; 2009, 70, 300 p.
96. Song, Y. S.; and Youn, J. R.; Modeling of rheological behavior of nanocomposites by Brownian dynamics simulation. *Korea-Aust. Rheol. J.* 2004, 16(4), 201-212.
97. Dror, Y.; et al. Carbon nanotubes embedded in oriented polymer nanofibers by electrospinning. *Langmuir.* 2003, 19(17), 7012-7020.
98. Gates, T.; et al. Computational materials: multi-scale modeling and simulation of nanostructured materials. *Compos. Sci. Technol.* 2005, 65(15), 2416-2434.
99. Agic, A.; Multiscale mechanical phenomena in electrospun carbon nanotube composites. *J. Appl. Polym. Sci.* 2008, 108(2), 1191-1200.
100. Teo, W.; and Ramakrishna, S.; Electrospun nanofibers as a platform for multifunctional, hierarchically organized nanocomposite. *Compos. Sci. Technol.* 2009, 69(11), 1804-1817.
101. Silling, S.; and Bobaru, F.; Peridynamic modeling of membranes and fibers. *Int. J. Non-Linear Mech.* 2005, 40(2), 395-409.
102. Berhan, L.; et al. Mechanical properties of nanotube

sheets: alterations in joint morphology and achievable moduli in manufacturable materials. *J. Appl. Phys.* 2004, 95(8), 4335-4345.

103. Heyden, S.; *Network Modelling for the Evaluation of Mechanical Properties of Cellulose Fibre Fluff*. Lund University; 2000.

104. Collins, A. J.; et al. The value of modeling and simulation standards. Virginia Modeling, Analysis and Simulation Center. Virginia: Old Dominion University; 2011, 1-8 p.

105. Kuwabara, S.; The forces experienced by randomly distributed parallel circular cylinders or spheres in a viscous flow at small Reynolds numbers. *J. Phys. Soc. Jpn.* 1959, 14, 527.

106. Brown, R.; *Air Filtration: An Integrated Approach to the Theory and Applications of Fibrous Filters*. New York: Pergamon Press New York; 1993.

107. Buysse, W. M.; et al. A 2D model for the electrospinning process. In: Department of Mechanical Engineering. Eindhoven: Eindhoven University of Technology; 2008, 75.

108. Ante, A.; and Budimir, M.; Design Multifunctional Product by Nanostructures. *Sciyo. com.* 2010, 27.

109. Jackson, G.; and James, D.; The permeability of fibrous porous media. *Can. J. Chem. Eng.* 1986, 64(3), 364-374.

110. Sundmacher, K.; Fuel cell engineering: toward the design of efficient electrochemical power plants. *Ind. Eng. Chem. Res.* 2010, 49(21), 10159-10182.

111. Kim, Y.; et al. Electrospun bimetallic nanowires of PtRh and PtRu with compositional variation for methanol electrooxidation. *Electrochem. Commun.* 2008, 10(7), 1016-1019.

112. Kim, H.; et al. Pt and PtRh nanowire electrocatalysts for cyclohexane-fueled polymer electrolyte membrane fuel cell. *Electrochem. Commun.* 2009, 11(2), 446-449.

113. Formo, E.; et al. Functionalization of electrospun TiO<sub>2</sub> nanofibers with Pt nanoparticles and nanowires for catalytic applications. *Nano Lett.* 2008, 8(2), 668-672.



114. Xuyen, N.; et al. Hydrolysis-induced immobilization of Pt (acac) 2 on polyimidebased carbon nanofiber mat and formation of Pt nanoparticles. *J. Mater. Chem.* 2009, 19(9), 1283-1288.
115. Lee, K.; et al. Nafion nanofiber membranes. *ECS Transact.* 2009, 25(1), 1451-1458.
116. Qu, H.; Wei, S.; and Guo, Z.; Coaxial electrospun nanostructures and their applications. *J. Mater. Chem. A.* 2013, 1(38), 11513-11528.
117. Thavasi, V.; Singh, G.; and Ramakrishna, S.; Electrospun nanofibers in energy and environmental applications. *Energ. Environ. Sci.* 2008, 1(2), 205-221.
118. Dersch, R.; et al. Nanoprocessing of polymers: applications in medicine, sensors, catalysis, photonics. *Polym. Adv. Technol.* 2005, 16(2-3), 276-282.
119. Yih, T.; and Al-Fandi, M.; Engineered nanoparticles as precise drug delivery systems. *J. Cell. Biochem.* 2006, 97(6), 1184-1190.
120. Kenawy, E.; et al. Release of tetracycline hydrochloride from electrospun poly (ethylene-co-vinylacetate), poly (lactic acid), and a blend. *J. Controlled Release.* 2002, 81(1), 57-64.
121. Verreck, G.; et al. Incorporation of drugs in an amorphous state into electrospun nanofibers composed of a water-insoluble, nonbiodegradable polymer. *J. Controlled Release.* 2003, 92(3), 349-360.
122. Zeng, J.; et al. Biodegradable electrospun fibers for drug delivery. *J. Controlled Release.* 2003, 92(3), 227-231.
123. Luu, Y.; et al. Development of a nanostructured DNA delivery scaffold via electrospinning of PLGA and PLA-PEG block copolymers. *J. Controlled Release.* 2003, 89(2), 341-353.
124. Zong, X.; et al. Structure and process relationship of electrospun bioabsorbable nanofiber membranes. *Polym.* 2002, 43(16), 4403-4412.
125. Yu, D.; et al. PVP nanofibers prepared using co-axial electrospinning with salt solution as sheath fluid. *Mater. Lett.* 2012, 67(1), 78-80.

126. Verreck, G.; et al. Preparation and characterization of nanofibers containing amorphous drug dispersions generated by electrostatic spinning. *Pharm. Res.* 2003, 20(5), 810-817.
127. Jiang, H.; et al. Preparation and characterization of ibuprofen-loaded poly (lactide-co-glycolide)/poly (ethylene glycol)-g-chitosan electrospun membranes. *J. Biomater. Sci. Polym. Edn.* 2004, 15(3), 279-296.
128. Yang, D.; Li, Y.; and Nie, J.; Preparation of gelatin/PVA nanofibers and their potential application in controlled release of drugs. *Carbohydr. Polym.* 2007, 69(3), 538-543.
129. Kim, K.; et al. Incorporation and controlled release of a hydrophilic antibiotic using poly (lactide-co-glycolide)-based electrospun nanofibrous scaffolds. *J. Controlled Release.* 2004, 98(1), 47-56.
130. Xu, X.; et al. Ultrafine medicated fibers electrospun from W/O emulsions. *J. Controlled Release.* 2005, 108(1), 33-42.
131. Zeng, J.; et al. Poly (vinyl alcohol) nanofibers by electrospinning as a protein delivery system and the retardation of enzyme release by additional polymer coatings. *Biomacromol.* 2005, 6(3), 1484-1488.
132. Yun, J.; et al. Effect of oxyfluorination on electromagnetic interference shielding behavior of MWCNT/PVA/PAAc composite microcapsules. *Euro. Polym. J.* 2010, 46(5), 900-909.
133. Jiang, H.; et al. A facile technique to prepare biodegradable coaxial electrospun nanofibers for controlled release of bioactive agents. *J. Controlled Release.* 2005, 108(2), 237-243.
134. He, C.; Huang, Z.; and Han, X.; Fabrication of drug-loaded electrospun aligned fibrous threads for suture applications. *J. Biomed. Mater. Res. Part A.* 2009, 89(1), 80-95.
135. Qi, R.; et al. Electrospun poly (lactic-co-glycolic acid)/halloysite nanotube composite nanofibers for drug encapsulation and sustained release. *J. Mater. Chem.* 2010, 20(47), 10622-10629.

136. Reneker, D. H.; et al. Electrospinning of nanofibers from polymer solutions and melts. *Adv. Appl. Mech.* 2007, 41, 343-346.
137. Haghi, A. K.; and Zaikov, G.; *Advances in Nanofibre Research*. Smithers Rapra Technology; 2012, 194 p.
138. Maghsoodloo, S.; et al. A detailed review on mathematical modeling of electrospun nanofibers. *Polym. Res. J.* 2012, 6, 361-379.
139. Fritzson, P.; *Principles of object-oriented modeling and simulation with Modelica 2.1*. Wiley-IEEE Press; 2010.
140. Robinson, S.; *Simulation: The Practice of Model Development and Use*. Wiley; 2004, 722 p.
141. Carson, I. I.; and John, S.; Introduction to modeling and simulation. In: *Proceedings of the 36th Conference on Winter Simulation*. Washington, DC: Winter Simulation Conference; 2004, 9-16 p.
142. Banks, J.; *Handbook of Simulation*. Wiley Online Library; 1998, 342 p.
143. Pritsker, A. B.; and Alan, B.; *Principles of Simulation Modeling*. New York: Wiley; 1998, 426 p.
144. Yu, J. H.; Fridrikh, S. V.; and Rutledge, G. C.; The role of elasticity in the formation of electrospun fibers. *Polym.* 2006, 47(13), 4789-4797.
145. Han, T.; Yarin, A. L.; and Reneker, D. H.; Viscoelastic electrospun jets: initial stresses and elongational rheometry. *Polym.* 2008, 49(6), 1651-1658.
146. Bhattacharjee, P. K.; et al. Extensional stress growth and stress relaxation in entangled polymer solutions. *J. Rheol.* 2003, 47, 269-290.
147. Paruchuri, S.; and Brenner, M. P.; Splitting of a liquid jet. *Phys. Rev. Lett.* 2007, 98(13), 134502-134504.
148. Ganan-Calvo, A. M.; On the theory of electrohydrodynamically driven capillary jets. *J. Fluid Mech.* 1997, 335, 165-188.
149. Liu, L.; and Dzenis, Y. A.; Simulation of electrospun nanofibre deposition on stationary and moving substrates. *Micro Nano Lett.* 2011, 6(6), 408-411.

150. Spivak, A. F.; and Dzenis, Y. A.; Asymptotic decay of radius of a weakly conductive viscous jet in an external electric field. *Appl. Phys. Lett.* 1998, 73(21), 3067-3069.
151. Jaworek, A.; and Krupa, A.; Classification of the modes of EHD spraying. *J. Aerosol Sci.* 1999, 30(7), 873-893.
152. Senador, A. E., Shaw, M. T.; and Mather, P. T.; Electrospinning of polymeric nanofibers: analysis of jet formation. In: *Mater. Res. Soc. California, USA: Cambridge Univ Press; 2000, 11 p.*
153. Feng, J. J.; The stretching of an electrified non-Newtonian jet: a model for electrospinning. *Phys. Fluids.* 2002, 14(11), 3912-3927.
154. Feng, J. J.; Stretching of a straight electrically charged viscoelastic jet. *J. Non-Newtonian Fluid Mech.* 2003, 116(1), 55-70.
155. Spivak, A. F.; Dzenis, Y. A.; and Reneker, D. H.; A model of steady state jet in the electrospinning process. *Mech. Res. Commun.* 2000, 27(1), 37-42.
156. Yarin, A. L.; Koombhongse, S.; and Reneker, D. H.; Bending instability in electrospinning of nanofibers. *J. Appl. Phys.* 2001, 89, 3018.
157. Gradoń, L.; Principles of momentum, mass and energy balances. *Chem. Eng. Chem. Process Technol.* 1, 1-6.
158. Bird, R. B.; Stewart, W. E.; and Lightfoot, E. N.; *Transport Phenomena.* New York: Wiley & Sons, Incorporated, John; 1960, 2, 808.
159. Peters, G. W. M.; Hulsen, M. A.; and Solberg, R. H. M.; A Model for Electrospinning Viscoelastic Fluids, in Department of Mechanical Engineering. Eindhoven: Eindhoven University of Technology; 2007, 26 p.
160. Whitaker, R. D.; An historical note on the conservation of mass. *J. Chem. Educ.* 1975, 52(10), 658.
161. He, J. H.; et al. Mathematical models for continuous electrospun nanofibers and electrospun nanoporous microspheres. *Polym. Int.* 2007, 56(11), 1323-1329.
162. Xu, L.; Liu, F.; and Faraz, N.; Theoretical model for

the electrospinning nanoporous materials process. *Comput. Math. Appl.* 2012, 64(5), 1017-1021.

163. Heilbron, J. L.; *Electricity in the 17th and 18th Century: A Study of Early Modern Physics*. University of California Press; 1979, 437 p.

164. Orito, S.; and Yoshimura, M.; Can the universe be charged? *Phys. Rev. Lett.* 1985, 54(22), 2457-2460.

165. Karra, S.; Modeling electrospinning process and a numerical scheme using Lattice Boltzmann method to simulate viscoelastic fluid flows. In: *Indian Institute of Technology*. Chennai: Texas A & M University; 2007, 60 p.

166. Hou, S. H.; and Chan, C. K.; Momentum equation for straight electrically charged jet. *Appl. Math. Mech.* 2011, 32(12), 1515-1524.

167. Maxwell, J. C.; *Electrical Research of the Honorable Henry Cavendish*, 426, in *Cambridge University Press*, Cambridge, Editor. Cambridge, UK: Cambridge University Press; 1878.

168. Vught, R. V.; Simulating the dynamical behaviour of electrospinning processes. In: *Department of Mechanical Engineering*. Eindhoven: Eindhoven University of Technology; 2010, 68.

169. Jeans, J. H.; *The Mathematical Theory of Electricity and Magnetism*. London: Cambridge University Press; 1927, 536.

170. Truesdell, C.; and Noll, W.; *The Non-Linear Field Theories of Mechanics*. Springer; 2004, 579 p.

171. Roylance, D.; Constitutive equations. In: *Lecture Notes*. Department of Materials Science and Engineering. Cambridge: Massachusetts Institute of Technology; 2000, 10 p.

172. He, J. H.; Wu, Y.; and Pang, N.; A mathematical model for preparation by AC-electrospinning process. *Int. J. Nonlinear Sci. Numer. Simul.* 2005, 6(3), 243-248.

173. Little, R. W.; *Elasticity*. Courier Dover Publications; 1999, 431.

174. Clauset, A.; Shalizi, C. R.; and Newman, M. E. J.; Power-law distributions in empirical data. *SIAM Rev.* 2009,

51(4), 661-703.

175. Man, Y.; Guo, Q.; and Pan, N.;  
Thermo-electro-hydrodynamic model for electrospinning  
process. *Int. J. Nonlinear Sci. Numer. Simul.* 2004, 5(1),  
5-8.

176. Giesekus, H.; Die elastizität von flüssigkeiten.  
*Rheol. Acta.* 1966, 5(1), 29-35.

177. Giesekus, H.; The physical meaning of Weissenberg's  
hypothesis with regard to the second normal-stress  
difference. In: *The Karl Weissenberg 80th Birthday  
Celebration Essays*. Eds. Harris, J.; and Weissenberg, K.;  
East African Literature Bureau; 1973, 103-112 p.

178. Wiest, J. M.; A differential constitutive equation for  
polymer melts. *Rheol. Acta.* 1989, 28(1), 4-12.

179. Bird, R. B.; and Wiest, J. M.; Constitutive equations  
for polymeric liquids. *Ann. Rev. Fluid Mech.* 1995, 27(1),  
169-193.

180. Giesekus, H.; A simple constitutive equation for  
polymer fluids based on the concept of  
deformation-dependent tensorial mobility. *J. Non-Newtonian  
Fluid Mech.* 1982, 11(1), 69-109.

181. Oliveira, P. J.; On the numerical implementation of  
nonlinear viscoelastic models in a finite-volume method.  
*Numer. Heat Transfer: Part B: Fundam.* 2001, 40(4),  
283-301.

182. Simhambhatla, M.; and Leonov, A. I.; On the  
rheological modeling of viscoelastic polymer liquids with  
stable constitutive equations. *Rheol. Acta.* 1995, 34(3),  
259- 273.

183. Giesekus, H.; A unified approach to a variety of  
constitutive models for polymer fluids based on the  
concept of configuration-dependent molecular mobility.  
*Rheol. Acta.* 1982, 21(4-5), 366-375.

184. Eringen, A. C.; and Maugin, G. A.;  
Electrohydrodynamics. In: *Electrodynamics of Continua II*.  
Springer; 1990, 551-573 p.

185. Hutter, K.; *Electrodynamics of continua* (A. Cemal  
Eringen and Gerard A. Maugin). *SIAM Rev.* 1991, 33(2),  
315-320.

186. Kröger, M.; Simple models for complex nonequilibrium fluids. *Phys. Rep.* 2004, 390(6), 453-551.
187. Denn, M. M.; Issues in viscoelastic fluid mechanics. *Ann. Rev. Fluid Mech.* 1990, 22(1), 13-32.
188. Rosky, P. J.; Doll, J. D.; and Friedman, H. L.; Brownian dynamics as smart monte carlo simulation. *J. Chem. Phys.* 1978, 69, 4628-4633.
189. Chen, J. C.; and Kim, A. S.; Brownian dynamics, molecular dynamics, and monte carlo modeling of colloidal systems. *Adv. Colloid Interf. Sci.* 2004, 112(1), 159-173.
190. Pasini, P.; and Zannoni, C.; *Computer Simulations of Liquid Crystals and Polymers*. Erice: Springer; 2005, 177, 380 p.
191. Zhang, H.; and Zhang, P.; Local existence for the FENE-dumbbell model of polymeric fluids. *Arch. Rat. Mech. Anal.* 2006, 181(2), 373-400.
192. Isihara, A.; Theory of high polymer solutions (the dumbbell model). *J. Chem. Phys.* 1951, 19, 397-343.
193. Masmoudi, N.; Well-posedness for the FENE dumbbell model of polymeric flows. *Commun. Pure Appl. Math.* 2008, 61(12), 1685-1714.
194. Stockmayer, W. H.; et al. Dynamic properties of solutions. Models for chain molecule dynamics in dilute solution. *Discuss. Faraday Soc.* 1970, 49, 182-192.
195. Graham, R. S.; et al. Microscopic theory of linear, entangled polymer chains under rapid deformation including chain stretch and convective constraint release. *J. Rheol.* 2003, 47, 1171-1200.
196. Gupta, R. K.; Kennel, E.; and Kim, K. S.; *Polymer Nanocomposites Handbook*. CRC Press; 2010.
197. Marrucci, G.; The free energy constitutive equation for polymer solutions from the dumbbell model. *J. Rheol.* 1972, 16, 321-331.
198. Reneker, D. H.; et al. Electrospinning of nanofibers from polymer solutions and melts. *Adv. Appl. Mech.* 2007, 41, 43-195.

199. Kowalewski, T. A.; Barral, S.; and Kowalczyk, T.; Modeling electrospinning of nanofibers. In: IUTAM Symposium on Modelling Nanomaterials and Nanosystems. Aalborg, Denmark: Springer;; 2009, 279-292 p.
200. Macosko, C. W.; Rheology: principles, measurements, and applications. Poughkeepsie. Newyork: Wiley-VCH; 1994, 578 p.
201. Kowalewski, T. A.; Blonski, S.; and Barral, S.; Experiments and modelling of electrospinning process. Tech. Sci. 2005, 53(4), 385-394.
202. Ma, W. K. A.; et al. Rheological modeling of carbon nanotube aggregate suspensions. J. Rheol. 2008, 52, 1311-1330.
203. Buysse, W. M.; A 2D Model for the Electrospinning Process, in Department of Mechanical Engineering. Eindhoven: Eindhoven University of Technology; 2008, 71 p.
204. Silling, S. A.; and Bobaru, F.; Peridynamic modeling of membranes and fibers. Int. J. Non-Linear Mech. 2005, 40(2), 395-409.
205. Teo, W. E.; and Ramakrishna, S.; Electrospun nanofibers as a platform for multifunctional, hierarchically organized nanocomposite. Compos. Sci. Technol. 2009, 69(11), 1804-1817.
206. Wu, X.; and Dzenis, Y. A.; Elasticity of planar fiber networks. J. Appl. Phys. 2005, 98(9), 93501.
207. Tatlier, M.; and Berhan, L.; Modelling the negative poisson's ratio of compressed fused fibre networks. Phys. Status Solidi (b). 2009, 246(9), 2018-2024.
208. Kuipers, B.; Qualitative Reasoning: Modeling and Simulation with Incomplete Knowledge. The MIT Press; 1994, 554 p.
209. West, B. J.; Comments on the renormalization group, scaling and measures of complexity. Chaos Solitons Fractals. 2004, 20(1), 33-44.
210. De Gennes, P. G.; and Witten, T. A.; Scaling Concepts in Polymer Physics. Cornell University Press; 1980, 324 p.
211. He, J. H.; and Liu, H. M.; Variational approach to nonlinear problems and a review on mathematical model of



- electrospinning. *Nonlinear Anal.* 2005, 63, e919-e929.
212. He, J. H.; Wan, Y. Q.; and Yu, J. Y.; Allometric scaling and instability in electrospinning. *Int. J. Nonlinear Sci. Numer. Simul.* 2004, 5(3), 243-252.
213. He, J. H.; Wan, Y. Q.; and Yu, J. Y.; Allometric scaling and instability in electrospinning. *Int. J. Nonlinear Sci. Numer. Simul.* 2004, 5, 243-252.
214. He, J. H.; and Wan, Y. Q.; Allometric scaling for voltage and current in electrospinning. *Polym.* 2004, 45, 6731-6734.
215. He, J. H.; Wan, Y. Q.; and Yu, J. Y.; Scaling law in electrospinning: relationship between electric current and solution flow rate. *Polym.* 2005, 46, 2799-2801.
216. He, J. H.; Wan, Y. Q.; and Yu, J. Y.; Application of vibration technology to polymer electrospinning. *Int. J. Nonlinear Sci. Numer. Simul.* 2004, 5(3), 253-262.
217. Kessick, R.; Fenn, J.; and Tepper, G.; The use of AC potentials in electrospinning and electrospinning processes. *Polym.* 2004, 45(9), 2981-2984.
218. Boucher, D. F.; and Alves, G. E.; Dimensionless Numbers. Part 1 and 2. 1959.
219. Ipsen, D. C.; Units Dimensions and Dimensionless Numbers. New York: McGraw Hill Book Company Inc; 1960, 466 p.
220. Langhaar, H. L.; Dimensional Analysis and Theory of Models. New York: Wiley; 1951, 2, 166
221. McKinley, G. H.; Dimensionless groups for understanding free surface flows of complex fluids. *Bull. Soc. Rheol.* 2005, 2005, 6-9.
222. Carroll, C. P.; et al. Nanofibers from electrically driven viscoelastic jets: modeling and experiments. *Korea-Aust. Rheol. J.* 2008, 20(3), 153-164.
223. Saville, D.; Electrohydrodynamics: the Taylor-Melcher leaky dielectric model. *Ann. Rev. Fluid Mech.* 1997, 29(1), 27-64.
224. Ramos, J. I.; Force fields on inviscid, slender, annular liquid. *Int. J. Numer. Methods Fluids.* 1996, 23,

221-239.

225. Saville, D. A.; Electrohydrodynamics: the Taylor-Melcher leaky dielectric model. *Ann. Rev. Fluid Mech.* 1997, 29(1), 27-64.

226. Senador, A. E.; Shaw, M. T.; and Mather, P. T.; Electrospinning of polymeric nanofibers: analysis of jet formation. In: *MRS Proceedings*. Cambridge Univ Press; 2000.

227. Reneker, D. H.; et al. Bending instability of electrically charged liquid jets of polymer solutions in electrospinning. *J. Appl. Phys.* 2000, 87, 4531.

228. Peters, G.; Hulsen, M.; and Solberg, R.; A Model for Electrospinning Viscoelastic Fluids.

229. Wan, Y.; et al. Modeling and simulation of the electrospinning jet with archimedean spiral. *Adv. Sci. Lett.* 2012, 10(1), 590-592.

230. Dasri, T.; Mathematical models of bead-spring jets during electrospinning for fabrication of nanofibers. *Malailak J. Sci. Technol.* 2012, 9.

231. Solberg, R. H. M.; Position-Controlled Deposition for Electrospinning. Eindhoven: Eindhoven University of Technology; 2007, 75 p.

232. Holzmeister, A.; Yarin, A. L.; and Wendorff, J. H.; Barb formation in electrospinning: experimental and theoretical investigations. *Polym.* 2010, 51(12), 2769-2778.

233. Karra, S.; Modeling electrospinning process and a numerical scheme using Lattice Boltzmann method to simulate viscoelastic fluid flows. 2012.

234. Arinstein, A.; et al. Effect of supramolecular structure on polymer nanofibre elasticity. *Nat. Nanotechnol.* 2007, 2(1), 59-62.

235. Lu, C.; et al. Computer simulation of electrospinning. Part I. Effect of solvent in electrospinning. *Polym.* 2006, 47(3), 915-921.

236. Greenfeld, I.; et al. Polymer dynamics in semidilute solution during electrospinning: a simple model and experimental observations. *Phys. Rev.* 2011, 84(4), 41806-41815.

237. Ly, H. V.; and Tran, H. T.; Modeling and control of physical processes using proper orthogonal decomposition. *Math. Comput. Modell.* 2001, 33(1), 223-236.
238. Peiró, J.; and Sherwin, S.; Finite difference, finite element and finite volume methods for partial differential equations. In: *Handbook of Materials Modeling*. London: Springer; 2005, 2415-2446 p.
239. Kitano, H.; Computational systems biology. *Nature*. 2002, 420(6912), 206-210.
240. Gerald, C. F.; and Wheatley, P. O.; *Applied Numerical Analysis*. Ed. 7th. AddisonWesley; 2007, 624 p.
241. Burden, R. L.; and Faires, J. D.; *Numerical Analysis*. Thomson Brooks/Cole; 2005, 8, 850 p.
242. Lawrence, C. E.; *Partial Differential Equations*. American Mathematical Society; 2010, 749 p.
243. Quarteroni, A.; Quarteroni, A. M.; and Valli, A.; *Numerical Approximation of Partial Differential Equations*. Springer; 2008, 23, 544 p.
244. Butcher, J. C.; A history of Runge-Kutta methods. *Appl. Numer. Math.* 1996, 20(3), 247-260.
245. Cartwright, J. H. E.; and Piro, O.; The dynamics of Runge-Kutta methods. *Int. J. Bifurcat. Chaos.* 1992, 2(03), 427-449.
246. Zingg, D. W.; and Chisholm, T. T.; Runge-Kutta methods for linear ordinary differential equations. *Appl. Numer. Math.* 1999, 31(2), 227-238.
247. Butcher, J. C.; *The Numerical Analysis of Ordinary Differential Equations: RungeKutta and General Linear Methods*. Wiley-Interscience; 1987, 512 p.
248. Reznik, S. N.; et al. Evolution of a compound droplet attached to a core-shell nozzle under the action of a strong electric field. *Phys. Fluids.* 2006, 18(6), 062101-062101-13.
249. Reznik, S. N.; et al. Transient and steady shapes of droplets attached to a surface in a strong electric field. *J. Fluid Mech.* 2004, 516, 349-377.
250. Donea, J.; and Huerta, A.; *Finite Element Methods for*

Flow Problems. Wiley. com. 2003, 362 p.

251. Zienkiewicz, O. C.; and Taylor, R. L.; The Finite Element Method: Solid Mechanics. Butterworth-Heinemann; 2000, 2, 459 p.

252. Brenner, S. C.; and Scott, L. R.; The Mathematical Theory of Finite Element Methods. Springer; 2008, 15, 397 p.

253. Bathe, K. J.; Finite Element Procedures. Prentice Hall Englewood Cliffs; 1996, 2, 1037 p.

254. Reddy, J. N.; An Introduction to the Finite Element Method. New York: McGrawHill; 2006, 2, 912 p.

## 2 2. Aluminium-Coated Polymer Films as Infrared Light Shields for Food Packing

1. Aihong G.; Xuejiao T.; Sujuan Z.; Key Eng. Mater. 2011, 474-476, 195-199.
2. Dombrowsky, L. A.; Rev. Gen. Therm. 1998, 37, 925-933.
3. King, D. E.; Drewry, D. G.; Sample, J. L.; Clemons, D. E.; Caruso, K. S.; Potocki, K. A.; Eng, D. A.; Mehoke, D. S.; Mattix, M. P.; Thomas, M. E.; Nagle, D. C.; Int. J. Appl. Ceram. Technol. 2009, 6(3), 355-361.
4. Shahidi, S.; Ghoranneviss, M.; Moazzenchi, B.; Anvari, E.; Rashidi, A.; Surf. Coat. Technol. 2007, 201, 5646-5650.
5. Takano, I.; Inoue, N.; Matsui, K.; Kokubu, S.; Sasase, M.; Isobe, S.; Surf. Coat. Technol. 1994, 66, 509-513.
6. O'Hare, L.; A., Leadley, S.; Parbhoo, B.; Surf. Interface Anal. 2002, 33, 335-342.
7. Greer, J.; Street R.; A.; Acta Mater. 2007, 55, 6345-6349.
8. Fortunato, E.; Nunes, P.; Marques, A.; Costa, D.; Aguas, H.; Ferreira, I.; Costa, M. E. V.; Godinho, M. H.; Almeida, P. L.; Borges, J. P.; Martins, R.; Surf. Coat. Technol. 2002, 151-152, 247-251.
9. Yanaka, M.; Henry, B., M.; Roberts, A. P.; Grovenor, C., R., M., Briggs, G., A., D., Sutton, A., P.; Miyamoto, T.; Tsukahara, Y.; Takeda, N.; Chjater, R., J., Thin Solid Films. 2001, 397, 176-185.
10. Bichler, C. H.; Kerbstadt, T.; Langowski, H. C.; Moosheimer, U. Surf. Coat. Technol. 1999, 112, 373-378.
11. Bichler, C. H.; Langowski, H. C.; Moosheimer, U.; Seifert, B.; J. Adhes. Sci. Technol. 1997, 11(2), 233-246.
12. Moosheimer, U.; Bichler, C. H.; Surf. Coat. Technol. 1999, 116, 812-819.
13. Oishi, T.; Goto, M.; Pihosh, Y.; Kasahara, A.; Tosa, M.; Appl. Polym. Sci. 2005, 241, 223-226.
14. Qi-Jia He; Ai-Min Zhang; Ling-Hong Guo; Polym. Plast. Technol. Eng. 2004, 43(3) 951-961.

15. Qui J.; Liu L. H.; Hsu P. F.; Appl. Surf. Sci. 2005, 111, 1912-1920.
16. Rahmatollahpur R.; Tahidi T.; Jamshidi-Chaleh K. J. Mat. Sci. 2010, 45, 1937.
17. Ozmihci, F.; Balkose, D.; Ulku, S.; J. Appl. Polym. Sci. 2001, 82, 2913-2921.
18. Balkose, D.; Oguz, K.; Ozyuzer, L.; Tari, S.; Arkis, E.; Omurlu, F.O.; J. Appl. Polym. Sci. 2012, 120, 1671-1678.
- 19.
20. Luongo, JP.; Infrared study of polypropylene. J. App. Polym. Sci. 1960, 9, 302-309.

#### 4 4. Trends on New Biodegradable Blends on the Basis of Copolymers 3-Hydroxybutyrate with Hydroxyvalerate and Segmented Polyetherurethane

1. Tian, H.; Tang, Z. et al.; *Progress in Polymer Science*. 2012, 37, 237. doi:10.1016/j.progpolymsci.2011.06.004.
2. Suyatma, N. E.; Copinet, A. et al.; *J Polym Environ*. 2004, 12(1), 1. doi: 15662543/04/0100-01/0.
3. Bonartsev, A. P.; Boskhomodgiev, A. P. et al.; *Mol. Cryst. Liquid Cryst*. 2012, 556 (1), 288.
4. Bagdi, K.; Molnar, K. et al.; *EXPRESS Polym. Lett*. 2011, 5(5), 417. doi: 10.3144/expresspolymlett.2011.41.
5. Shi, R.; Chen, D. et al.; *Int. J. Mol. Sci*. 2009, 10, 4223. doi:10.3390/ijms10104223.
6. Sanche z-Garcia, M. D.; Gimene z, E. et al.; *Carbohydr. Polym*. 2008, 71(2), 235. doi:10.1016/j.carbpol.2007.05.041.
7. Yang, K-K.; Wang, X.-L. et al.; *J. Ind. Eng. Chem*. 2007, 13(4), 485.
8. Iordanski, A. L.; Rogovina, S. Z. et al.; *Dokl. Phys. Chem*. 2010, 431, Part 2, 60. doi:10.1134/S0012501610040020.
9. Smirnov, A. I.; Belford, R. L. et al.; (Ed. Berliner, L. J.). New York: Plenum Press; 1998, Ch. 3, 83-108.
10. Karpova, S. G.; Iordanskii, A. L. et al.; *Russ. J. Phys. Chem. B*. 2012, 6(1), 72.
11. Bloembergen, S.; Holden, D. A. et al.; *Marchessault: Macromolecules*. 1989, 22, 1656.
12. Di Lorenzo, M. L.; Raimo, M. et al.; *J. Macromol. Sci.-Phys*. 2011, B40(5), 639.
13. Selikhova, V. I.; Shcherbina, M. A. et al.; *Polym. Chem*. 2002, 22(4), 605 (in Russian).
14. Kamaev, P. P.; Aliev, I. I. et al.; *Polymer*, 2001, 42, 515.
15. Freier, T.; Kunze, C. et al.; *Biomaterials*, 2002,

23(13), 2649.

16. Artsis, M. I.; Bonartsev, A. P. et al.; *Mol. Cryst. Liq. Cryst.* 2012, 555, 232. doi: 10.1080/15421406.2012.635549.

17. Zaikov, G. E.; Iordanskii, A. L. et al.; *Diffusion of Electrolytes in Polymers. Ser. New Concepts in Polymer Science.* Utrecht-Tokyo: VSP BV; 1988, 229-231.



## 5 5. New Biologically Active Composite Materials on the Basis of Dialdehyde Cellulose

1. Khashirova, S. Yu.; Zaikov, G. E.; Malkanduev, U. A.; Sivov, N. A.; Martynenko, A. I.; Synthesis of new monomers on diallyl guanidine basis and their ability to radical (co) polymerization, *J. Biochemistry and Chemistry: Research and developments*. New York: Nova Science Publishers Inc; 2003, 39-48.
2. Sivov, N. A.; Martynenko, A. I. Kabanova, E. Yu.; Popova, N. I.; Khashirova, S. Yu.; Ésmurziev, A. M.; Methacrylate and acrylate guanidines: synthesis and properties. *Petrol. Chem.* 2004, 44(1), 43-48.
3. Sivov, N. A.; Khashirova, S. Yu.; Martynenko, A. I.; Kabanova, E. Yu.; Popova, N. I.; NMR <sup>1</sup>H spectral characteristics of diallyl monomers derivatives, *handbook of condensed phase chemistry*. Nova Science Publishers; 2011, 293-301.

## 6.6. Microheterogeneous Titanium Ziegler-Natta Catalysts: The Influence of Particle Size on the Isoprene Polymerization

1. Kissin, Yu. V.; *J. Catal.* 2012, 292, 188-200.
2. Hlatky, G. G.; *Chem. Rev.* 2000, 100, 1347-1376.
3. Kamrul Hasan, A. T. M.; Fang, Y.; Liu, B.; Terano, M.; *Polymer*, 2010, 51, 3627-3635.
4. Schmeal, W. R.; Street, J. R.; *J. Polym. Sci: Polym. Phys. Ed.* 1972, 10, 2173-2183.
5. Ruff, M.; Paulik, C.; *Macromol. React. Eng.* 2013, 7, 71-83.
6. Taniike, T.; Thang, V. Q.; Binh, N. T.; Hiraoka, Y.; Uozumi, T.; Terano, M.; *Macromol. Chem. Phys.* 212, 2011, 723-729.
7. Morozov, Yu. V.; Nasyrov, I. Sh.; Zakharov, V. P.; Mingaleev, V. Z.; Monakov, Yu. B.; *Russ. J. Appl. Chem.*, 2011, 84, 1434-1437.
8. Zakharov, V. P.; Berlin, A. A.; Monakov, Yu. B.; Deberdeev, R. Ya.; *Physicochemical fundamentals of rapid liquid phase processes*. Moscow: Nauka; 2008, 348 p.
9. Monakov, Y. B.; Sigaeva, N. N.; Urazbaev, V. N.; *Active sites of polymerization. Multiplicity: stereospecific and kinetic heterogeneity*. Leiden: Brill Academic, 2005, 397 p.
10. Grechanovskii, V. A.; Andrianov, L. G.; Agibalova, L. V.; Estrin, A. S.; Poddubnyi, I. Ya.; *Vysokomol. Soedin.*, 1980, Ser. A 22, 2112-2120.
11. Guidetti, G.; Zannetti, R.; Ajò, D.; Marigo, A.; Vidali, M.; *Eur. Polym. J.* 1980, 16, 1007-1015. This page intentionally left blank

## 7 7. The Role and Mechanism of Bonding Agents in Composite Solid Propellants

1. Agrawal, J. P.; High Energy Materials Propellants, Explosives and Pyrotechnics. Weinheim: WILEY-VCH Verlag GmbH & Co. KGaA; 2010.
2. Allen, H. C.; Bonding Agent for Nitramines in Rocket propellants. US Patent 4389263, 1983.
3. Chung, H. L.; Kawata, K.; Itabashi, M.; Tensile strain rate effect in mechanical properties of dummy HTPB propellants. J. Appl. Polym. Sci. 1993, 50, 57-66.
4. Uscumlic, G. S.; Zreigh, M. M.; Dusan, Z. M.; Investigation of the interfacial bonding in composite propellants. 1,3,5-Trisubstituted isocyanurates as universal bonding agents, J. Serb. Chem. Soc. 2006, 71, 445-458.
5. Behera, S.; Effect of RDX on elongation properties of AP/HTPB based case bonded composite propellants. Sci. Spectrum, 2009, 31-36.
6. Li, X.; Jiao, J.; Yao, J.; Wang, L.; Study on the relationship between microscopic structure and mechanical properties of HTPB propellant. Adv. Mater. Res. 2011, 4, 1151-1155.
7. Duterque, G.; Lengellej, G.; Combustion mechanisms of nitramine-based propellants with additives. J. Propul. Power, 1990, 6, 718-725.
8. Shokri, S.; Sahafian, A.; Afshani, M. E.; Bonding agents and their performance mechanisms in composite solid propellants. MSc Thesis, K.N. Toosi University of Technology, Iran, 2005.
9. Davenas, A.; Solid Rocket Propulsion Technology. Oxford: Pergamon Press; 1993.
10. Kim, C. S.; Youn, C. H.; Nobel, P. N.; Gao, A.; Development of neutral polymeric bonding agents for propellants with polar composites filled with organic nitramine crystals. Propell. Explos. Pyrot. 1992, 17, 38-42.
11. Kim, C.; Sue, N.; Paul, N.; Youn, C. H.; Tarrant, D.; Gao, A.; The mechanism of filler reinforcement from addition of neutral polymeric bonding agents to energetic polar propellants. Propell. Explos. Pyrot. 1992, 5, 51-58.

12. Hamilton, R. S.; Wardle, R.; Hinshaw, J.; Oxazoline Bonding Agents in Composite Propellants. US Patent 5366572, 1994.
13. Ducote, M. E.; Carver, J. G.; Amine Salts as Bonding Agents. US Patent 4493741, 1987.
14. Wallace, I. A.; Ambient Temperature Mix, Cast, and Cure Composite propellant Formulations. US Patent 5472532, 1995.
15. Allen, H. C.; Clarke, F.; Tetra-Alkyl Titanates as Bonding Agents for Thermoplastic Propellants. US Patent 4597924, 1986.
16. Hamilton, R. S.; Wardle, R.B.; Hinshaw, J. C.; Vinyl Ethers as Nonammonia Producing Bonding Agents In Composite Propellant Formulations. US Patent 5336343, 1994.
17. Hasegawa, K.; Takizuka, M.; Fukuda, T.; Bonding Agents for AP and Nitramine/ HTPB Composite Propellants. AIAA/SAE/ASME, 19th Joint Propulsion Conference, Washington, 1983.
18. Consaga, J. P.; Dimethyl Hydantoin Bonding Agents in Solid Propellants. US Patent 4,214,928; 1980.
19. Leu, A. L.; Shen S. M.: The effects of silane bonding agent on the improvement of thermal stability and mechanical properties of HTPB/HMX composite system. Technol. Polym. Compd. Energ. Mater. 1990, 101-1.
20. Kim, C. S.; Filler reinforcement of polyurethane binder using a Neutral Polymeric Bonding Agent. US Patent 4915755, 1990.
21. Perrault, G.; Lavertu, R.; Drolet, J. F; High-Energy Explosives or Propellant Composition. US Patent 4289551, 1981. This page intentionally left blank

## 8 8. A Study on Adsorption of Methane on Zeolite 13X at Various Pressures and Temperatures

1. Blaha, D.; Bartlett, K.; Czepiel, P.; Harriss, R.; Crill, P.; Natural and anthropogenic methane sources in New England, *Atmos. Environ.* 1999, 33, 243-255.
2. Hui, K. S.; Chao, C. Y. H.; Kwong, C. W.; Wan, M. P.; Use of multitransition-metalionexchanged zeolite 13X catalysts in methane emissions abatement, *Combust. Flame.* 2008, 153, 119-129.
3. Wang, Y.; Hashim, M.; Ercan, C.; Khawajah, A.; Othman, R.; High Pressure Methane Adsorption on Granular Activated Carbons, 21st Annual Saudi-Japan Symposium, November 2011, Catalysts in Petroleum Refining & Petrochemicals, Dhahran, Saudi Arabia; 2011.
4. Behvandi, A.; Tourani, S.; Equilibrium modeling of carbon dioxide adsorption on zeolites. *World Acad. Sci. Eng. Technol.* 2011, 76.
5. Salil, U.; Rege, R.; Yang, T.; Qian, K.; Buzanowski, M. A.; Air-purification by pressure swing adsorption using single/layered beds. *Chem. Eng. Sci.* 2001, 56, 2745- 2759.
6. Jee, J. G.; Kim, M. B.; Lee, C. H.; Adsorption characteristics of hydrogen mixtures in a layered bed: binary, ternary and five component mixtures. *Ind. Eng. Chem. Res.* 2001, 40, 868-878.
7. Cavenati, S.; Grande, C. A.; Rodrigues, A. E.; Adsorption equilibrium of methane, carbon dioxide, and nitrogen on zeolite 13X at high pressures. *J. Chem. Eng.* 2004, 49, 1095-1101.
8. Moghadaszadeha, Z.; Towfighib, J.; Mofarahi, M.; Four-bed pressure swing adsorption for oxygen separation from air with zeolite 13X, iran international zeolite conference (IIZC'08), 29 April 2008, Tehran, Iran; 2008.
9. Mofarah, M.; Sadrameli, M.; Towfighi, J.; Four-bed vacuum pressure swing adsorption process for propylene/propane separation. *Ind. Eng. Chem.* 2005, 44, 1557-1564.
10. Yoshida, S.; Ogawa, N.; Kamioka, K.; Hirano, S.; Mori, T.; The study of zeolite molecular sieves for production of oxygen by using pressure swing adsorption. *Kluwer Acad.*

Pub. 1999, 5, 57-61.

11. Subotic, M.; Tuba, M.; Bacanin, N.; Simian, D.;  
Parallelized cuckoo search algorithm for unconstrained  
optimization. World Sci. Eng. Acad. Soc. 2012.

12. Santos, J.C.; Cruz, P.; Regala, T.; Magalhaes, F. D.;  
Mendes, A.; High-purity oxygen production by pressure  
swing adsorption. Ind. Eng. Chem. 2007, 46, 591-599. This  
page intentionally left blank

## 9 9. Importance of the Phase Behavior in Biopolymer Mixtures

1. Hidalgo, J.; Hansen, P. M. T. J.; Dairy Sci. 1971, 54, 1270-1274.
2. Wang, Y.; Gao, J. Y.; Dubin P. L.; Biotechnol. Prog. 1996, 12, 356-362.
3. Dubin, P. L.; Gao, J.; Mattison, K.; Sep. Purif. Methods, 1994, 23, 1-16.
4. Strege, M. A.; Dubin, P. L.; West, J. S.; Flinta, C. D.; Protein separation via polyelectrolyte complexation. In Symposium on Protein Purification: From Molecular Mechanisms to Large-scale Processes. Ed. Ladisch, M.; Willson, R. C.; Paint C. C.; Builder, S. E.; ACS Symposium Series 427, Chapter 5. Washington: American Chemical Society; 1990, 66 p.
5. Antonov, Yu. A.; Grinberg, V. Ya.; Zhuravskaya, N. A.; Tolstoguzov, V. B.; Carbohydrate polymers, 1982, 2, 81-90.
6. Antonov, Yu. A.; Application of the Membraneless osmosis method for protein concentration from molecular-dispersed and colloidal dispersed solutions. Review. Applied Biochem. Microbiol. (Russia) Engl. Transl., 2000, 36, 382-396.
7. Kiknadze, E. V.; Antonov, Y. A.; Appl. Biochem. Microbiol. (Russia) Engl. Transl., 1998, 34, 462-465.
8. Xia, J.; Dubin P. L.; Protein-polyelectrolyte complexes In: Macromolecular Complexes in Chemistry and Biology, Ed. Dubin P. L.; Davis R. M.; Schultz, D.; Thies C.; Berlin: Springer-Verlag, 1994, Chapter 15.
9. Ottenbrite, R. M.; Kaplan, A. M.; Ann. N. Y. Acad. Sci. 1985, 446, 160-168.
10. Magdassi, S.; Vinetsky, Y.; Microencapsulation: methods and industrial applications. In Microencapsulation of oil-in-water Emulsions by Proteins. Ed. Benita, S.; New York: Marcel Dekker Inc.; 1997, 21-33.
11. Regelson, W.; J Bioact. Compat. Polym. 1991, 6, 178-216.
12. Albertsson, P.-Å.; Johansson, G.; Tjerneld, F.; In Separation Processes in Biotechnology, Ed. Asenjo, J. A.; New York: Marcel Dekker, 1990, 287-327.

13. Harding, S.; Hill, S. E.; Mitchell, J. R.; Biopolymer Mixtures. Nottingham: University Press; 1995, 499 p.
14. Tolstoguzov, V. B.; Functional properties of protein-polysaccharide mixtures. In: Functional Properties of Food Macromolecules. Ed. Hill, S. E.; Ledward, D. A.; Mitchel, J. R.; Gaitherburg, Maryland: Aspen Publishers Inc.; 1998.
15. Piculell, L.; Bergfeld, K.; Nilsson, S.; Factors determining phase behaviour of multicomponent polymer systems. In Biopolymer Mixtures. Ed. Harding, S. E.; Hill, S. E.; Mitchell, J. R.; Nottingham: Nottingham University Press; 1995, 13-36.
16. Antonov, Y. A.; Van Puyvelde P.; Moldenaers, P.; Biomacromolecules, 2004, 5(2), 276-283.
17. Antonov, Y. A.; Van Puyvelde P.; Moldenaers, P.; IJBM, 2004, 34, 29-35.
18. Antonov, Y. A.; Wolf, B.; Biomacromolecules, 2006, 7(5), 1582-1567.
19. Walter, H.; Brooks, D. E.; Fisher, D. In Partitioning in Aqueous Two-Phase Systems: Theory, Methods, Uses and Applications to Biotechnology. London: Academic Press; 1985.
20. Hellebust, S.; Nilsson, S.; Blokhuis, A. M. Macromolecules, 2003, 36, 5372- 5382.
21. Scott, R. J.; Chem. Phys. 1949, 17, 3, 268-279.
22. Tompa, H.; Polym. Solut. London: Butterworth; 1956.
23. Flory, P. J.; Principles of Polymer Chemistry. Ithaca, NY: Cornell University Press; 1953.
24. Prigogine, I.; The Molecular Theory of Solution. Amsterdam: North-Holland; 1967.
25. Patterson, D.; Polym. Eng. Sci. 1982, 22 (2), 64-73.
26. Gottschalk, M.; Linse, P.; Piculell, L.; Macromolecules. 1998, 31, 8407-8416.
27. Lindvig, T.; Michelsen, M. L.; Kontogeorgis, G. M.; Fluid Phase Equilib. 2002, 203, 247-260.



28. Piculell, L.; Nilsson, S.; Falck, L.; Tjerneld, F.; Polym. Commun. 1991, 32, 158-160.
29. Bergfeldt, K.; Piculell, L.; Tjerneld, F.; Macromolecules. 1995, 28, 3360-2270.
30. Bergfeldt, K.; Piculell, L. J.; Phys. Chem. 1996, 14, 5935-5840.
31. Antonov, Y. A.; Grinberg, V. Ya.; Tolstoguzov, V. B.; Starke. 1975, 27, 424-431.
32. Antonov, Y. A.; Grinberg, V. Ya.; Zhuravskaya, N. A.; Tolstoguzov, V. B. J.; Texture Studies. 1980, 11(3), 199-215.
33. Rha, C. K.; Pradipasena, P.; In Functional Properties of Food Macromolecules. Ed. Mitchell, J. R.; Ledward, D. A.; London: Elsevier Applied Science; 1986, 79-119.
34. Whistler, R. L.; Industrial Gums, 2nd edn. New York: Academic Press; 1973.
35. Capron, I.; Costeux, S.; Djabourov, M.; Rheol. Acta. 2001, 40, 441-456.
36. Van Puyvelde, P.; Antonov, Y. A.; Moldenaers, P.; Food Hydrocolloids. 2003, 17, 327- 332.
37. Koningsveld, R.; Staverman, A. J.; J. Polym. Sci. A-2, 1968, 305-323.
38. Polyakov, V. I.; Grinberg, V. Ya.; Tolstoguzov, V. B.; Polym. Bull. 1980, 2, 760-767.
39. Dubois, M.; Gilles, K. A.; Hamilton, J. K.; Revers, P. P.; Smith, T.; Anal. Chem. 1956, 18, 350-356.
40. Zaslavsky, B. Y.; Aqueous Two Phase Partitioning: Physical Chemistry and Bioanalytical Applications. New York: Marcel Dekker; 1995.
41. Grinberg, V. Ya.; Tolstoguzov, V. B.; Food Hydrocolloids. 1997, 11, 145-158.
42. Van Puyvelde, P.; Antonov, Y. A.; Moldenaers, P.; Food Hydrocolloids. 2003, 17, 327- 332.
43. Overbeek, J. T. G.; Voorn, M. J. J.; Cell Comp.

Physiol. 1957, 49, 7-39.

44. Kaibara, K.; Okazaki, T.; Bohidar, H.P.; Dubin, P.;  
Biomacromolecules. 2000, 1, 100- 107.

45. Antonov, Yu. A.; Dmitrochenko, A. P.; Leontiev, A. L.;  
Int. J. Biol. Macromol. 2006, 38 (1), 18-24.

46. Antonov, Y. A.; Gonçalves, M. P.; Food Hydrocolloids.  
1999, 13, 517-524.

47. Michon,C.; Konate, K.; Cuvelier, G.; Launay, B.; Food  
Hydrocolloids. 2002, 16, 613-618.

48. Galazka, V. B.; Ledward, D. A.; Sumner, I. G.;  
Dickinson, E.; Agric. Food Chem. 1997, 45, 3465-3471.

49. Dickinson, E.; Trends Food Sci. Technol. 1988, 9,  
347-354.

50. Snoeren, T. H. M.; Payens, T. A. J.; Jevnink, J.; Both,  
P. Milchwissenschaft. 1975, 30, 393-395.

51. Kabanov, V. A.; Evdakov, V. P.; Mustafaev, M. I.;  
Antipina, A. D.; Mol. Biol. 1977, 11, 582-597.

52. Noguchi, H.; Biochim. Biophys. Acta. 1956, 22, 459-462.

53. Kumihiko, G.; Noguchi, H.; Agricul. Food Sci. 1978, 26,  
1409-1414.

54. Sato, H.; Nakajima, A.; Colloid Polym. Sci. 1974, 252,  
294-297.

55. Sato, H.; Maeda, M.; & Nakajima, A.; J. Appl. Polym.  
Sci. 1979, 23, 1759-1767.

56. Bungenberg de Jong, H. G.;  
Crystallisation-Coacervation-Flocculation. In Colloid  
Science. Ed. Kruyt, H. R.; : Amsterdam: Elsevier Publishing  
Company; 1949, Vol. II, Chapter VIII, 232-258.

57. Gurov, A. N.; Wajnerman, E. S.; Tolstoguzov, V. B.;  
Stärke. 1977, 29 (6), 186-190.

58. Antonov, Y. A.;Lefebvre, J.; Doublier, J. L. Polym.  
Bull. 2007, 58, 723-730.

59. Antonov, Y. A.;Lashko N. P.;.Glotova, Y. K.;  
Malovikova, A.; Markovich, O. Food Hydrocolloids. 1996, 10

(1), 1-9.

60. Polyalov, V. I.; Grinberg, V. Ya.; Antonov, Y. A.; Tolstoguzov, V. B.; Polym. Bull. 1979, 1, 593-597.

61. Polyalov, V. I.; Kireeva, O. K.; Grinberg, V. Ya.; Tolstoguzov, V. B.; Nahrung. 1985, 29, 153-160.

62. Swaisgood, H. E.; In Advanced Dairy Chemistry-1:Proteins. Ed. Fox, P. F.; London: Elsevier Applied Science; 1992.

63. Langendorff, V.; Cuvelier, G.; Launay, B.; Michon, C.; Parker, A.; De Kruif, C. G.; Food Hydrocolloids. 1999, 13, 211-218.

64. Bowman, W. A.; Rubinstein, M.; Tan, J. S.; Macromolecules. 1997, 30(11), 3262- 3270

65. Junhwan, J.; Dobrynin, A.; Macromolecules. 2005, 38(12), 5300-5312.

66. Smid, J.; Fish, D.; In: Encyclopedia of Polymer Science and Engineering, 2nd ed. Polyelectrolyte Complexes. Ed. Mark, H. F.; Bikales, N. M.; Overberger, C. G.; Menges, G.; New York: Wiley/Interscience; 1988, Vol. 11, 720 p.

67. Striolo, A.; Ward, J.; Prausnitz, J. M.; Parak, W. J.; Zanchet, D.; Gerion, D.; Milliron, D.; Alivisatos, A. P. J.; Phys. Chem. 2002. B, 106(21), 5500-5505.

68. Antonov, Y. A.; Van Puyvelde P.; Moldenaers, P.; Biomacromolecules. 2004, 5(2), 276-283.

69. Antonov, Y. A.; Van Puyvelde, P.; Moldenaers, P.; Food Hydrocolloids. 2009, 23, 262- 270. This page intentionally left blank Applied Methodologies in Polymer Research and Technology Editors PhD Abbas Hamrang, Devrim Balköse, Applied Methodologies in and Polymer Research Technology

Applied Methodologies in Polymer Research and Technology

This book covers a broad range of polymeric materials and presents the latest developments

and trends in advanced polymer materials and structures. It discusses the developments of

advanced polymers and respective tools to characterize and

predict the material properties

and behavior. This book has an important role in advancing polymer materials in macro and

nanoscale. Its aim is to provide original, theoretical, and important experimental results that

use non-routine methodologies. It also includes chapters on novel applications of more familiar

experimental techniques and analyses of composite problems that indicate the need for new

experimental approaches.

This new book:

- highlights some important areas of current interest in key polymeric materials and

technology

- gives an up-to-date and thorough exposition of the present state of the art of key

polymeric materials and technology

- describes the types of techniques now available to the engineers and technicians and

discusses their capabilities, limitations, and applications

- provides a balance between materials science and chemical aspects and basic and

applied research

- focuses on topics with more advanced methods

- explains modification methods for changing of different materials properties

ABOUT THE EDITORS

Abbas Hamrang, PhD, is a professor of polymer science and technology. He is currently a

senior polymer consultant and editor and a member of the academic board of various

international journals. His previous involvement in academic and industry sectors at the

international level includes deputy vice-chancellor of research and development, senior

lecturer, manufacturing consultant, and science and technology advisor. His research interests

include degradation studies of historical objects and archival materials, cellulose-based

plastics, thermogravimetric analysis, and accelerated ageing processes and stabilization of

polymers by chemical and non-chemical methods.

Devrim Balköse, PhD, is a retired Professor and Head of the Chemical Engineering

Department of Izmir Polytechnic Institute in Turkey. She has been an associate professor in

macromolecular chemistry and a professor in process and reactor engineering. She has also

worked as research assistant, assistant professor, associate professor, and professor at Ege

University in İzmir, Turkey. Her research interests are in polymer reaction engineering,

polymer foams and films, adsorbent development, and moisture sorption, with her research

projects focusing on nanosized zinc borate production, ZnO polymer composites, zinc borate

lubricants, antistatic additives, and metal soaps.

Reviewers and Advisory Board Members: Gennady E. Zaikov, DSc, and A. K. Haghi, P h D H a m r a n g B a l k ö s e  
ISBN: 978-1-77188-040-4 9 781771 880404 00009

www.appleacademicpress.com Applied Methodologies in  
Polymer Research and Technology Editors PhD PhD Abbas  
Hamrang, Devrim Balköse, A p p l i e d M e t h o d o l o g  
i e s i n a n d P o l y m e r R e s e a r c h T e c h n o l  
o g y

## Applied Methodologies in Polymer Research and Technology

This book covers a broad range of polymeric materials and presents the latest developments

and trends in advanced polymer materials and structures. It discusses the developments of

advanced polymers and respective tools to characterize and predict the material properties

and behavior. This book has an important role in advancing polymer materials in macro and

nanoscale. Its aim is to provide original, theoretical, and important experimental results that

use non-routine methodologies. It also includes chapters on novel applications of more familiar

experimental techniques and analyses of composite problems that indicate the need for new

experimental approaches.

This new book:

- highlights some important areas of current interest in key polymeric materials and technology
- gives an up-to-date and thorough exposition of the present state of the art of key polymeric materials and technology
- describes the types of techniques now available to the engineers and technicians and discusses their capabilities, limitations, and applications
- provides a balance between materials science and chemical aspects and basic and applied research
- focuses on topics with more advanced methods
- explains modification methods for changing of different materials properties

### ABOUT THE EDITORS

Abbas Hamrang, PhD, is a professor of polymer science and

technology. He is currently a

senior polymer consultant and editor and a member of the academic board of various

international journals. His previous involvement in academic and industry sectors at the

international level includes deputy vice-chancellor of research and development, senior

lecturer, manufacturing consultant, and science and technology advisor. His research interests

include degradation studies of historical objects and archival materials, cellulose-based

plastics, thermogravimetric analysis, and accelerated ageing processes and stabilization of

polymers by chemical and non-chemical methods.

Devrim Balköse, PhD, is a retired Professor and Head of the Chemical Engineering

Department of Izmir Polytechnic Institute in Turkey. She has been an associate professor in

macromolecular chemistry and a professor in process and reactor engineering. She has also

worked as research assistant, assistant professor, associate professor, and professor at Ege

University in İzmir, Turkey. Her research interests are in polymer reaction engineering,

polymer foams and films, adsorbent development, and moisture sorption, with her research

projects focusing on nanosized zinc borate production, ZnO polymer composites, zinc borate

lubricants, anistatic additives, and metal soaps.

Reviewers and Advisory Board Members: Gennady E. Zaikov, DSc, and A. K. Haghi, PhD Hamrang Balköse  
ISBN: 978-1-77188-040-4 9 781771 880404 00009 Applied Methodologies in Polymer Research and Technology Editors  
PhD PhD Abbas Hamrang, Devrim Balköse, Applied Met

h o d o l o g i e s i n a n d P o l y m e r R e s e a r c h  
T e c h n o l o g y Applied Methodolog e in Polymer Re  
arch and Technology This bo k covers a broad range of  
polymeric materials and pres nts the latest devel pments  
and tr ds in advanc d polymer materials and structures. It  
discusses the developments of advanced polymers and  
respective tools to characterize and predict the material  
properties and behavior. This book has an important role  
in advancing polymer materials in macro and nanoscale. Its  
aim is to provide original, theoretical, and important  
experimental results that use non-routine methodologies.  
It also includes chapters on novel applications of more  
familiar experimental techniques and analyses of composite  
problems that indicate the need for new experimental  
approaches. This new book: • highlights some important  
areas of current interest in key polymeric materials and  
technology • gives an up-to-date and thorough exposition  
of the present state of the art of key polymeric materials  
and technology • describes the types of techniques now  
available to the engineers and technicians and discusses  
their capabilities, limitations, and applications •  
provides a balance between materials science and chemical  
aspects and basic and applied research • focuses on  
topics with more advanced methods • explains modification  
methods for changing of different materials properties  
ABOUT THE EDITORS Abbas Hamrang, PhD, is a professor of  
polymer science and technology. He is currently a senior  
polymer consultant and editor and a member of the academic  
board of various international journals. His previous  
involvement in academic and industry sectors at the  
international level includes deputy vice-chancellor of  
research and development, senior lecturer, manufacturing  
consultant, and science and technology advisor. His  
research interests include degradation studies of  
historical objects and archival materials, cellulose-based  
plastics, thermogravimetric analysis, and accelerated  
ageing processes and stabilization of polymers by chemical  
and non-chemical methods. Dev im Balköse, PhD, is a  
retired Professor and Head of the Chemical Engineering  
Department of Izmir Polytechnic Institute in Turkey. She  
has been an associate prof ssor in macromolecular  
chemistry and a professor in process and reactor  
engineering. She has also worked as research assistant,  
assistant professor, associate professor, and professor at  
Ege University in İzmir, Turkey. Her research interests  
are in polymer reaction engineering, polymer foams and  
films, adsorbent development, and moisture sorption, with  
her research projects focusing on nanosized zinc borate  
production, ZnO polymer composites, zinc borate  
lubricants, antistatic additives, and metal soaps.



Reviewers and Advisory Board Members: Gennady E. Zaikov, DSc, and A. K. Haghi, PhD Hamrang Balköse  
ISBN: 978-1-77188-040-4 9 781771 880404 00009 Applied Methodologies in Polymer Research and Technology Editors PhD PhD Abbas Hamrang, Devrim Balköse, Applied Methodologies in Polymer Research and Technology Applied Methodologies in Polymer Research and Technology This book covers a broad range of polymeric materials and presents the latest developments and trends in advanced polymer materials and structures. It discusses the developments of advanced polymers and respective tools to characterize and predict the material properties and behavior. This book has an important role in advancing polymer materials in macro and nanoscale. Its aim is to provide original, theoretical, and important experimental results that use non-routine methodologies. It also includes chapters on novel applications of more familiar experimental techniques and analyses of composite problems that indicate the need for new experimental approaches. This new book: • highlights some important areas of current interest in key polymeric materials and technology • gives an up-to-date and thorough exposition of the present state of the art of key polymeric materials and technology • describes the types of techniques now available to the engineers and technicians and discusses their capabilities, limitations, and applications • provides a balance between materials science and chemical aspects and basic and applied research • focuses on topics with more advanced methods • explains modification methods for changing of different materials properties

ABOUT THE EDITORS Abbas Hamrang, PhD, is a professor of polymer science and technology. He is currently a senior polymer consultant and editor and a member of the academic board of various international journals. His previous involvement in academic and industry sectors at the international level includes deputy vice-chancellor of research and development, senior lecturer, manufacturing consultant, and science and technology advisor. His research interests include degradation studies of historical objects and archival materials, cellulose-based plastics, thermogravimetric analysis, and accelerated ageing processes and stabilization of polymers by chemical and non-chemical methods. Devrim Balköse, PhD, is a retired Professor and Head of the Chemical Engineering Department of Izmir Polytechnic Institute in Turkey. She has been an associate professor in macromolecular chemistry and a professor in process and reactor engineering. She has also worked as research assistant, assistant professor, associate professor, and professor at Ege University in İzmir, Turkey. Her research interests

are in polymer reaction engineering, polymer foams and films, adsorbent development, and moisture sorption, with her research projects focusing on nanosized zinc borate production, ZnO polymer composites, zinc borate lubricants, antistatic additives, and metal soaps.  
Reviewers and Advisory Board Members: Gennady E. Zaikov, DSc, and A. K. Haghi, PhD Hamrang Balköse  
ISBN: 978-1-77188-040-4 9 781771 880404 00009